Synthesis of peptide-loaded chitosan nanoparticles for the treatment of sexually transmitted infections (STI's)

UNIVERSITY *of the*
WESTERN CAPE

By

Bonke Phathekile

A thesis submitted in partial fulfilment of the requirements for the degree of

Magister Scientiae in Chemistry

Faculty of Natural Science

University of the Western Cape

Cape Town, South Africa

Supervisor: Prof Martin Onani

Co-supervisors: Prof Mervin Meyer

Prof Emily. G Okuthe (Walter Sisulu University)

November 2019

DECLARATION

I declare that *Synthesis of peptide loaded chitosan nanoparticles for the treatment of sexually transmitted infections (STI's)* is my own work, that it has not been submitted for any degree or examination in any other university, and that all the sources I have used or quoted have been indicated and acknowledged by complete references.

Bonke Phathekile Year: January 2020

Signature.. .....

DEDICATION

I dedicate my MSc dissertation to my amazing family, father, Mr Ndodemnyama Phathekile; mother, Mrs Nozukile Phathekile, sister, Miss Alindile Phathekile and brother, Mr Lusindiso Phathekile who have been my motivation throughout my academic career. Your words of encouragement, support and love have helped me to always strive to do my best no matter how difficult the task at hand. A heartfelt thank you for all you have done for me.

ACKNOWLEDGEMENTS

First and foremost many praises to our Heavenly Father for his sacred grace and blessings on me without which I would not have been able to accomplish anything.

I'm truly grateful to everyone who directly or indirectly assisted me with my project. Your expertise has led me to acquire a true passion for my work. This has been a difficult yet fruitful journey. My heartfelt gratitude goes to my parents and siblings for their caring support system at home, in particular the cups of coffee when I least expected it. All your love, encouragements and above all support has played a huge role in my journey.

I would like to thank my supervisor Prof Martin Onani, Group Leader of the Organometallics and Nanomaterials research group, for all his guidance, advice and continuous encouragements throughout my research. Thank you for teaching me the first fundamental rules of research.

To my co-supervisors Prof Mervin Meyer and Prof. Emily Okuthe for the insight to the project and valuable contributions which have led to the success of my thesis. Thank you for always being available when I needed your guidance.

Many thanks to the Biolabels, Organometallic and Nanomaterials research group members for their support, sharing of knowledge and endless debates. Thank you for your kind support and lending a helping hand in the laboratory during my experiments.

I humbly thank everyone within the Chemical Science Department for all your help and respect. Special thanks to Ms Dawn Mcmahon for all your support, kind assistance, and always making me smile. Many thanks to the sensor laboratory team, especially Dr Masikini Milua for allowing me access their analytical instruments; Mr Adrian Josephs of the Electron Microscopy Unit (EMU) for carrying out Transmission Electron Microscopy (TEM) and Scanning ELctron Microscopy (SEM) analysis of my samples; Miss Nasheeta of the University of Cape Town for SEM analysis of my samples.

I thank all my family and friends for all your continuous prayers, love and support.

Finally, I wish to acknowledge and thank the following organisations for their financial support. This work would not have been possible without the dire financial need they provided. This research work was supported by National Research Foundation (NRF) through Grant

holder linked Bursary to Prof. Okuthe GE (NRF - Thuthuka Rating Track, Ref. No. TTK150625121238; UID: 99307), DST Mintek (NIC) and HWSETA.

Without everyone, this would not have been possible. Many thanks.

PUBLICATION AND CONFERENCE CONTRIBUTIONS

This work has been presented in part at the following different scientific fora:

1. Nobonke Phathekile, Martin O. Onani, Mervin Meyer, Emily Okuthe, The Synthesis of peptide-loaded chitosan nanoparticles for the treatment of sexually transmitted diseases (STIs). **HORIZONS OF SCIENCE Forum of Diploma Theses 2018**, 22-23-05-2018. Krakow, Poland. Oral Presentation.

2. Nobonke Phathekile, Martin O. Onani., Prof M. Meyer and G.E Okuthe. The Synthesis of peptide-loaded chitosan nanoparticles for the treatment of sexually transmitted diseases (STIs). **BIO Africa Convention**, 27-29-08-2018. Durban ICC. Poster Presentation.

3. Miss N. Phathekile, Prof M.O. Onani, Prof M. Meyer and G.E Okuthe. The Synthesis of peptide-loaded chitosan nanoparticles for the treatment of sexually transmitted diseases (STIs). **DST Nanotechnology Innovation Centres' 10 Year Anniversary Workshop**. 14-16-10-2018, CSIR International Convention Centre, Pretoria. Poster presentation.

KEYWORDS

Synthesis of peptide-loaded chitosan nanoparticles for the treatment of sexually transmitted infections

Phathekile, Bonke

Chitosan

Kn2-7

HBd-3

Microbicides

Tripolyphosphate

Poly acrylic acid

Antimicrobial activity

Encapsulation

Controlled release

Sexual Transmitted Infections

ABSTRACT

Synthesis of peptide-loaded chitosan nanoparticles for the treatment of STI's

Phathekile, Bonke

MSc thesis, Department of Chemistry, University of the Western Cape

Peptides are among the main drugs which attract much attention because of their great potential in treating sexually transmitted diseases and other chronic diseases. There has been a major challenge of delivering these drugs in mucosal sites with low pH environment. The aim of this study is to synthesize acidic pH stable peptide loaded chitosan nanoparticles gels that could penetrate mucus layers covering the epithelial cells and kill HIV virus. Chitosan nanoparticles were synthesized by crosslinking method called Ionic gelation with Sodium tripolyphosphate~~TPP~~. A series of peptide-loaded chitosan nanoparticles of different concentrations of tripolyphosphate~~TPP~~ were produced using medium molecular weight (MW) of chitosan. The nanoparticles were characterized by ultraviolet-visible absorption spectroscopy (UV-Vis), scanning electron microscopy (SEM), dynamic light scattering (DLS) and high resolution transmission electron microscopy (HRTEM). The sizes of chitosan nanoparticles were obtained at the range of 327-416 nm with zeta potential of +9.61-23.9 mV when these nanoparticles were prepared at room temperature. After the loading of two peptides Kn2-7 and HBd-3 in chitosan nanoparticle, the sizes increased from 340.2-753.7nm with an increase in Zeta potential of 15.9-67.7 mV which showed a good stability and monodispersed nanoparticles. The highest loading capacity and entrapment efficiency was obtained from the nanoparticles that were crosslinked with 1mg/mL of TPP at 85.6% and 78.3%. The peptide loaded chitosan nanoparticles were further exposed to different pH conditions to test their stability in the environment that mimic the vaginal mucus. The results showed that antimicrobial peptide loaded chitosan nanoparticles~~AMP-CNPs~~ are not stable at low pH, they do not release the peptide in a sustained manner. The loaded nanoparticles were further coated with polyacrylic acid (PAA) using layer by layer method to form polyelectrolyte that provide a slow release at low pH. The polyacrylic acid~~PAA~~-peptide loaded chitosan nanoparticles were also characterised using the same characterization technique. The tests of stability on nanoparticles showed that the antimicrobial peptide loaded chitosan nanoparticles~~AMP-CP~~ do not release the peptide immediately after exposing them to low pH conditions. The antibacterial assay confirmed that the polyacrylic~~PAA~~ coated kn2-7 chitosan nanoparticle~~CNP~~s inhibited

the bacterial better than Kn2-7 alone at the pH of 3.8. In conclusion, from the obtained results these nanoparticles serve as promising candidates for the delivery of these antimicrobial peptides safely in vaginal sites.

TABLE OF CONTENTS

LIST OF FIGURES

CHAPTER 1

CHAPTER 2

CHAPTER 3

CHAPTER 4

LIST OF TABLES.

LIST OF ABBREVIATIONS

AMP	Antimicrobial peptide
Hβd-3	Human beta defensin-3
CS	Chitosan
TPP	Tripolyphosphate
CNPs	Chitosan nanoparticles
PAA	poly acrylic acid
NPs	Nanoparticles
Amp	Ampicillin
MIC	Minimum inhibitory concentration
EE	Encapsulation Efficiency
LC	Loading Capacity
FTIR	Fourier Transform Spectroscopy
UV-VIS	Ultraviolet Visible
DLS	Dynamic Light Spectroscopy
HRSEM	High Resolution Scanning Electron Microscope
HRTEM	High Resolution Transmission Electron Microscope
µg/mL	Microgram per millilitre
nm	Nanometer
rpm	Rate per minute
mm	Milimitre
KBr	Potassium bromide
LBL	Layer by Layer
PDI	Polydispersity index

ND	Not determined
Ac	Acetic acid
KCP	Kn2-7-chitosan-poly(acrylic acid)
HCP	Human beta defensin-3-chitosan-poly(acrylic acid)
AMP-CP	Antimicrobial peptide-chitosan-poly(acrylic acid)
LB	Luria-Bertani

CHAPTER 1

INTRODUCTION

Background

1.1 Sexually transmitted infections

Sexually transmitted infections (STIs) are infections that can be caught or transmitted when having unprotected sex with another person who is already infected by an STI[1]. Each year, over 9 million women are diagnosed with these infections[2]. STI is a major cause of critical illness, infertility, long-term disability, and death, with severe medical and psychological consequences for millions people around the world. According to the World Health Organization (WHO), STIs are among the top five diseases in developing countries forcing patients to seek healthcare[3].

Various issues are cited as contributing factors to the high incidence of STIs. , These factors include lack of sexual education more especially in rural areas where teenagers are more sexually active, and change in people's behaviour for example by alcohol consumption which leads to unprotected sexually activities. Among all those factors, the vulnerability of women due to gender power in relationships and shortage of women controlled protective methods lead to the high number of ~~women getting affected by the transmission of~~ STIs infections [4]. New cases of STIs such as HIV, human herpes virus, human papilloma virus and hepatitis B virus occur annually. All these infections constitute a huge health and economic burden, especially for developing countries where they account for 17% of economic losses caused by ill health. STIs affect both genders with women suffering the most of the epidemic because of their heightened risk of infection due to biological, economic and social vulnerabilities. In general, the spread of viruses is primarily from man to woman, rather than from woman to man. Currently, the most effective method available for protection against STIs is the use of a condom, but it can be improved by applying microbicidal coatings on the condom[5].

1.2 Vaginal Microbicides

VA ~~v~~aginal microbicides can be defined as chemical agents that are topically applied within the vagina in order to prevent infection by HIV and other sexually transmitted pathogens

through causing the death of the infectious organism [6]. Microbicides are considered as a promising tool to protect women from acquiring STI's. The administration of microbicides is controlled by women, who can apply them before sexual intercourse without the sexual partner's involvement [7].There are many examples of different types of vaginal microbicides which include tablets, surfactants, ring microbicide, films and gels but they fail on clinical trials. Some of these microbicides lack bioavailability and , need high dosages which might lead to the damage of damage other cells [8]. Fortunately,, therefore with our approach we can solve the stability of these microbicides on low pH, bioavailability and bio-distribution in mucus. The increase in number of topical microbicides on the market today such as, tenofovir, Pro 2000 and savvy, which are not peptide based for the prevention of HIV transmission is a reflection of the advances that have been made in understanding the pathophysiology of HIV infection. It is clear that the development of a topical microbicide to prevent the sexual transmission of HIV is scientifically, ethically, and culturally complicated [9]. Microbicidal agents are capable of decreasing the rate of transmission of viruses through sexual contact[10]. Antimicrobial peptides such as Kn2-7 peptide and Human β-defensin-3, which are capable of killing viruses and bacteria have been identified and can potentially also be used as microbicidal agents to fight STIs.

1.3 The antimicrobial peptides (AMPs)

Antimicrobial peptides (AMPs) are host defence peptides that exist in various organisms such as, bacteria, fungi and plants. These peptides have attracted more attention because of their antibacterial, anti-fungi, anti-virus properties and can also overcome bacterial drug resistance[11]. Our focus in this study is on the following AMPs, human beta defensin-3 Hβd-3 and Kn2-7.

1.3.1 The antimicrobial peptide, Kn2-7

Kn2-7 is an antimicrobial peptide that was derived from the venom of the scorpion *Buthus martensii Karsch* (BmK)[12]. Chen and co-workers in their study reported that Kn2-7 has a high antibacterial activity against clinical antibiotic-resistant strains such as methicillin-resistant *Staphylococcus aureus* (MRSA), *Staphylococcus aureus* and *Escherichia coli*[13]. Recent studies revealed that this peptide has a high level of anti-HIV activity and it can be used to prevent the transmission of HIV/AIDS. It was reported that the Kn2-7 peptide could inhibit HIV-1 by direct interaction with viral particles and was described as a promising candidate for

the development of novel microbicidal agent[14]. Kn2-7 was also shown to have growth inhibitory effects against gram negative and gram positive bacteria[15].

1.3.2 The antimicrobial peptide, Human beta-defensin-3

Human beta defensin-3 (Hβd-3) is the member of host defence that is recently discovered and has attracted much attention because of its antimicrobial properties[16]. There is growing evidence that the activity of this peptide also involves the adaptive immunity[17]. Hβd-3 has been reported to have strong broad-spectrum antibacterial activity. It has been reported to have antibacterial activities towards Gram-negative and Gram-positive bacteria as well as an ability to act as a chemo-attractant [18]. Chen Zhu and co-workers reported the evaluation of the effects of Hβd-3 on *Staphylococcus epidermidis* ATCC 35984 (methicillin-resistant strain), MRSE287, and MRSA (ATCC43300) by evaluating bacterial adhesion, biofilm formation, and maturation[19]. Since there is considerable current interest in developing Hβd-3 for possible pharmaceutical applications, studies to further our understanding on the determinants of antibacterial activities and immunomodulatory function of Hβd-3 are considered to be highly significant[20].

1.4 Chitosan

Chitosan (CS) is a natural polysaccharide produced by the partial deacetylation of chitin fig 1.1, the structural element in the exoskeleton of crustaceans such as crabs and shrimps[21]. The amino group in chitosan has a pKa value of approximately 6.5, which leads to protonation in an acidic solution with a charge density dependent on the pH and the % deacetylation value. CS has water soluble and bioadhesive properties to negatively charged surfaces, which make CS ideal for drug delivery to cells that are part of mucosal membranes[22]. CS has drawn attention because of its mucoadhesive properties. It has an ability to promote transport of drugs, peptides and proteins across mucosal barriers. The study of CNPs is intended for cancer therapy[23].

It is also ideal for drug delivery in acidic environments where it can be degraded slowly, thereby releasing the drug to the desired site. This polymer is biocompatible and biodegradable and is widely used as a pharmaceutical excipient in a range of formulations such as powders, tablets, emulsions, and gels[24]. The use of CS as a mucoadhesive polymer for vaginal delivery systems has been studied by several researchers. The CS as a natural polymer has been also

applied in wound healing because of its adhesive nature together with the antifungal character [25].

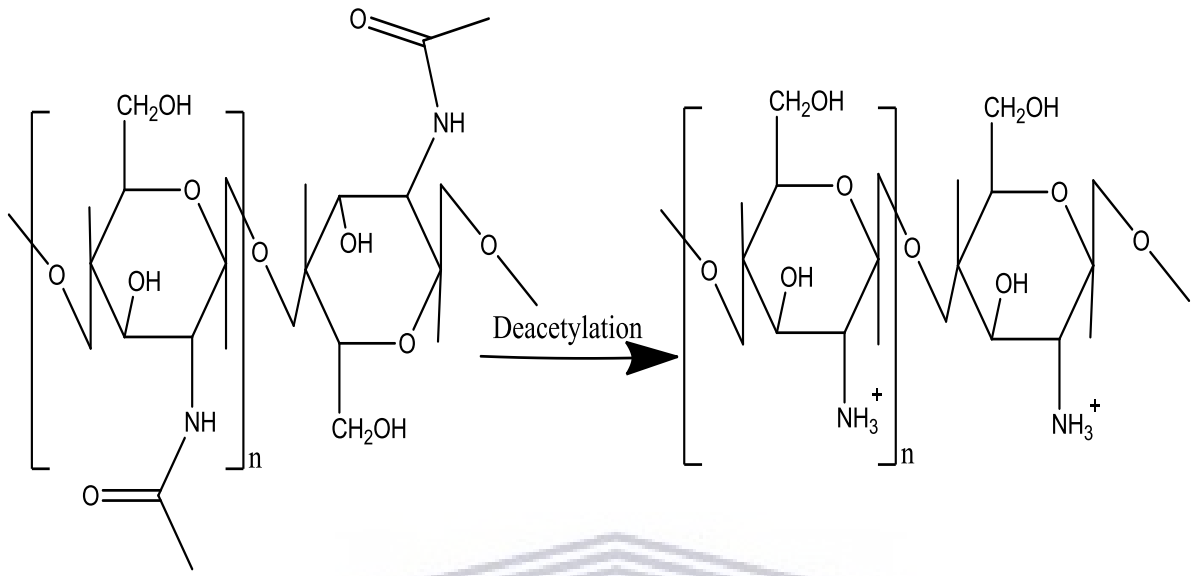

Figure 1. 1: Illustration on the formation of CS[26]

The chitosan nanoparticles(CNPs) can be synthesised from CS using inotropic gelation method[27]. These NPs can be used as carriers for protein drugs like insulin and also to get the improved mucus penetrating properties. The use of CNPs for drug delivery can enhance the mucus diffusion efficiency of drugs. CNPs are prepared by crosslinking of CS with triphosphate as coreshell nanocarriers. CNPs as is illustrated in fig 1.2 has been prepared by reacetylation of CS and used as vehicles for gastric drug delivery. The CNPs ensure the controlled release of active antimicrobial agents, such as have amoxycillin and metronidazole in the gastric cavity[28].

In addition to its biocompatibility and biodegradability, one of the main advantages of chitosan over other equivalent drug delivery excipients is its favourable toxicological profile. It is commonly regarded as a non-toxic, non-irritant material and has been approved for use in cosmetics and as a food supplement in several countries [29]. Nevertheless, analysis of the toxicological data of chitosan and derivatives is not an easy task since the wide range of CS brands and derivatives that have been described in the literature often results in contradictory toxicity profiles among similar and different kinds of CS [30]. Mucus is a viscoelastic and adhesive gel that protects the tissues by trapping and removing unwanted substances[31]. According to Stoke-Einstein equation for diffusion, mucus has a high viscosity such that it is

very difficult for molecules and small particles to penetrate it [32]. The development of NPs that can penetrate high viscoelastic human mucosal tissues has become a main interest in nanotechnology[33]. Polymeric NPs have attracted interest due to their mucus penetrating properties. These NPs have a size ranging from 10-1000nm[34]. Polymer NPs possess a number of desirable features such as their penetration to mucosal deep tissues due to their Nano size, cellular uptake and subcellular trafficking[35]. Mucus penetrating polymers have an excellent binding capacity with mucosal tissues over a considerable period of time. Several studies have been conducted on the encapsulation of tragacanth, Carbopol, Poloxamer 407, pectin, sodium alginate, cellulose derivatives, and chitosan, among others, into intravaginal drug formulations in order to increase the residence time of these formulations at the site of action[36]-[37].

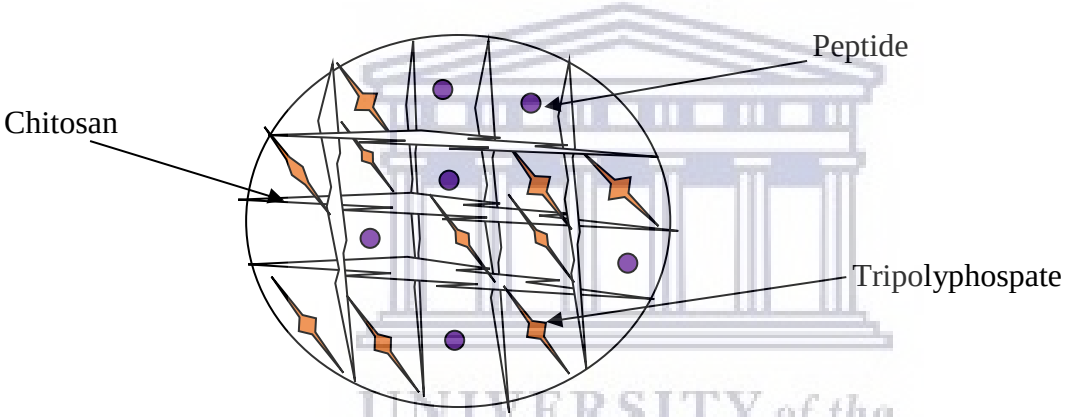

Figure 1. 2: Formation of the peptide loaded CS

However, the antibacterial activity of CNPs has only rarely been reported in the literature. The unique character of CNPs due to their small size and quantum size effect could make these NPs exhibit useful antibacterial activities [38].

1.5 Problem Statement

STIs such as HIV, hepatitis B, herpes, and the human papilloma virus (HPV), chlamydia, gonorrhoea, and syphilis can be passed on from person to person during sexual intercourse. Microbicides can be applied as topical agents in the vagina or rectum to prevent the transmission of STIs during sexual intercourse[9]. These drugs are capable of killing these infectious organisms on contact. However, the normal environment of the vagina is inhospitable to many microbicidal agents. To begin with, the pH within the upper vagina is acidic with a pH below 5. The low pH normally provides protection against the growth of bacteria. The vaginal lining contains large amounts of glycogen, which is broken down by anaerobic lactobacilli within the vagina resulting in the production of lactic acid. Lactic acid is the cause for the low pH within the vagina. Many microbicidal agents are denatured in acidic environments, which can neutralize the protective effects of the microbicide. Microbicidal agents must thus be able to function in an acidic pH to be effective.

Secondly, the vagina also contains cervical mucus. The mucus function as an almost impenetrable barrier to the cervix. This can affect the biodistribution of a microbicidal agent within the vagina and cervix[39]. If the microbicide is not well distributed throughout the vagina, the microbicide will not be able to destroy the infectious organisms effectively.

To overcome these limitations what is thus required is a drug delivery system that can protect the microbicidal agent in an acidic environment and ensure the efficient biodistribution of the microbicidal agent in an environment that has high mucus content. Nanotechnology can provide drug delivery solutions for the slow release of the microbicidal agent in an acidic environment. Nanomaterials that can effectively traverse mucus, so called mucus penetrating nanoparticles can also resolve the problem of biodistribution. The mucus penetrating properties of CNPs has been well demonstrated previously[40]. These NPs are also slowly degraded in acidic environments, which will result in the slow release of drugs that are incorporated into the NP.

AMPs are synthetic or naturally occurring peptides with a broad-spectrum antibacterial and antiviral activity. Human β-defensin3 (Hβd-3) and Kn2-7 peptide is 2 examples of AMPs that was shown to inhibit the growth of STIs These peptides can thus be used as microbicides to prevent the transmission of STIs, in particular HIV. However, peptides are also vulnerable to degradation in acidic pH environments. By loading CNPs with these peptides a more effective intravaginal microbicidal treatments that is not affected by the low pH of the vagina and which

will be efficiently distributed throughout the mucus rich environment of the vagina can be developed. CNPs loaded with these peptides could for example be incorporated into a vaginal gel.

1.6 Research aims and objectives

Aim

To synthesize AMP loaded CNPs that can maintain the antimicrobial activity of antimicrobial peptides in conditions that simulate the pH of the vaginal environment.

Objectives:

- To synthesize chitosan nanoparticles (CNPs).
- To load the chitosan nanoparticles (CNPs) with antimicrobial peptides (AMPs) to produce AMP-CNPs.
- To characterize the AMP-CNPs.
- To evaluate the stability of AMP-CNPs in low and high pH conditions.
- To coat AMP-CNPs with polyacrylic acid (PAA) to produce AMP-CP NPs.
- To characterize the AMP-CS/PAA NPs.
- To evaluate the stability of AMP-CP NPs in low and high pH conditions.
- To investigate the antimicrobial activity of the AMP-CNPs in low and high pH conditions.

1.7 Outline of the dissertation

The following outline gives a brief description about the contents of each chapter:

Chapter 1

An introduction to the study with aims and objectives

Chapter 2

Literature reports on the methods of synthesis and characterization techniques. The application and drug delivery of chitosan NPs is also briefly highlighted.

Chapter 3

Deals with the synthesis and methods of characterization of PAA/CNPs containing peptide. Antibacterial aessay and release studies methods.

Chapter 4

Focuses on the synthesis and characterization of peptide loaded CNPs, stability tests on loaded NPs, peptide loaded CS/poly acrylic acid NPs. The release studies on peptide loaded CS/polyacrylic acid NPs and antibacterial activity of Kn2-7 peptide and peptide loaded NPs. Results obtained are interpreted and discussed.

Chapter 5

Conclusions based on the interpretation of the data obtained are drawn in this chapter. Recommendations for future work are also put forward in this chapter.

Appendix

Selected spectra are presented in this section.

CHAPTER 2

LITERATURE REVIEW

2.1 Introduction

The development of high quality drug transport systems that can transport and deliver drugs precisely and safely to the site of action is turning into a fairly necessary research area for pharmaceutical researchers. As a result, promising ways of delivering poorly soluble drugs, peptides and proteins are being devised and improved. Although there are many workable enhancements to be made in the field drug transport and diagnostics, nanotechnology provides benefits that permit a greater targeted delivery and controlled release of the therapeutic compounds[41].

In previous years CNPs were introduced as promising carriers for oral protein delivery, because they can protect these peptides/proteins from denaturing. Other proteins, such as insulin show low therapeutic activity when administered orally due to degradation by proteolytic enzymes [42]. In addition to that, a number of *in vivo* and *in vitro* studies of different animal and cell models, have confirmed that CS-based NPs produced water-soluble derivatives which increases the oral availability of the peptide octreotide[47,48]. However the toxicity of CS and its derivatives is the major concern in drug delivery. This literature focuses on different ways that were previously explored to deliver dugs through mucus barriers using Cchitosan NPs, t. The problems that were faced by those researchers and their successes in delivering drugs across mucosal sites. Furthermore, the behaviour of NPs when exposed to low pH environment as nanocarriers.

2.2 Polymeric NPs

These are solid, submicron-sized particles or drug carriers. The term "nanoparticle" here is used as a collective term for both nanospheres and nanocapsules, relying on the method of preparation[45]. Nanospheres have a matrix type of structure with drugs absorbed at the surface or encapsulated inside the particle. Nanocapsules are vesicular systems in which the drug is confined to a cavity consisting of an internal liquid core surrounded by using a polymeric membrane (Fig. 2.1).

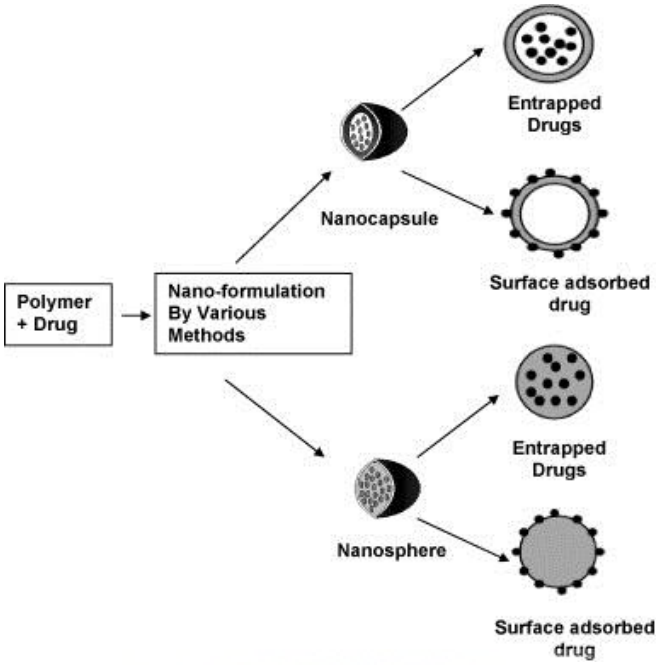

Figure 2. 1: Biodegradable NPs according to the structural organization biodegradable NPs [50]

Drugs can both be entrapped into the NPs or adsorbed on their surface. In general, fragile molecules are highly preserved from enzymatic degradation occurring in biological medium when they are entrapped in the nanocarriers[46]. In this case, their association with the drug carrier have to be determined at some stage in the preparation of the nanocapsules or the nanospheres[47]. However, if the drug is particularly inclined to degradation, which might also show up in the course of the preparation method of the drug carrier or when it is no longer an associate in the course of the preparation of the drug carrier, it can be loaded by means of adsorption on the surface of already prepared carriers[48].

Nanocapsules as active substance carriers have added benefits including high drug encapsulation efficiency due to optimized drug solubility in the core, low polymer content in contrast to nanospheres, drug polymeric shell safety in opposition to degradation factors such as pH, light and the reduction of tissue infection due to the polymeric shell[47]. Some polymeric NPs are insoluble in water at physiological temperature and pH. They swell drastically in an aqueous medium and are successful in imbibing massive quantities of water into the network structure. These NPs are additionally recognised as nanogels[49].

Nanogels are hydrogels that are at the nanoscale. These are materials with water swollen constructions composed of more often than not hydrophilic polymers. They are insoluble in water due to the presence of chemical or physical cross linkers. The physical cross linkers can be weak associations formed through Van der Waals interactions or hydrogen bonds and these

grant them network structures and physical integrity[50]. Being insoluble, polymeric hydrogel NPs can hold a massive quantity of water that not only contributes to their top compatibility but also keeps a certain degree of structural integrity and elasticity. Hydrophilic functional groups such as -OH, -COOH, -CONH2 present in the hydrogel are capable of absorbing water barring causing dissolution[51].

2.2.1 Treatment of NPs after preparation

Several types of therapy can be utilized to nanoparticle suspension after synthesis. These consist of purification, sterilization and drying.

2.2.2 Purification of nanoparticle suspension

Once nanoparticle suspensions are obtained, purification can also be further needed to remove impurities and excess reagents involved throughout preparation. Depending on the approach of synthesis, impurities encompass solvents, oil, surfactants, large polymer aggregates and residual polymers. Methods of purification include evaporation under decreased pressure, centrifugation and filtration[52].

Evaporation under decreased pressure is the most frequent method to eliminate volatile organic solvents and a section of water. This manner is usually used after acquiring suspensions with the aid of Nano precipitation, and emulsification-solvent diffusion[52].

Filtration is applied to eliminate large particles or polymer aggregates which form throughout preparation. Such purification is mainly utilized on nanoparticle suspensions designed for intravenous injection[53].

Centrifugation at low gravity force can additionally be applied to get rid of aggregates and large particles on most of the polymer nanoparticle suspensions. However, it does not guarantee the removal of all particles with a diameter above a very particular size as filtration, since NPs having an excessive density may also sediment with aggregates[54].

2.2.3 Drying of NPs

As in the case of many pharmaceutical preparations, storage of NPs as suspensions provides many disadvantages such as risk of microbial contamination, polymer degradation by using hydrolysis, physicochemical instability due to particle aggregation and sedimentation and loss of biological activity of the drug. To keep away from such problems, pharmaceutical preparations are stored in dry form. The transformation of a liquid preparation into a dry product can be accomplished by freeze-drying or spray drying approaches[55].

2.2.3.1 Freeze drying

Also recognized as lyophilization, is a very frequent method of conservation used to make sure long time period stability of pharmaceutical and biological products, preserving their authentic properties[56]. The basic principle of this technique relies upon getting rid of water content of a frozen sample by way of sublimation and desorption in vacuum. In general, freeze drying, (carried out via a freeze-drier (Fig. 2.2) can be divided into three steps: freezing of the pattern (solidification), primary drying, corresponding to the ice sublimation and secondary drying, corresponding to desorption of unfrozen water[57].

Figure 2. 2: Samples in a freeze drier [62]

2.2.3.2 Spray drying

The spray drying approach transforms liquids into dried particles under a continuous process. Nanoparticle formulations submitted to spray drying are normally aqueous suspensions and include one soluble compound introduced as drying auxiliary e.g. silicon dioxide, lactose and

mannitol. Spray-drying method includes four necessary steps: 1) atomization of the nanoparticle suspension into a spray, 2) spray-air contact, 3) drying of the spray and 4) separation of product from the drying gas [58].

2.3 Applications of polymeric NPs

Over the years, nanoparticle drug delivery systems have shown big potential in biological, clinical and pharmaceutical applications. The novel properties of these carriers propose that they will have an essential role in the biomedical field. In anticancer therapy, one of the worst challenges is the low tumour response to treatment, due to the fact of the non-specific bioavailability of administered anticancer agents. Use of NPs as transports for anticancer agents achieves bioaccumulation of drug in the target tissue. Paclitaxel and doxorubicin are examples of anticancer drugs that have been effectively encapsulated in polymeric NPs (polyalkylcyanoacrylate NPs) and used in the treatment of cancer[59].

One most important challenge with protein transport is the loss of therapeutic efficacy of the protein due to the degradation/denaturing of the protein. Insulin-loaded ALG/CNPs produced by polyelectrolyte complexation approach have been shown to provide more advantageous intestinal absorption of insulin following oral administration. The physiological effect used to be observed for extra than 18 hours per dose. Thus ALG/CNPs are promising as an oral transport system for proteins and other drugs[60].

2.4 Drug-loaded CNPs for the treatment of diseases

The model of anti-HIV microbicide tenofovir encapsulated in CNPs prepared by ionic gelation technique was reported for the first time in 2011 by Jianing Meng and co-workers. The release studies, cytotoxicity aessays and studies of interaction of the loaded NPs with mucus revealed that large CNPs have a potential of the controlled release, safe, and bioadhesive delivery system. These characteristics makes CNPs the suitable candidates for delivery of microbicide across vaginal mucus for the prevention of HIV transmission[61].

Isabel Haro and co-workers[62] reported a novel polymeric NPs covered with glycol-CS, which was successfully used to incorporate an HIV-1 inhibitor peptide, derived from GB virus C. The observation results revealed that NPs have interesting physicochemical and

morphological features that provide their mobility across the mucus, to get to the vaginal epithelium and release the peptide. However, the localization of the loaded nanopartices at the upper-layers of the epithelial mucosa considered as a key aspect, since the peptide may be released at the site where HIV transmission occurs. Calcitonin encapsulated in CNPs resulted in a pronounced hypocalcemic effect and a corresponding pharmacological availability. These data suggest that, these systems are promising and safe carriers for pulmonary peptide delivery which was investigated in rats[63],[64]. Another study using chitosan-loaded systems exhibited an important capacity to improve the intestinal absorption of the model peptide, salmon calcitonin, as shown by the significant and long-lasting decrease in the blood calcemia levels[65]. The reports suggested that polyionic coacervation process for fabricating BSA loaded CNPs offers mild preparation conditions and a clear processing window for manipulation of physiochemical properties of these NPs, which can be conditioned to be applied as control over protein encapsulation efficiency and subsequent release profile. Particle degradation did not offer a second wave of significant release because they were entrapped inside the polymer[66]

Wan Ajun and co-workers reported the CNPs loaded with aspirin and probucol for the treatment of restenosis. These NPs were prepared by ionic gelation method and loaded with the combination of aspirin and probucol under different preparation conditions. In their study they focused on the release, loading capacity and encapsulation efficiency of the drug. Even though the drug was successfully loaded into CNPs, the loading capacity and encapsulation efficiency were affected by the pH and concentration of the TPP. The release of the drug from CNPs showed a prolonged and sustained release for over 24 hours[67].

CNPS loaded with curcumin were investigated for the treatment of plasmodium yoelii infected mice. This was conducted to improve the stability and bioavailability of the curcumin [27]. The findings revealed that curcumin loaded in CNPs do not degrade rapidly when compared to the free curcumin by the time these particles were incubated in mouse plasma[68]. The uptake of the encapsulated curcumin by CNPs was much better than the free curcumin. The oral delivery of curcumin loaded chitosan-based NPs showed that they can diffuse through mucosal barrier intact[69]. The mice that were infected with plasmodium yoelii survived when treated with 1 mg of curcumin loaded CNPs. Further findings showed that loading of the curcumin in CNPs increase the chemical stability and enhance the bioavailability of the drug when fed to mice[70].

Salmon calcitonin loaded in CNPs prepared by ionic gelation technique is reported[71]. These loaded NPs were able to be absorbed into mannitol forming inhalable microparticles by spray drying process. The results suggested that loaded CNPs were released from spray dried microparticles upon exposure to lung fluid[72]. Yamamoto and coworkers studied Surface-modified dl-lactide/glycolide copolymer (PLGA) nanospheres with chitosan which were prepared by the emulsion solvent diffusion technique for pulmonary delivery of peptide. The pharmacological motion of CS-modified nanospheres loaded with elcatonin was once extended extensively in contrast with that of the unmodified nanospheres[71].

Thymoquinone loaded CNPs were successfully prepared by Sanjar Alarm et.al. A physical analysis and electron microscope screening confirmed the acceptability for intranasal administration. The invitro studies study in rats revealed that intranasal administration delivers thymoquinone to the brain rapidly and more effectively than previous methods[73]. The accumulation of loaded CNPs within interstitial spaces and delivery of the drug to the brain may be due the nano size range and the stretching of tight junctions within the nasal mucosa.

The finding also supported the potential of the loaded NPs on penetration. The studies suggest intranasal delivery of thymoquinone loaded CNPs to be a promising approach for brain targeting [74]. However, benefit-to-risk ratio and clinical details need to be found scientifically for its suitability in clinical practice in the management of Alzheimer symptoms. The encapsulation of the thymoquionone inside the CNPs showed in Fig. 2.3 was functionalized by the attachment of the carbonyl groups of the thymoquinone and amino groups of the chitosan[75]. The following structure shows the clear picture of the interaction between thymoquinone and this polymer.

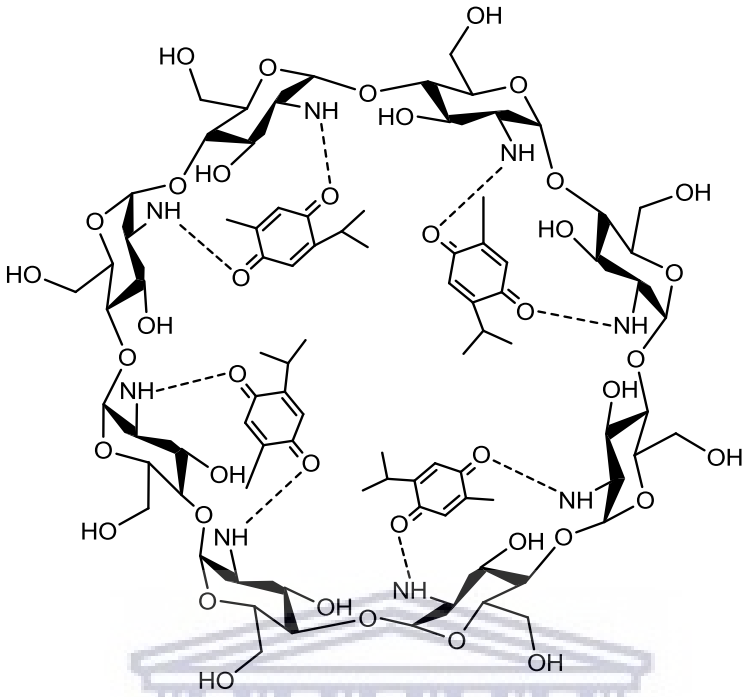

Figure 2.3: The reaction that shows the interaction between CNPs and thymoquinone

Alignic acid coated with CNPs as transport to deliver legumain DNA drug was reported. Although a number of issues needs to be considered and addressed before the application of oral DNA drug can occur. The purpose of this study was to provide the insight into a potential therapeutic strategy for the treatment of breast cancer. The findings revealed that alignic acid coated CNPs may be a safe and efficient tool for oral delivery of a DNA drug. Furthermore, a legumain DNA drug delivered orally with alignic acid coated with CNPs can effectively improve autoimmune response and protect against breast cancer in mice[76].

The nasal delivery of hepatitis B antigen in alginate coated CNPs were developed for intranasal therapy. The aim of developing these NPs was to protect the antigen from enzymatic degradation at mucosal sites[77]. Encapsulation of alginate CNPs with hepatitis B antigen, administered nasally to mice, led to the humoral mucosal immune responses. The production of systemic antibodies, predominantly the 1-type antibodies, was observed when the hepatitis B antigen captured in the particles was administered simultaneously with the adjuvant, CpG ODN, in solution[78].

Kai Zhao *et.al* investigated the delivery of Newcastle disease virus vaccine loaded CNPs for treating Newcastle disease (NDV). NDV- loaded CNPs demonstrated the advantages of live vaccines and inactivated vaccines, while compensating for their defects. Further tests on

significant mucosal immune responses after intranasal administration of NDV-CNPs in chickens showed a wide range of potential applications of NDV-loaded CNPs[79]. Curcumin loaded in different molar masses of CNPs prepared by nanoprecipitation method was studied. All the particles investigated indicated the similar behaviour showing the same morphology of the particles. The optimization of the conditions was performed to obtain a monodisperse size distribution of the loaded NPs[80]. The encapsulation of curcumin with chitosan, favored by the strong H-bonds between poloxamer and chitosan, was confirmed by the changes in particle size and zeta potential values. To add more, the resulting NPs showed high loading efficient of curcumin (99%). Finally, loaded NPs demonstrated the strong ability to interact with mucus through electrostatic forces that highlight their potential as mucoadhesive carriers for the transportation of curcumin[81].

The study of the delivery of DNA loaded in the nanocarier made of hyaluronan and chitosan was investigated by Seijo *et al*. This gene transfer system was considered as the system that is promising for the treatment of chronic diseases that affect the ocular surface. The purpose of their work was to study the efficacy and mechanism action of the DNA loaded NPs. The transfection efficiency of the loaded NPs was evaluated in a human corneal epithelium cell model followed by the investigation of the bioadhesion and internalization of the loaded NPs in the ocular epithelia of the rabbit[82]. The study on the formulation of the NPs that can be used the intranasal transport RHT has been done. The effect of different variables on NPs preparation was investigated. The encapsulation efficiency, was at 85.3 ± 3.5%, and the reproducibility of the preparations were satisfactory. They found 89.27 ± 2.672 of the RHT released in invitro tests over 24 h and those results indicated a controlled and sustained release profile of CS-RHT NPs. An improved brain uptake of CS–RHT NPs was clearly observed on the delivery from nose to brain. From these investigations it was found that RHT loaded CNPs could be a novel colloidal drug transportation system for the Alzheimer's diseases therapy via nose to brain[83].

Qun Wang and co-workers reported alignate chitosan-PLGA nano carriers, the purpose of the study was to use these NPs to deliver Ac-PLP-BPI-NH2-2 peptide as a vaccine for autoimmune ancephalomyelitis. One of the things they considered in the study was the controlled release of the peptide from the NPs during the delivery[84]. CNPs loaded with peptide in freeze dried cylinders for sexually transmitted diseases was investigated by MarziaMarciello *et.al*. In this

work, a straightforward and efficient strategy for the vaginal application and release of peptide-loaded mucoadhesive NPs was developed. This strategy essentially consists of CNPs encapsulated in suitable hydrophilic freeze-dried cylinders whereby CNPs are responsible for carrying the peptide drug and allowing adhesion to the vaginal mucosal epithelium [85]. Kim and co-workers studied a brain targeting way where the CNPs were used to carry RVG peptide to the brain. Brain-targeted delivery of drug or was not easy to achieve efficiently due to the infiltrative nature of the blood-brain barrier (BBB). In addition, the findings revealed that delivery of RVG protein to brain tissue was further limited by the size and physic-chemical properties of proteins[86]

2.5 CNPs on Drug delivery

Fu Chen and coworkers studied the FITC-BSA loaded alignate modified N-trimethyl CNPs. In their study they compared the permeability of alignate modified trimethyl CNPs with the ones that are not modified. Alignate modified NPs were able to improve the diffusion of FITC-BSA than non-modified trimethyl CNPs. It was also suggested that alignate modified trimethyl CNPs had a stronger effect on improving the transport of FITC-BSA though transcellular pathway but had more or less the same effect on enhancing the drug delivery through paracellular pathway[87].

Mesobuthus eupeus venom-loaded CNPs were investigated by Dounighi *et.al*. Loaded NPs were prepared using ionic gelation technique which employed TPP as a crosslinker. This investigation was done to see the physicochemical properties of the loaded CNPs. The release studies revealed that the release of venom from CNPs can be sustained over a long period. Therefore, the CNPs prepared via ionic gelation method appeared to be an alternative option to deliver venom peptide to its target side than other traditional adjuvant systems. [88].

In their study Yu-chuan Huang and co-workers demonstrated that spherical and mono dispersed chondroitin sulphate. CNPs can be prepared by an ionic gelation method. It was suggested that, the aggregates or NPs formation can be easily predicted by means of calculating the weight ratio of chondroitin sulphate/chitosan. There is a linear relationship between the particle size and zeta potential with the final concentration of chondroitin sulphate at a fixed chondroitin sulphate/chitosan ratio. The loading of FITC-BSA in chondroitin sulphate-CNPs exhibited a higher formation yield and a degree of concentration than chitosan TPP NPs. A high encapsulation efficiency of FITC–BSA was achieved, and the release profile of FITC–BSA from chondroitin–CNPs indicated a small burst release followed by a continued and

controlled release. Ex vivo cellular uptake studies using Caco-2 and HEK-293 cells showed that chondroitin–CNPs were endocytosed into the cells. It was concluded that, this new NPs system offers an interesting potential as a transport for hydrophilic compounds such as drugs and proteins[89].

The study of encapsulation of Najanaja oxiana (Indian or speckled cobra) venom in CNPs and investigation of physicochemical structure of NPs was conducted. CNPs were prepared based on the ionic gelation method crosslinking the TPP and chitosan. Chitosan exhibited the formation of stable cationic NPs. The increase in concentration of chitosan concentration led to the formation of aggregates with large diameter. Optimum loading capacity and encapsulation efficiency of venom at a concentration of 500 μg/ mL were achieved for low-molecular-weight (low-MW) chitosan [90]. Tacrine-loaded CNPs were prepared by Barnabas Wilson *et.al* using spontaneous emulsification method. The loaded NPs prepared by this method showed good drug-loading capacity. The *in vitro* release studies showed that after the initial burst, all the drug-loaded batches provided a continuous and slow release of the drug. Coating of NPs with Polysorbate 80 slightly reduced the drug release from the NPs. Release kinetics studies showed that the release of drug from NPs was diffusion-controlled, and the mechanism of drug release was fickian diffusion. The biodistribution of these particles after intravenous injection in rats showed that of NPs coated with 1% Polysorbate 80 altered the biodistribution pattern of NPs[91].

Ana Grenha *et.al*.in their study demonstrated the proposed technologies that are appropriate to obtain complexes between phospholipids and preformed NPs, as well as to produce microspheres that contain the referred complexes, which show the suitable properties for pulmonary delivery. The suggested phospholipids composition greatly affects the complexes physicochemical characteristics, and also suggesting that a stronger lipid/ NPs interaction occurs when a negatively charged phospholipid is incorporated in the lipid film. As a result it proceeded in a more efficient lipidic coating of the CNPs[92].

The study of the evaluation of pH sensitive CNPs was conducted by Abdallah Makhlof and co-workers. CNPs were prepared by ionic cross-linking with hydroxypropyl methylcellulose phthalate (HPMCP) and evaluated for the oral delivery of insulin. *In vitro* results revealed a superior acid stability of CNPs with a significant control over insulin release and degradation in simulated acidic conditions with or without pepsin[93]. Deng et.al loaded lysozyme in CNPs applying ionotropic gelation method in environmental friendly condition. Their main focus in

their work was specifically to check the effect of molecular weight during the delivery of lysozyme[94].

Gavin and co-workers reported the mucoadhesive vaginal tablets of acriflavine loaded chitosan microspheres. The purpose of the study was to develop the vaginal tablets that will be able to release the drug in a sustained and prolonged manner. These tablets were prepared by spray drying method using different ratios of drug to polymer weights. The *in vitro* adhesion tests, carried out on the same formulation, showed a good adhesive behaviour [95]. Tzeyung *et.al.* Loaded Rotigotine in CNPs, fabricated and optimized these encapsulated NPs for nose to brain delivery. Data obtained from *in vitro* release kinetics exhibited the prolonged release of the drug from the formulation. No signs of toxicity or structural damage was seen upon histopathological examination of nasal mucosa[96]. The study on new formulations of CMCS/AA hydrogels with varying composition of Carboxymethyl chitosan,acrylic acid, and ethylene glycol dimethacrylate (EGDMA) that were prepared by free radical polymerization technique using benzoyl peroxide as catalyst. Since the bioavailability of 5-FU through the oral route is very limited owing to its rapid metabolism and clearance from the general circulation. The investigation was aimed at increasing the bioavailability of 5-FU via smart hydrogels and at investigating their potential in delivering 5-FU to target colon cancer[97].

Vanic and co-workers developed the optimized chitosan-coated liposomes to ensure the efficacy and efficient topical therapy to avoid systemic absorption of the clotrimazole. This drug was chosen as a therapy for pregnant patients who were suffering from vaginal infections. Mucoadhesive polymer chitosan was selected as a candidate to prolong system's retention at the vaginal site and act on biofilms responsible for high recurrence of infections[98]. Perioli *et.al*. Investigated the topical administration of the antibacterial metronidazole. In their study they focused on the representation of the most common therapy in the treatment of bacterial vaginosis. It was confirmed that this kind of delivery system is suitable for formulating metronidazole for topical application representing a good alternative to traditional dosage forms for vaginal topical administration[99].

2.6 Investigation on stability of loaded chitosan nanoparticle at low pH

On other reports CNPs were coated with poly acrylic acid (PAA) to improve their stability at low pH conditions[100]. Makhlof *et.al* reported the stability of CNPs at low pH when crosslinked with trypolyphosphate (TPP) versus CNPs that are crosslinked with hydroxypropyl methyl cellulose phthalate (HPMSP), chitosan/HPMSP NPs displayed excellent stability[93].

Zhong *et.al* prepared cyclodextrin/chitosan nanoparticle for delivery of ovalbumin, the results suggested that OVA loaded CNPs had been more stable than CNPs without OVA in acidic medium, probable due to stabilization impact of protein corona thru OVA covered on the surface of NPs with the aid of electrostatic interaction, which can guard chitosan from degradation by gastric acid [101].

In our study we are focusing on the synthesis of CNPs via ionic gelation method in different concentrations of Sodium TPP, then optimize the NPs. After the optimization, the best NPs will be chosen as a vehicle to proceed and carry the Kn2-7 which has been identified to have a high level of anti-HIV activity and Hβd-3 which has been reported to have similar properties as Kn2-7. These peptides will be transported through vaginal mucus to reach the target sites and kill HIV. The purpose of using chitosan as a vehicle, is to increase the residence time of the peptide in the mucosal tissue by protecting it from the harsh conditions caused by pH, to overcome the mucus barrier and also to decrease the side effects. Owing to the amino groups on chitosan polymer chains, it is protonated and easily dissolved at low pH, so to prevent this protonation we coat peptide loaded CNPs with poly acrylic acid to ensure the stability of these NPs in acidic conditions.

CHAPTER 3

MATERIALS AND METHODS~~EXPERIMENTAL SECTION~~

3.1 Chemicals

The Kn2-7 and Hβd-3 peptides were purchased from GL Biochem (Shanghai) China. The medium molecular weight Chitosan (degree of deacetylation of 85%), phosphathe buffer saline pH (7.4) and sodium TPP were purchased from Sigma Aldrich.Poly (acrylic acid) 1800 Da was purchased from DLD. All other reagents used were of analytical grade.

3.2 Procedure for synthesis of CNPs

CNPs were prepared in a vial according to the method described by Aminu Kura *et.al*[102] with few changes. Chitosan solution was prepared by dissolving 2% of a polymer in 1% v/v acetic acid. The solution was stirred at room temperature for 10 minutes. Sodium TPP solution was prepared by deionized water at concentrations of 0.3 mg/ml, 0.5 mg/ml, 1mg/ml, 3mg/ml and 5mg/ml, the solution was added dropwise to the chitosan solution while stirring. Chitosan TPP in fig 3.1 was formed, the reaction was sonicated for 20 minutes, and remaining suspension was centrifuged for 30 minutes at 14.5 rpm and dried at room temperature.

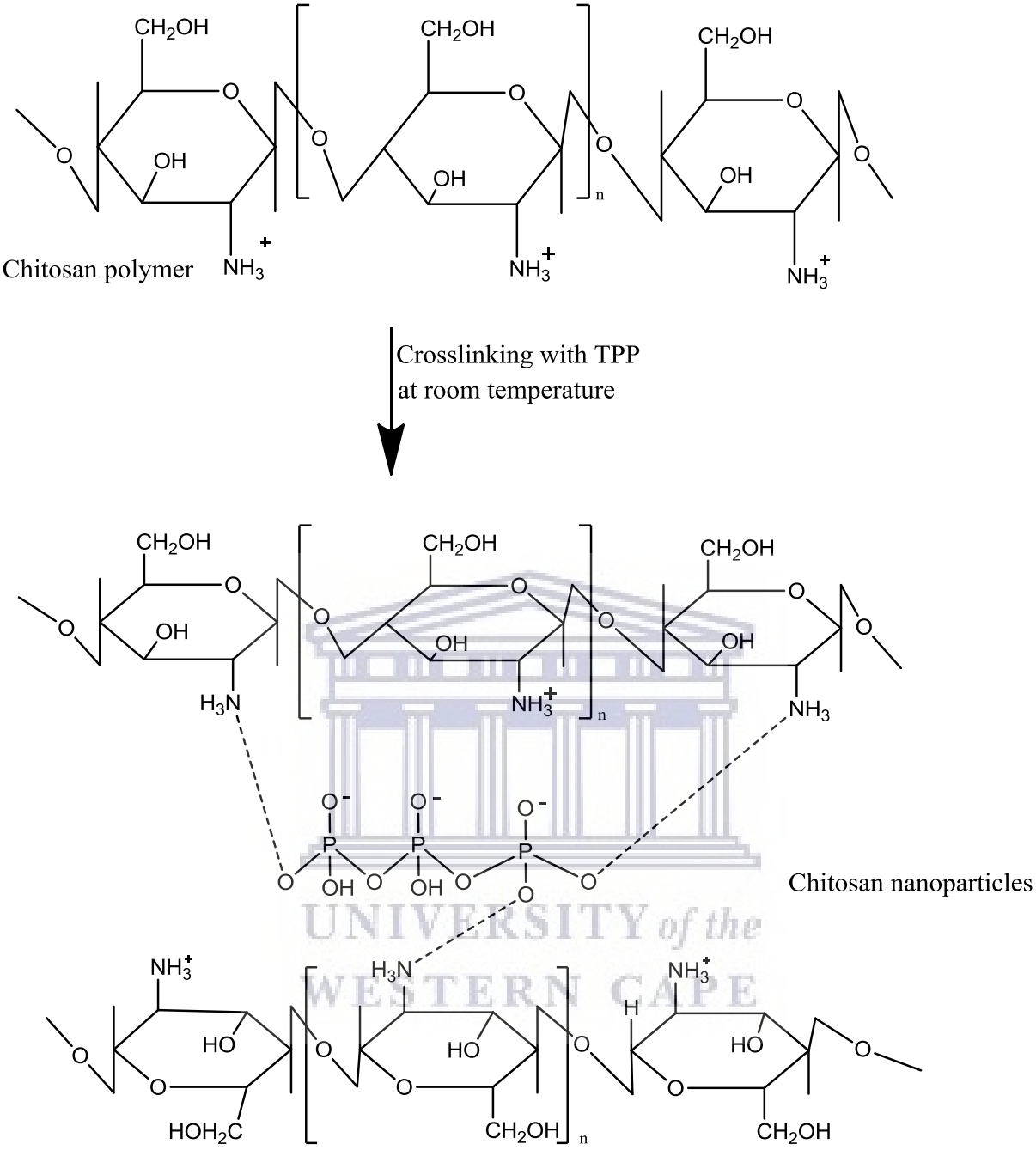

Figure 3. 1: Reaction for the synthesis of CNPs by ionic gelation

3.3 Synthesis of Kn2-7-loaded CNPs

Chitosan solution (0.5% in 1% v/v acetic acid solution) was stirred at room temperature for 10 minutes. The peptide (1mg/ml) was added to the solution and the solution was left stirring for 15 minutes. The TPP solution was prepared by deionized water at concentration of 3mg/ml, it was then added to the Kn2-7/Chitosan solution drop wise using a syringe to form Kn2-7 CNPs explained in Fig 3.2. After 30 minutes the solution was sonicated for 20 minutes, centrifuged, washed and freeze dried.

3.3.1 Synthesis of Hβd-3-loaded CNPs

Chitosan solution (0.5% in 1% v/v acetic acid solution) was stirred at room temperature for 10 minutes. The peptide (1mg/ml) was added to the solution and the solution was left stirring for 15 minutes. TPP solution was prepared by deionized water at concentration of 3mg/ml, the TPP solution was then added to the Hβd-3 /Chitosan solution dropwise using a syringe. After 30 minutes the solution was sonicated for 20 minutes, centrifuged, washed and freeze dried.

3.3.2 Coating of Kn2-7 and Hβd-3-loaded CNPs with Poly(acrylic acid) PAA

The coated loaded NPs were prepared using layer by layer method reported by Yukun *et.al*[100]. 10 mg/ml of PAA was prepared by adding 10mg of PAA in 1 ml of double deionized water. The sample peptide loaded CNPs was added in PAA solution and stirred for 1 hour, then centrifuged for 30 minutes at 14.5 rpm. These NPs were redispersed in milliQ water by ultra-sonication of 45 kHz for min and freeze dried.

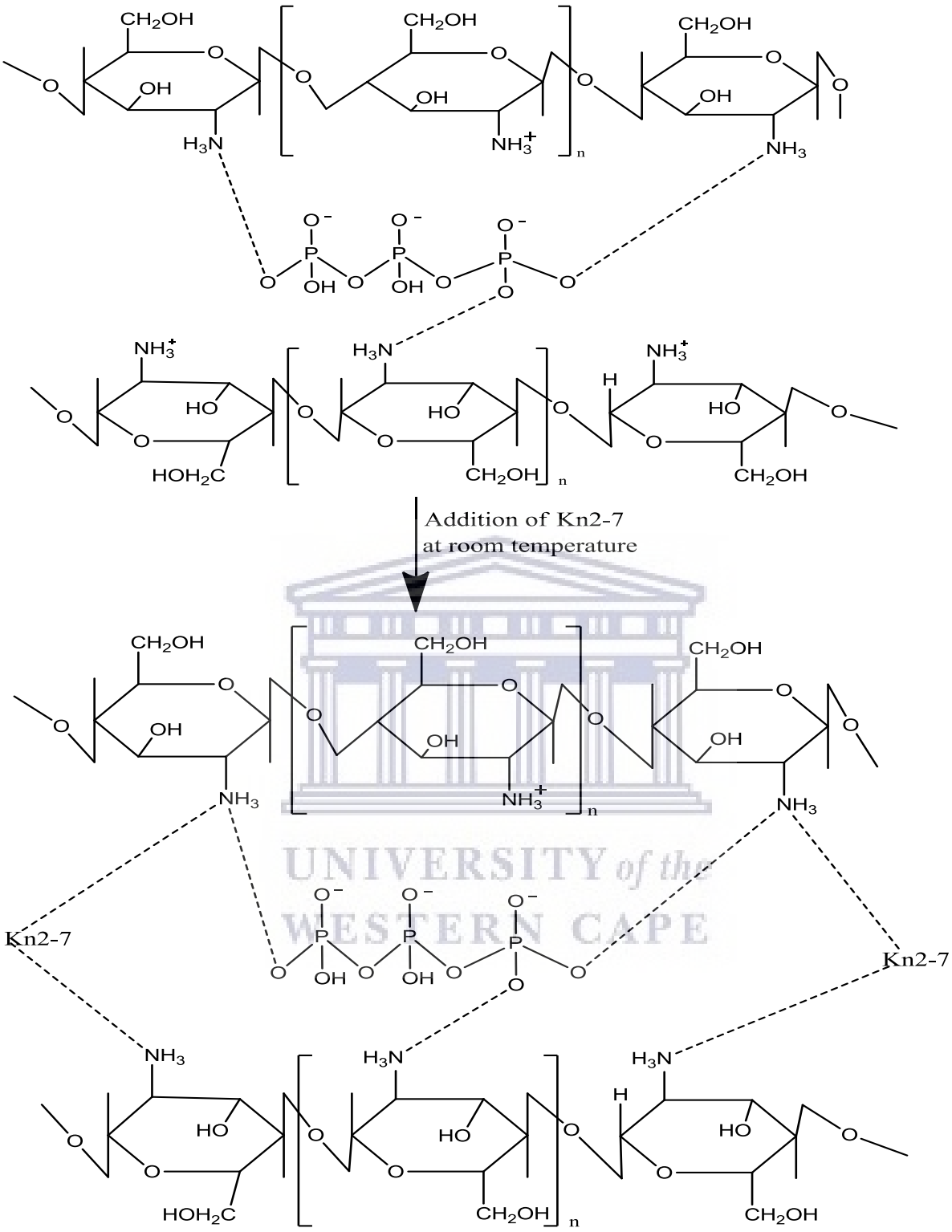

Figure 3. 2: The ionic interaction of CNPs with TPP and Kn2-7 peptide

3.4 Characterization techniques

The morphological characterization of free chitosan and Kn2-7 CNPs were investigated by high resolution transmission electron microscope (HRTEM) (Philips 400®, 80 kV, The Netherlands) and scanning electron microscopy (SEM).The particle size, size distribution [polydispersity index (PDI)] and zeta potential of particles were measured by Zetasizer (Malvern Instruments, UK), based on the dynamic light scattering (DLS) technique. The structural features of NPs were estimated by FTIR (Fourier transform infrared) (FTIR- 410® Jasco Colchester, United Kingdom), using KBr pellets. The absorption wavelengths of the NPs were obtained by ultra violet visible spectrum (UV-vis).

3.4.1 The morphological characterization

3.4.1.1 High Resolution Transmission Microscopy

HRTEM (Fig 3.3) is an ultimate tool that is used for the characterization of nanomaterials. This tool has been mostly applied for imaging, diffraction, and chemical analysis of solid and liquid materials. For example Carbon nanotubes were first identified by HRTEM. Analysis of such tubular structures need extensive development of electron microscopy. In this instrument conventional imaging and diffraction are the two most powerful methods in characterizing the phase structure and phase transformation of inorganic materials[103]. Most of the researches which involved the use of this instrument have been conducted to investigate the effect of particles size and its properties[104]. The sample is analysed in this technique by bombarding it with a focused beam of electrons under a high vacuum and accelerating voltage, in order to enable the sample to collect all the information using its high-resolution and high magnification imaging ranging at nanoscale dimensions. High resolution transmission electron microscopy also provides images of atomic resolution crystal lattice and chemical information by strategically focusing the electron probe of the HR-TEM. The image in the figure below shows the illustration of the High resolution transmission spectroscopy.

Figure 3. 3: HRTEM diagram [111]

3.4.1.2 Scanning electron Microscopy

This is a technique used for providing images of external morphology that are the same as those accessed by human eye. The images are obtained by impinging a finely focussed beam of electrons on the surface of the solid sample. The beam of electrons is scanned throughout the sample in a raster scan by scan coils. When electric current is directly passed through a coil-wound electric wire, a rotationally-symmetric magnetic field is formed and a lens action is produced on an electron beam to make a strong magnetic lens with a short focal length. It is necessary to increase the density of the magnetic line as shown in Fig. 3.4, the external parts of the coil are surrounded by yokes so that part of the magnetic field leaks from a narrow gap. A portion with a narrow gap, called "pole piece," is fabricated with a high accuracy. The main feature of the magnetic lens is that when you change the current passing through the coil, the strength of the lens is also changed[105].

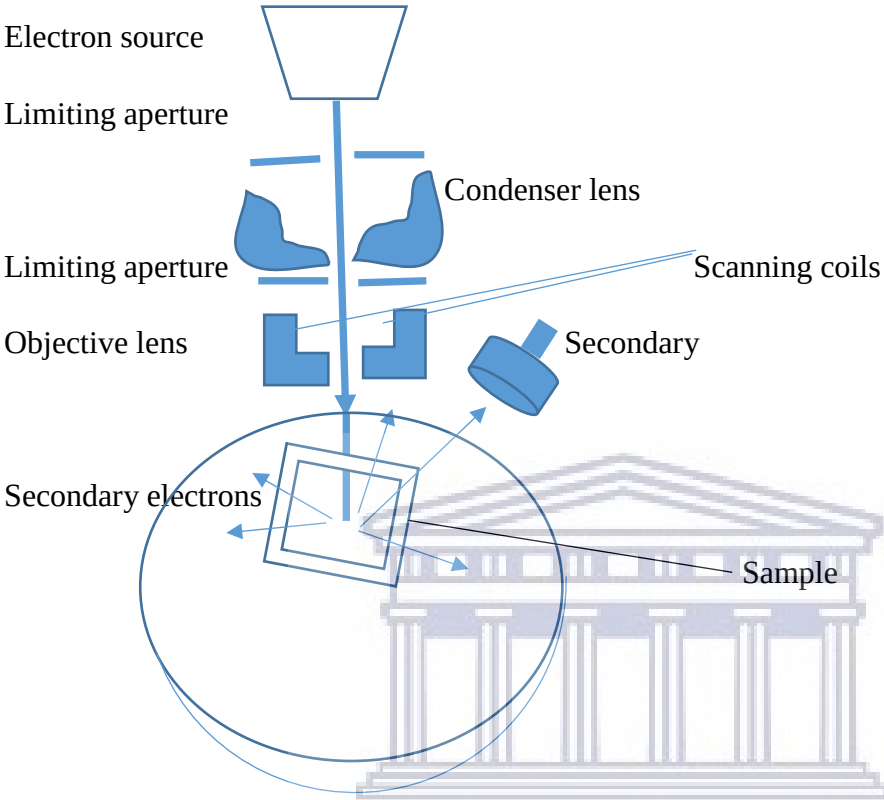

Figure 3. 4: Schematic diagram of SEM [113]

3.4.1.3 Dynamic Light scattering

The Dynamic light ~~S~~cattering is the method where the ~~of~~ particles are scattered by light. This technique is also known as photon correlation spectroscopy and quasi-elastic light scattering. It is a powerful method used for probing solution dynamics and measuring particle sizes. The size information can be obtained by dynamic light scattering technique in a few minutes for particles with diameters randing from nanometres to micrometres. DLS method involves the measuring of the Doppler broadening of Rayleigh scattered light as a result of Brownian motion of particles. The sample in the DLS experiment is illuminated by a single wavelength laser beam. The Doppler width in dynamic light scattering is measured by using the optical mixing or light-beating techniques to translate frequencies to frequencies that are near to zero hertz. DLS instrument show in Fig. 3.5 consists of a laser source, sample cell, a photo detector and a computer with an autocorrelation.

Figure 3. 5: Image of DLS spectrometer [114]

3.4.2 Ultraviolet Visible Absorption Spectroscopy

To understand why some compounds are coloured and others are not and to determine the relationship of conjugation to colour, we must make accurate measurements of light absorption at different wavelengths in and near the visible part of the spectrum. The energies noted above 200nm are sufficient to promote or excite a molecular electron to a higher energy orbital. Consequently, absorption spectroscopy carried out in this region is sometimes called "electronic spectroscopy". The diagram below shows the various kinds of electronic excitation that may occur in organic molecules. In all of the six transitions expected, only the two lowest energy ones are achieved by energies available in the 200-800nm spectrum.

As a rule, energetically favoured electron promotion will be from the highest occupied molecular orbital (HOMO) to lowest unoccupied molecular orbital (LUMO), and the resulting species is said to be an excited state Fig 3.6. An optical spectrometer records the wavelength at which absorption occurs, together with the degree of absorption in each wavelength. The resulting spectrum is presented as a graph of absorbance (A) versus wavelength.

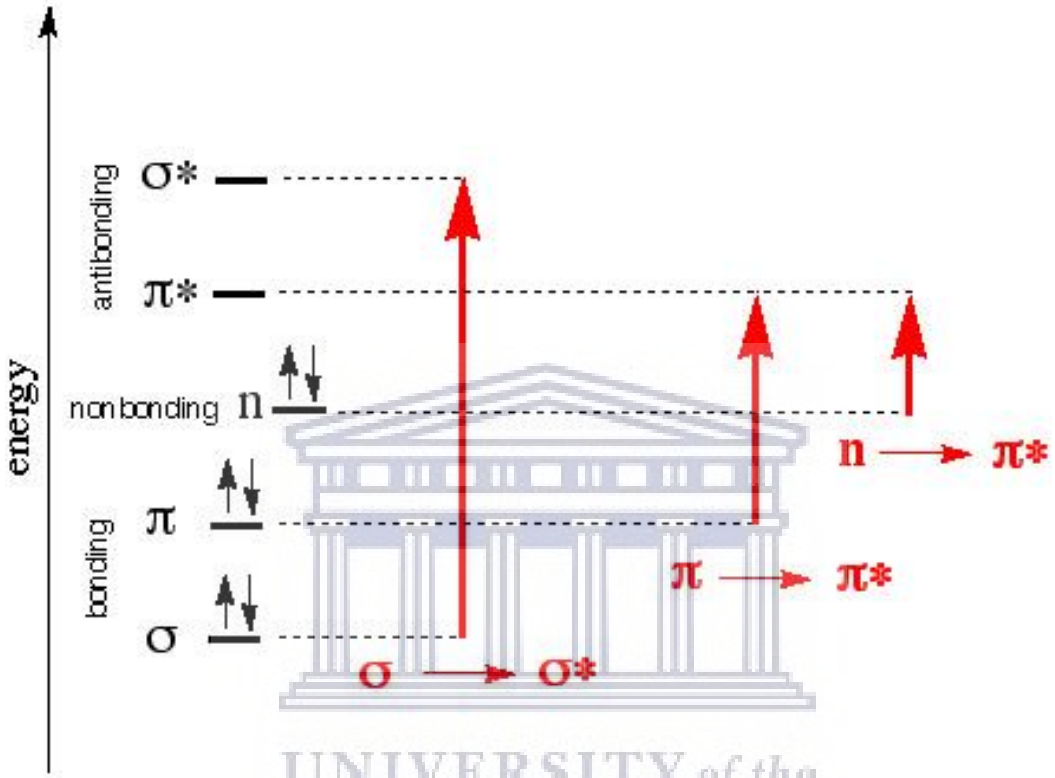

Figure 3. 6: Diagram illustrating the electron excitation [115]

The picture in Fig. 3.7 is a diagram of the components of typical double beam spectrometer. A beam of light from UV/visible light source is separated into its component wavelengths by a prism or diffraction grating. Each single wavelength beam in turn is split into two equal intensity beams by a half mirrored device. One beam, the simple beam, passes through a small transparent container (cuvette) containing a solution of the compound being studied in a transparent solvent. The other beam, the reverence, passes through an identical cuvette containing only a solvent. The intensities of these light beams are then measured by electronic detectors and compared. The intensity of the reference beam, which should have suffered little

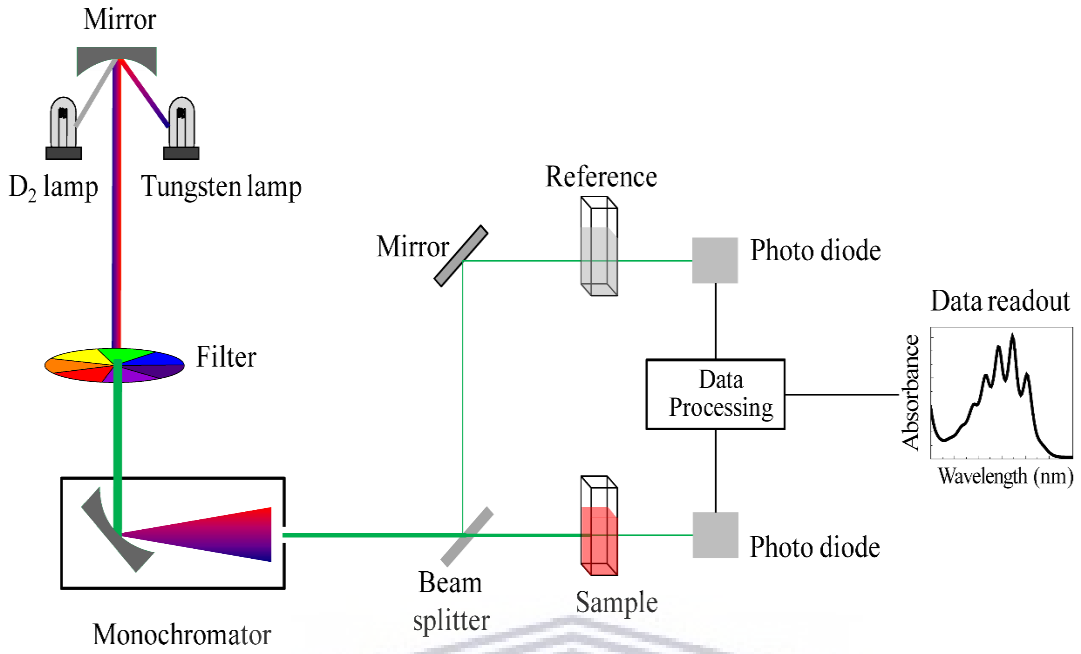

Figure 3. 7: Illustration of UV vis diagram [116]

or no light absorption, is defined as I_0.the intensity of the beam is defined as I. The spectrometer can be operated manually or programmed to automatically scan all component wavelengths.

3.4.3 Fourier Transform Infra-red Spectroscopy

FTIR is a characterization technique used to determine the chemical make-up of a compound. It exposes a chemical solution to light in infrared range or heat lamp region of the electromagnetic spectrum. A detector in fig 3.8 then measures the amount of light absorbed by the solution and records the amount absorbed by the spectrum. The infrared region of the electromagnetic spectrum is used because the molecules vibrate with energies in the infrared region. This vibrational motion is quantized and infrared radiation can promote transition between vibrational energy levels.

When energy of infrared radiation from the instrument matches the energy of the vibration of a molecule in the sample, radiation is absorbed. In this regard, the frequency in wavenumbers (cm^{-1}) of the infrared radiation matches the frequency of the vibration[106].

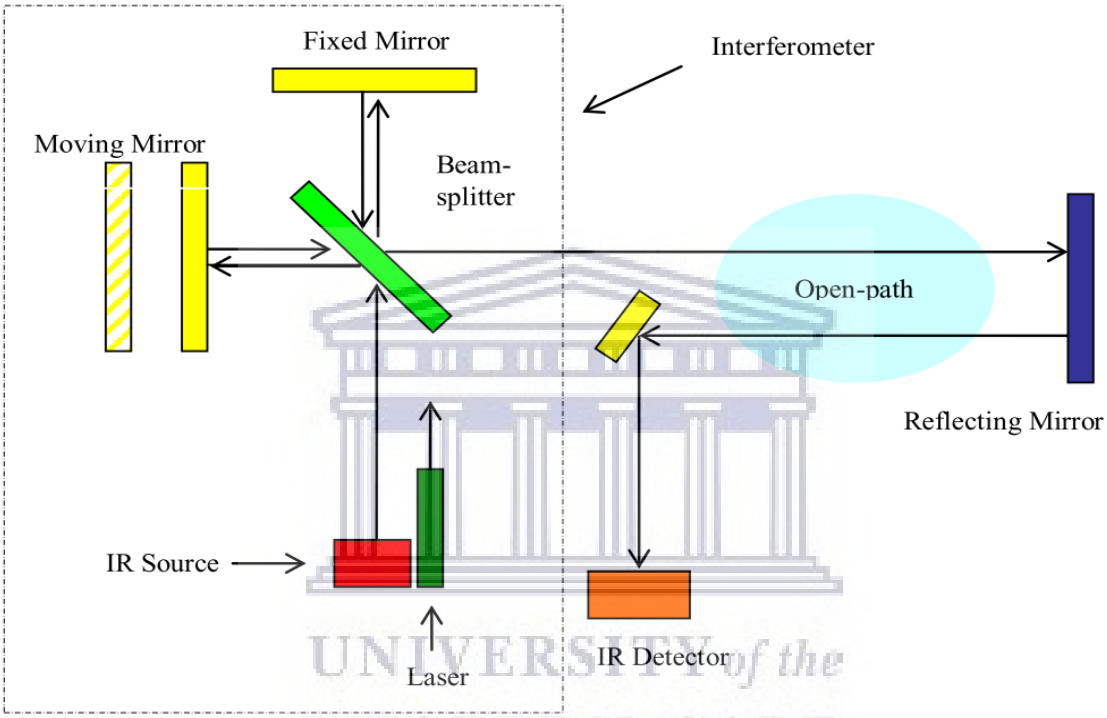

Figure 3. 8: Schematic diagram of FTIR [118]

3.5 Encapsulation efficiency (EE %) and Loading capacity (%) of NPs

The encapsulation efficiency and loading capacity of the NPs were determined by the separation of NPs from the aqueous medium containing free Kn2-7 peptide by cold centrifugation (Hitachi Centrifuge) at 14500 rpm for 1 hour. The amount of free Kn2-7 in the supernatant was measured by UV-Visible Spectrophotometer (Perkin Elmer Lambda 25) at 210 nm. The Kn2-7 and Hβd-3 in different concentrations of TPP loading capacity (LC) [102] of the NPs was calculated as follows.

$$\text{Loading capacity\%} = \frac{\text{Total peptide} - \text{free peptide}}{\text{NPs weight}} \text{ x}100$$

And the encapsulation efficiency was determined by the following equation[102]:

$$\text{Encapsulation efficiency \%} = \frac{\text{Total peptide amount} - \text{free peptide}}{\text{Total peptide amount}} \text{ x}100$$

3.6 Stability test of peptide loaded CNPs

The freeze dried NPs after characterizations were exposed in different buffer conditions. 0.5 mg of the sample was added in PBS pH 7.4 the readings were taken by qubit at time zero and recorded, the solution was further incubated for 24 hours followed by qubit reading. Another 0.5 of the same was added in PBS at pH 6.0, sonicated and the readings were taken after and recorded. The pH of PBS was reduced by 1% acetic to 3.44-3.96, 0.25 of the sample was added in the PBS, vortexed and incubated for 24 hour and the readings were taken before and after the action.

3.7 Evaluation of antibacterial activity of Kn2-7 peptide and KCP NPs

3.7.1 Assessing the growth kinetics of *S. aureus* in acidic medium

S. aureus was cultured in normal Luria-Bertani (LB) at pH 7.4 (high) and acidic LB at pH 3.8 (acidic) for 24 hours, the growth rate was assessed by measuring absorbance at OD600nm every hour for the first 6 hours and at 24 hours.

3.7.2 Determining the MIC of KCP NPs and KN2-7 peptide

The Minimum Inhibitory Concentration (MIC) was determined by a broth micro dilution[15]. The MIC for Kn2-7 peptide was evaluated only in pH 7.4 media. PAA coated CNPs loaded with Kn2-7 and Kn2-7 peptide were serially diluted in acidic and normal MH broth in a 96 well plates, *S. aereus* was added on each well. For the CNPs the dilution started from 25 – 1.56µg/mL n and the peptide concentration started from 50 – 3.13 µg/mL Ampicillin was used as a positive control and untreated cells as a negative control. The turbidity of the bacterial suspension was visually assessed after 24 h incubation at 37 °C as an indication of bacterial growth and confirmed by a plate reader (POLARstar Omega BMG LABTECH reading at OD 600nm). The lowest concentration that inhibited the visible growth of bacteria was recorded as the Minimum Inhibitory Concentration (MIC).

CHAPTER 4

RESULTS AND DISCUSSION

4.1 Dynamic light scattering

~~For measurement of the Zeta Potential, the NPs were placed in specific cuvettes with lateral electrodes. To perform this analysis, 0.25 mg of each loaded and unloaded CNPs in different concentrations of TPP were used. It was dispersed in 1000µL of double deionized water and then placed in specific cuvettes to measure the Zeta Potential and size of the NPs. Ten races per minute were performed in the Zetasizer (Malvern Instruments, UK).~~

The light scattering data and ζ-potential of Kn2-7-loaded NPs as a function of peptide concentration are given in Table 4.1. The mean particle size of the free CNPs at concentrations of 0.3 mg/ml, 1 mg/ml and 3mg/ml of TPP was found to be 327 nm, 416nm, and 382 nm. This is in agreement with the results obtained by Bodnar and co-workers who observed the CNPs at the average hydrodynamic diameter of single NPs between 290 and 340 nm[107]. The sizes we obtained were relatively larger but in the same range with the results that were previously reported by Wen Fen *et.al*. who prepared CNPs by ionic gelation method and obtained the optimized NPs from the DLS at a diameter of 138 nm [108]. ~~W~~whereas, During the loading of Kn2-7 peptide, the percentage amounts of chitosan were decreased from 2% to 0.5% to check the influence of chitosan amounts in the size of the NPs. Similarly, we observed a decrease in the size of the NPs in the DLS. Table 4.1 shows all the details about the different sizes among all the concentrations that were measured in both the free and loaded chitosan nanoparticle. As shown in Table 4.1(appendix, Fig.1 a-b, the PDIs of unloaded NPs were between 0.293 and 0.592, which showed that the particles size was well controlled with a narrow dispersity. Those of the loaded NPs were between 0.365 and 0.501, which also indicates that the NPs were monodispersed. The Zeta potential of the Kn2-7CNPs that were crosslinked by 0.3 mg/ml TPP was very poor for loaded and unloaded CNPs that were the clear indication that these NPs are not stable. The 1 mg/ml TPP Kn2-7 CNPs Zeta potential showed excellent results by increasing from +24.9 mV to + 54.3 mV, from these results it was concluded that these NPs can be made a first priority for drug delivery. From the literature it was reported that NPs with Zeta potentials close to +30 or -30 Mv, or above are the most stable NPs. From our results on table 1, the results for 1 mg/ml and 3mg/mlTPP show the stable NPs. Our PDI and Zeta potential were not that different from the ones that were previously reported in the literature.

Table 4. 1: Particle size, polydispersity index and Zeta potential of medium molecular weight CNPs and peptide-loaded NPs.

TPP Concentration (mg/ml)	% Chitosan		Particle size (nm)		Polydipersity Index		Zeta potential	
	- peptide	+ peptide	- peptide	+ peptide	- peptide	+ peptide	- peptide	+ peptide
0.3	2	0.5	327	495.0	0.592	0.501	9.61	15.9
1	2	0.5	416	289.4	0.540	0.341	24.9	54.3
2	2	0.5	382	340.2	0.293	0.365	23.9	46.6

Abbreviations: ND- not determined, CNPs- CNPs. Kn2-7 peptide concentration 0.5 mg/ml.

The given data on table 4.2 (appendix, Fig.1(c-d) gives the information about the size, polydispersity index (PDI) and Zeta potential of free chitosan and beta-defensin 3 loaded CNPs. The Hβd-3 CNPS-1 mg/ml TPP shows the most stable NPs at PDI of 0.341 and Zeta potential of 67.7, followed by 0.3 mg/ml and 3 mg/ml loaded NPs. In this case all the NPs revealed the best stability from both the Zeta potential and polydispersity index.

Table 4. 2: Particle size, polydispersity index and Zeta potential of medium molecular weight CNPs and peptide-loaded NPs.

[TPP] (mg/ml)	% Chitosan		Particle size (nm)		Polydipersity Index		Zeta potential	
	- peptide	+ peptide	- peptide	+ peptide	- peptide	+ peptide	- peptide	+ peptide
0.3	2	0.5	327	533.2	0.592	0.567	9.61	54.2
1	2	0.5	416	753.7	0.474	0.341	24.9	67.7
2	2	0.5	382	613.7	0.293	0.528	23.9	53.9

Abbreviations: ND- not determined, CNPs- CNPs. Beta-defensin peptide concentration 0.5 mg/ml.

4.2 UV-vis

For this analysis, free chitosan nanoparticle, peptide and the loaded NPs obtained were added in a cuvette diluted with 1% acetic acid, put in the cylindrical sample port of the spectrometer and the reference was put on the second cylindrical port (Thermo, model NICOLET evolution 100) and analysed between 190 -800nm.

4.2.1 CNPs

The absorption of CNPs and loaded CNPs was observed by UV-Vis spectrum. Fig. 4.1 shows three different peaks of CNPs from different concentrations at 272nm wavelength. When free CNPs were characterized by uv visible spectrum, the absorption peaks were very poor agreeing with the results of Jolanta et.al[109]. But we also noticed that when chitosan was crosslinked with 1mg/ml the absorption was poor but the peak was more intense than when it was crosslinked with 0.3mg/ml and 3mg/ml. The intensity of the NPs at 1mg/ml was referred to the previous reports by Megha and co-workers[110] who reported UV-vis of CNPs with a sharp peak at 226nm in 2018 after the NPs were kept for 20 days. They also reported about the paper that was published in 2014 which the reporters got 201 nm peak for CNPs. Whereas Krishnaveni et.al reported a peak at 310 nm of CNPs mixed with silver[111].

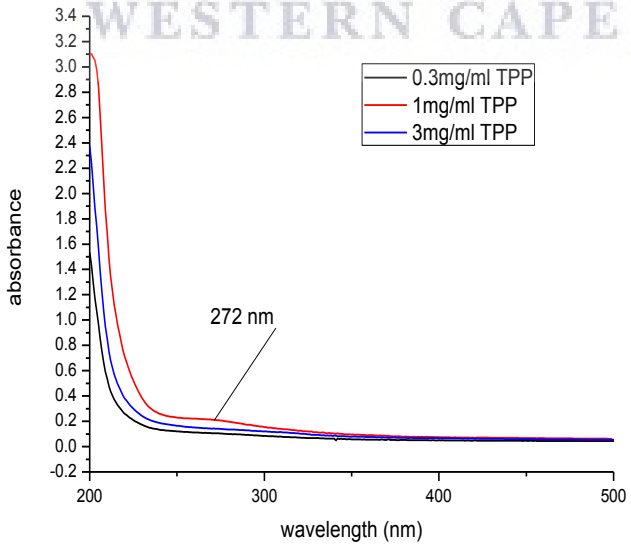

Figure 4. 1: UV-vis results for Free CNPs spectra

4.2.2 Kn2-7 CNPs

After the loading of the peptide in the chitosan nanoparticle Fig. 4 .2 the absorption peak shifted from 272 nm to 195 nm for 0.3 mg/ml, 206 for 1 mg/ml TPP Kn2-7 CNPs and 211nm for 3mg/ml TPP Kn2-7 CNPs. The peaks for Kn2-7CNPs were more intense when compared to the free CNPs which was also reported in an article by Martines *et.al*[112] . The peak obtained at 195 nm for 0.3 TPP Kn2-7 CNPs indicates that, the NPs at that concentration are optically inactive or the less concentration of TPP in CNPs resulted in less absorption. The other two peaks from 1mg/ml TPP and 3mg/ml TPP that were obtained at 206 nm and 211 nm showed that the more concentration of TPP added result to more intensity of the peaks in the uv-visible spectrum . From the peaks we obtained it can be concluded that the peptide was successfully loaded in CNPs because the Kn2-7 peptide absorbs in the same region as loaded NPs**.**

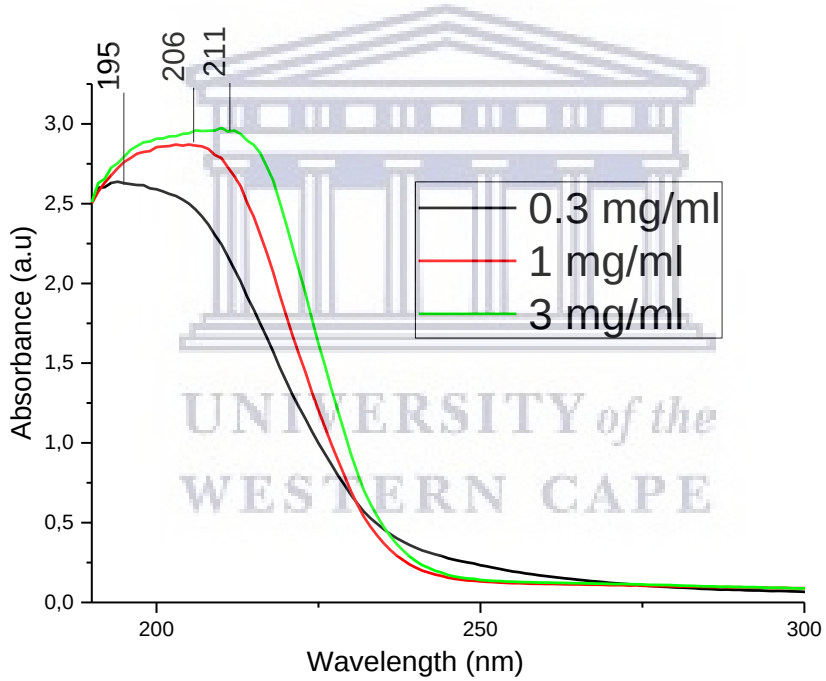

Figure 4. 2: UV-vis results for Kn2-7CNPs

4.2.3 Hβd-3 CNPs

After the loading of the peptide in the chitosan nanoparticle Fig. 4.3 the absorption peak shifted from 272nm to 194 nm, 200 nm for both 0.3 and 1 mg/ml TPP HβD-3 CNPs and 203nm for 3mg/ml TPP Hβd-3 CNPs. The peaks for Hβd-3 loaded CNPs were more intense when compared to the free CNPs this was also reported by Honary et.al[114] .We obtained a peak at 194 nm for 0.3 TPP Kn2-7 CNPs which indicates the NPs at that concentration are optically

inactive or the less concentration of TPP in CNPs resulted in less absorption. The other two peaks 1mg/ml TPP and 3mg/ml TPP were obtained at 203 nm and 200 nm attributed to the change in the concentration of TPP. From the peaks we obtained it can be concluded that the peptide was successfully loaded in CNPs because Hβd-3 peptide also showed the absorption in the same region.

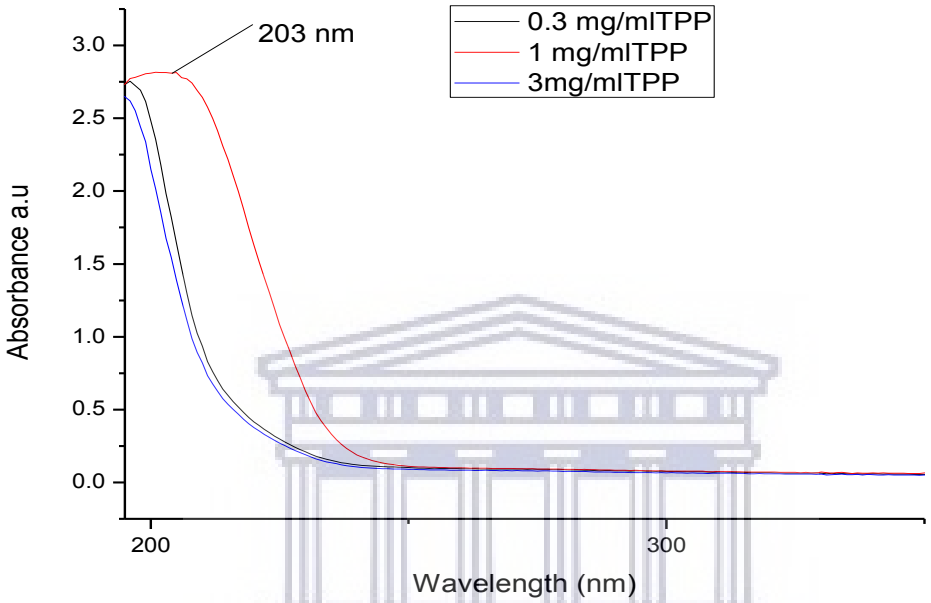

Figure 4. 3: UV-vis results for Hβd-3CNPs

4.3 FTIR

The raw materials, purified chitosan, the free and loaded CNPs obtained were mixed with potassium bromide (KBr), macerated and pressed for the formation of the pellets. The spectra were obtained in the infrared region of 400–4000cm^{-1} (PerkinElmer, model SPECTRUM Two, series 95058, software PerkinElmer spectrum, version 10.4.00, with a scanning number of 20 and resolution 4 cm^{-1})

The FTIR spectra of Hβd-3 and Kn2-7 where obtained from all the three concentrations of the cross linker TPP as shown in the appendix Fig.2 (a-i) page 85-93, but in our discussions we only focused on 1 mg/ml TPP spectra for discussions because they show excellent results than the other concentration. To add more, these spectra overlap, so this gives us more reasons to choose a spectrum for the next discussion of the FTIR results.

4.3.1 FTIR of Kn2-7 CNPs

In the discussions we selected the spectrum of 1mg/ml TPP Kn2-7 CNPs because they are the ones that have shown excellent stability and monodispersity in previous characterizations. The evidence of the interaction of chitosan with TPP in CNPs was obtained through FTIR data. Upon the formation NPs (appendix, Fig.2 b-f), four main peaks were observed that can be linked to the O-H and N-H stretching at 3278cm^{-1}, C-H stretching at 2945 cm^{-1}. The amide 1 peak at 1645 cm^{-1} which clearly shows the involvement of amine groups in electrostatic interaction with phosphate groups of tripolyphosphate(TPP), the –NH_2 bending vibration at 1553 and anti-symmetric stretching of C-O-C and C-H stretching at 1150 cm^{-1} and P=O at 1209[113].In peptide-loaded CSNPs (refer to table 4.3, appendix Fig 2a), the band at 3278 cm^{-1} in blank CNPs that corresponds to the O-H stretching, has disappeared and a new peak appeared at a higher frequency in 3400 cm^{-1} which corresponds to the formation of new amide formation from the ionic interaction between the carboxylic groups of Kn2-7 and amino groups of the chitosan. The intensity of amide I band at 1553 cm^{-1} (in CSNPs) has decreased and slightly shifted to a lower wavenumber (1541 cm^{-1}); this may be attributed to the electrostatic interactions between the negative charges of kn2-7 peptide and positive charges of chitosan [78].

The band at 1344 cm^{-1}(-CH3 antisymmetric deformation) underwent a shift towards 1381 cm^{-1} after peptide loading, showing that peptide fraction had been incorporated into CNPs Other reports confirmed the presence of the peptide by observing the shifts of (-CH3 antisymmetric deformation) which underwent a small shift towards 1484 cm^{-1} after peptide loading. Furthermore, the peak of 1413 cm^{-1} (C-H bending) which was present in the pure peptide spectra, appeared again in the spectra of peptide-containing CNPs, showing that peptide fraction had been incorporated into CNPs [70]. In addition, the band at 703 cm^{-1} was found in peptide-loaded NPs, most likely originated from -C-H rocking of CH_2 of the amino acid residues in peptides.

Table 4. 3: FTIR results for CNPS, Kn2-7 CNPs.

Wavenumber		Vibration	Functional groups		Shift
CNPs	**Kn2-7CNPs**		**CNPs**	**Kn2-7 CNPs**	
3278	3400	Stretching vibration	O-H,N-H	O-H, N-H	Yes
-	2929	Asymmetric stretch	-	C-H (alkane)	New peak
1645	1643	Bending vibration	Amide 1	Amide 1	Yes
1553	1540	Carbonyl stretch	Amide II	Amide II	Yes
1344	1381	Bending	-	C-H (CH_3)	Yes
1209	1226	Stretching vibrations	P=O	P=O	Yes
-	703	Rocking	-	C-H (C-H_2)	New peak

4.3.2 Hβd-3 CNPs FTIR data

The spectrum shows the Hβd-3CNPs in the same concentrations of TPP as of the Kn2-7CNPs. In HβD-3 loaded CSNPs (refer to table 4.4), the band at 3278 cm^{-1} in blank CNPs that corresponds to the O-H stretching, has disappeared and a new peak appeared at a higher frequency in 3400 cm^{-1} which corresponds to the formation of new amide formation from the ionic interaction between the carboxylic groups of Hβd-3 and amino groups of the chitosan. The intensity of amide I band at 1553 cm^{-1} (in CSNPs) has decreased and slightly shifted to a lower wavenumber (1541 cm^{-1}); this may be attributed to the electrostatic interactions between the negative charges of Hβd-3 peptide and positive charges of chitosan[115].The band at 1344 cm^{-1}(-CH_3 antisymmetric deformation) underwent a shift towards 1381 cm^{-1} after peptide loading, showing that peptide fraction had been incorporated into CNPs Other reports confirmed the presence of the peptide by observing the shifts of (-CH_3 antisymmetric deformation) which underwent a small shift towards 1484 cm^{-1} after peptide loading. Furthermore, the peak of 1413 cm^{-1} (C-H bending) which was present in the pure peptide spectra, appeared again in the spectra of peptide-containing CNPs, showing that peptide fraction had been encapsulated into CNPs [116]. In addition, the band at 703 cm^{-1} was found

in peptide-loaded NPs, most likely originated from-C-H rocking of CH2 of the amino acid residues in peptides.

Table 4. 4: FTIR results for CNPS, Hβd-3 CNPs.

Wavenumber		Vibration	Functional groups		Shift
CNPs	**Hβd-3CNPs**		**CNPs**	**Kn2-7 CNPs**	
3278	3253	Stretching vibration	O-H,N-H	O-H, N-H	Yes
-	2924	Asymmetric stretch	-	C-H (alkane)	New peak
1645	1634	Bending vibration	Amide 1	Amide 1	Yes
1553	1548	Carbonyl stretch	Amide II	Amide II	Yes
1344	-	Bending	-	C-H (CH3)	disappeared
1209	1260	Stretching vibration	P=O	P=O	Yes
-	797	Rocking	-	C-H (C-H2)	New peak

4.4 HRTEM analysis

4.4.1 CNPs

The CNPs which were prepared in three different concentrations were also characterized by HRTEM. The NPs obtained from chitosan that was cross-linked with 0.3mg/ml TPP exhibited the spherical NPs in the range of 2.5nm-3.4nm diameter as shown in Fig 4.4a. The chitosan that was cross-linked with 1mg/ml TPP (Fig. 4.4b) varied at 5.0 nm-15nm, and lastly in3mg/ml TPP (Fig. 4.4c) the size obtained was at the range of 2.3 nm-2.5 nm diameter. The smallest size obtain was from the NPs cross-linked with 3mg/ml of TPP. Because we wanted the NPs with

smallest size to load the peptide, chitosan-3mg/ml TPP was chosen as a candidate to carry kn2-7 peptide. The size of the cross-linked CNPs from TEM was observed in the range of 60-280 nm. The micrographs confirmed the nanosize of dried cross-linked CNPs. Banerjeet.al [68], obtained spherical CNPs with the size of 110 nm diameter.

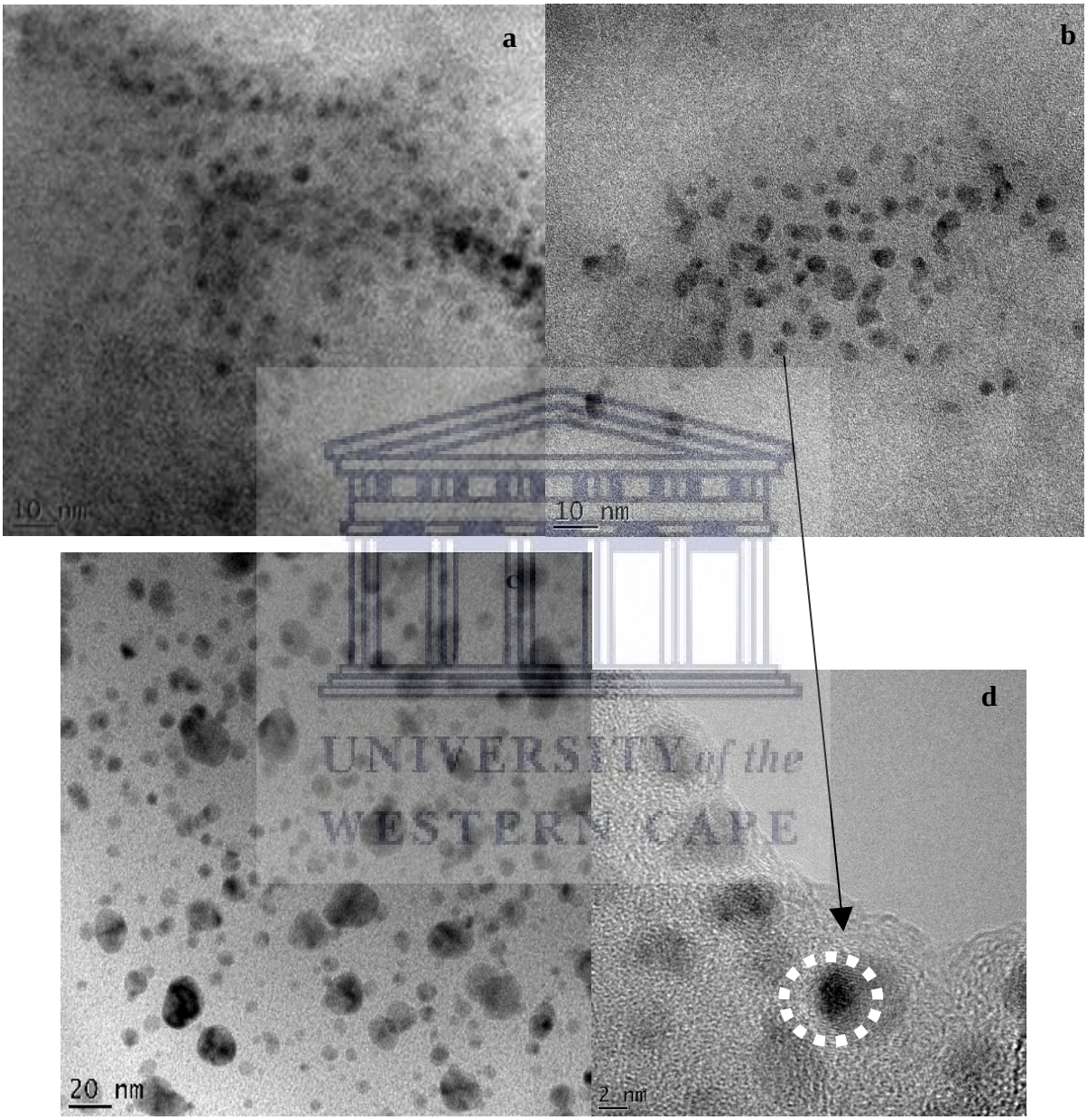

Figure 4. 4: HRTEM micrographs of CNPS Cross-linked with (a) 0.3 mg/ml (b) 1mg/ml and (c) 3mg/ml TPP. Magnified image (d) shows the shape of CNPs

4.4.2 Kn2-7 and Hβd-3 CNPs

The TEM image showed roughly spherical-shaped NPs (Fig.4.5), having smaller diameter than that obtained from the DLS measurements; this may be due to the shrinking of the NPs during the drying process (TEM sample preparation)[117]. The particle size and size distribution of the polymeric NPs are of great importance in using them as drug vehicles; as TEM images show the mean diameter of the peptide loaded NPs to be less than 100nm. The increase in size of the TEM image from 2.5 nm to 3.902 nm indicated the presence of the peptide inside the CNPs. The size of the crosslinked CNPs from TEM was observed in the range of 60-280 nm. The micrographs confirmed the nanosize of dried cross-linked chitosan particles. Banerje *et.al*[118] obtained spherical CNPs with the size of 110 nm diameter of the NPs prepared by modifying polymer reverse micelle method. The method they use involves organic solvents whereas in this study we prepared these NPs using ionic gelation method with deionised water as a solvent.

The observation froom the TEM gave us information on the particle shape and the determination of the particle size. Typical TEM images of Kn2-7CNPs and Hβd-3CNPs in Fig.4.5 show the loaded NPs in different concentrations of the TPP. The image in Fig. 4.5a revealed spherical shaped NPs with agglomerated NPs with size rage of 35-70nm. The Kn2-7 on the other hand in Fig. 4.5b showed dispersed NPs in spherical and smooth surfaces with size range of 20-25nm in diameter, which agrees with the work by Dounighi *et.al* who obtained spherical homogenous morphology with size approximately 137nm of Venom loaded CNPs[88]. In Fig. 4.5c Hβd-3CNPs showed dispersed heterogeneous morphology of the particles with size of 20-40 nm while Kn2-7CNPs cross-linked with the same concentration of TPP demonstrated spherical dispersed particles with size range of 15-20nm refer to Fig. 4.5d. When comparing these images from Fig. 4.5a-f, Hβd-3CNPs tend to have poor dispersion and Kn2-7CNPs from the low to high concentration of TPP cross linker showed solid consistent structures, agreeing with the results that were reported by Deng and co-workers[119].

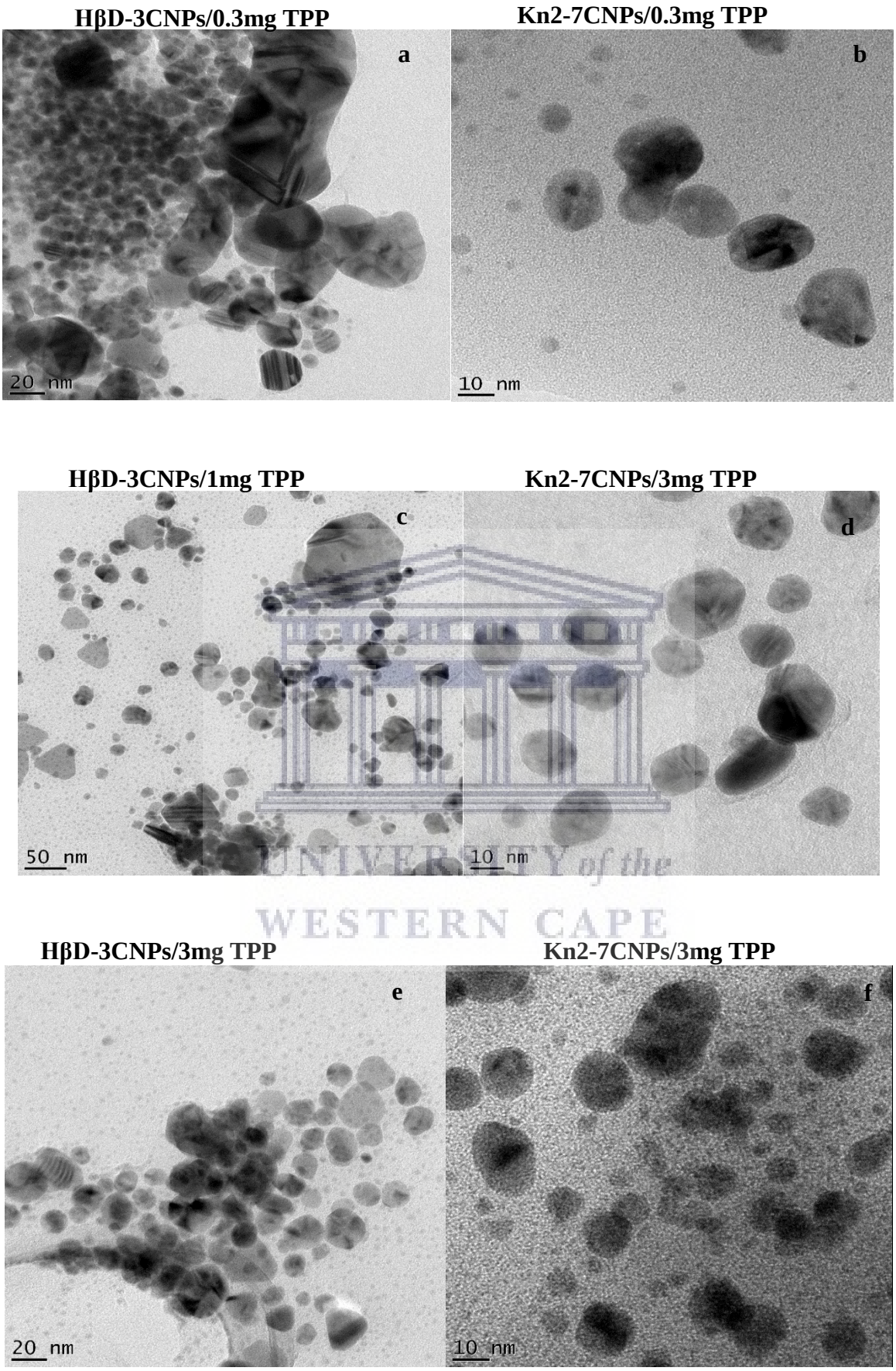

Figure 4. 5: HRTEM results for Kn2-7CNPs and EDS

4.5 Morphology by SEM

4.5.1 CNPs

SEM is a technique that provides that employs high energy beam of electrons to scan the surface of a sample. It provides a direct picture of the surface, size information and to investigate surface morphology of the sample[120]. The SEM images for free CNPs (Fig.4.6) showed spheroidal shape-NPs with smooth surfaces and the size at 100 nm. We also noticed that free CNPs have a smaller size than the loaded NPs possibly due to the loading of the peptide. Kiilll et.al synthesized crosslinked CNPs and characterized them with SEM. The results showed a spherical shape with smooth surfaces and had a homogeneous particle size distribution in the range of 70–100 nm [121]. Hasheminejad and co-workers also reported the spherical NPs with size ranging between 129-148 nm characterized by FESEM[122].

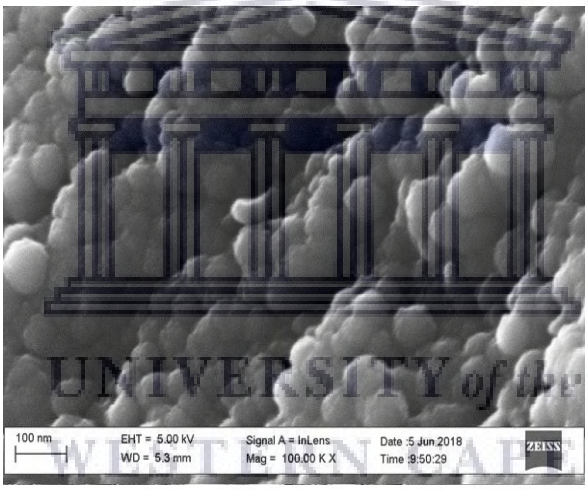

Figure 4. 6: SEM results for free CNPs

4.5.2 Kn2-7 and Hβd-3 CNPs

The SEM analysis was carried out on NPs, the results from the loaded CNPs (Fig.4.7) exhibited spherical morphology of the NPs arranged in sheet structures Fig 4.7(a,b,c,d and f). We also noticed that some of the Hβd-3 CNPs are arranged in the shapes that look like fibres (Fig 4.7 e) and the peptide inside them shown in dark. Amidi[123] and co-workers reported that from their SEM images that the loading of protein did not affect the size and morphology of the NPs. This is in contrast to our study results reported above.

The six images below confirm the change of the arrangement after the loading when compared to free CNPs in Fig. 4.6.

Hβd-3CNPs/0.3mg TPP

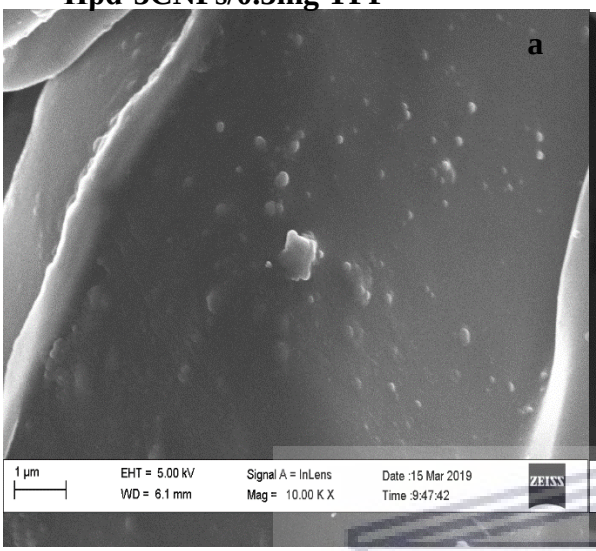

Kn2-7CNPs/0.3mg TPP

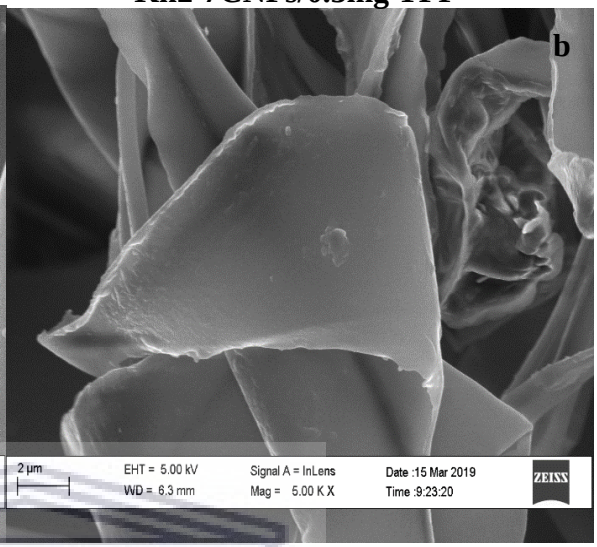

Hβd-3CNPs/1mg TPP

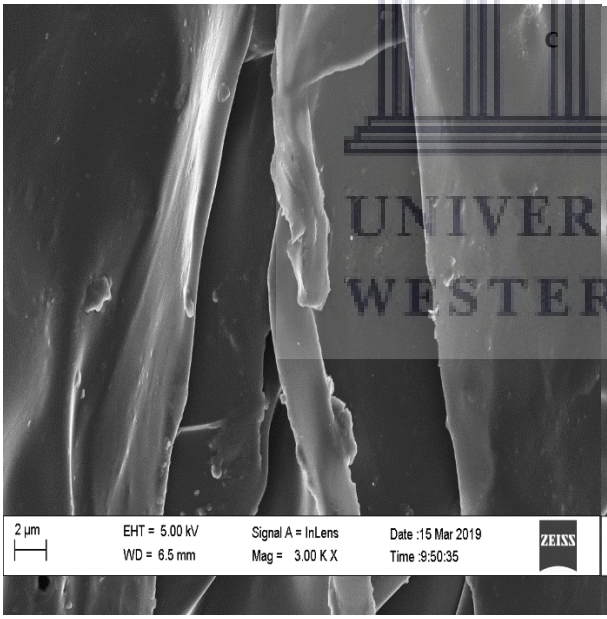

Kn2-7CNPs/1mg TPP

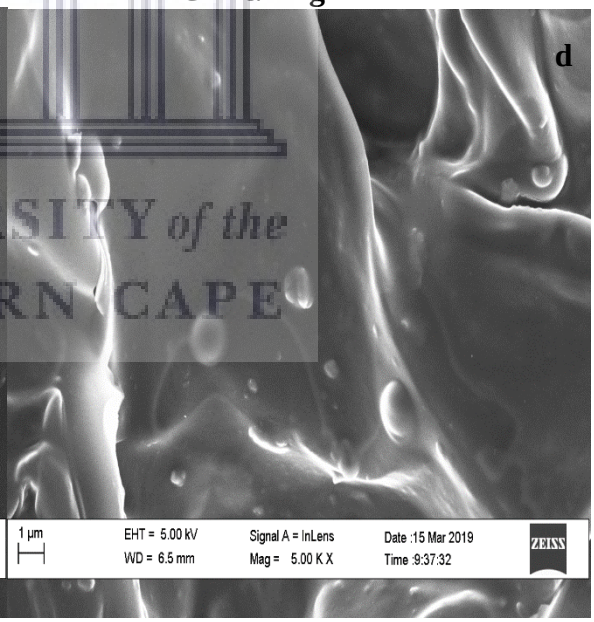

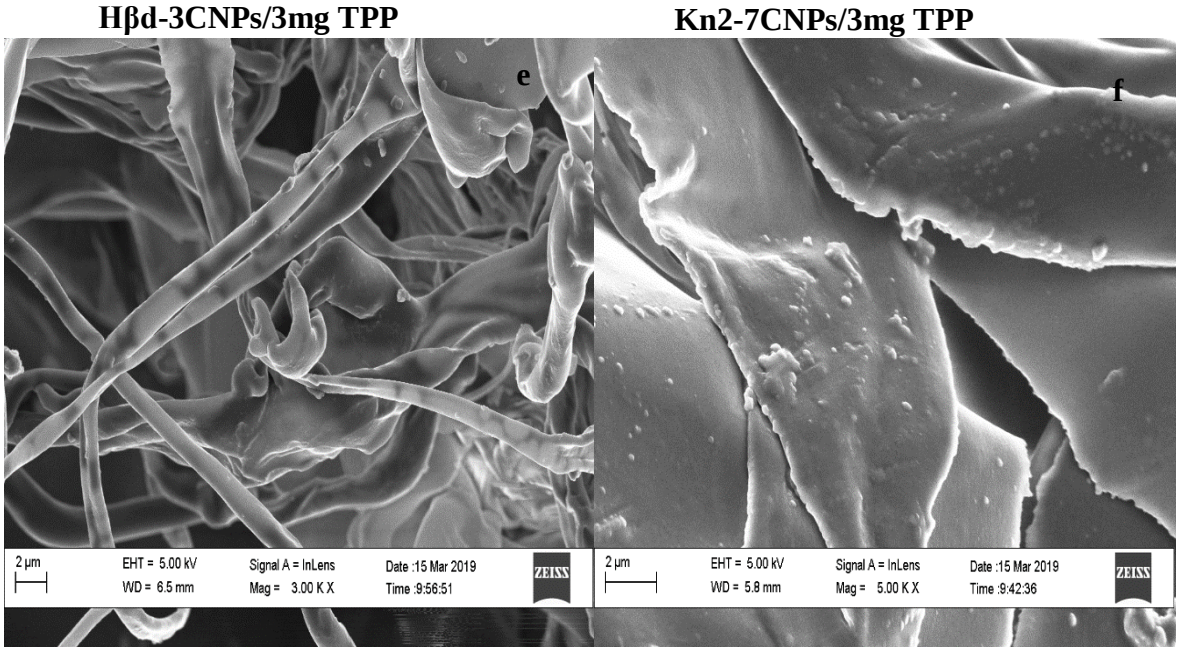

Figure 4. 7: SEM results for (a) HβD-3 chitosan NPs (b) Kn2-7 chitosan NPs

4.6 Loading capacity (LC) and encapsulation efficiency EE (%) of Kn2-7 and Hβd-3 CNPs

Both peptides were successfully incorporated into CNPs after testing different preparation with TPP concentrations (Table 4.5). The NPs loaded with peptide EE% and L.C% values were respectively of 78.3% and 85.6% (Table 4.5). The association of peptide to NPs with CS/TPP in different concentrations was successful but the NPs with 3mg/mL TPP showed poor loading and encapsulation of peptide due to the competition between TPP and peptide for the same positive charged sites on CS molecules[124]. Therefore, peptide was incorporated into NPs containing minor amount of TPP (0.3 mg/mL and 1mg/mL TPP concentrations) obtaining colloidal stable NPs. The highest percentage yield (approximately 34%) of peptide loaded NPs was obtained with the 3mg/ml TPP CNPs. 1mg/mL Kn2-7 CNPs shown an excellent loading capacity as well as entrapment efficiency in CNPs. On the other hand, shown less amount Hβd-3 loaded in CNPs which is 66.4% (Table 4.5) but still good when compared to other cross-linked concentrations of TPP such as 59.6% in Hβd-3 CNPs/0.3mg/mlTPP and 53.1 % in Hβd-3 CNPs/1mg/mlTPP .

Table 4. 5: EE% and L.C values of peptide CNPs prepared with different concentrations of TPP (mean, n=3).

TPP concentration mg/mL	EE%		LC%	
	Kn2-7 CNPs	Hβd-3 CNPs	Kn2-7 CNPs	Hβd-3 CNPs
0.3	50.7	59.6	38.3	21.5
1	78.3	66.4	85.6	48.8
3	55.6	53.1	46.9	29.0

4.7 Stability test of peptide-loaded CNPs in different pH conditions

Stability test of the NPs is method to check their quality and how the AMP-CNPs behave in different pH environments more especially those that simulate vaginal mucus. The results of this investigation determine the strength of the NPs to keep the peptide before the actual release, in other words this step gives the residence time of the peptide inside the NPs and amount of the peptide released over time.

The loaded NPs only exhibited the stability at pH of 6.0-7.4 this was investigated by firstly exposing the NPs in the buffer without any action taken, the readings in the qubit revealed that the NPs did not release the peptide. The release study was reported by Kavas *et.al*. They investigated the release of mitomycin-c from CNPs and showed the sustained release at pH of 6.0 and 7.4 although the release at pH 6 was slower[125]. Furthermore the NPs were sonicated with no observation of any disintegration but the NPs were dispersed. This was an indication that, these loaded NPs are stable in weak acids to basic environment. Peptide loaded CNPs were also tested to the lower pH medium and the readings on qubit in table 4.6 clearly shows that the loaded NPs are not stable in that pH. This was shown by applying different actions in the NPs within different time intervals.

As noticed in table 4.6 that some of the NPs after being exposed in the low pH buffer, were vortexed, incubated for 24 hour and others with no action taken but they read more or less the same reading in the qubit instrument which revealed that the NPs at low pH release immediately. This contradict with the previous report by Bhardwaj *et.al*[126] who found that

loaded CNPs have a low solubility at low pH which resulted to the poor release of the drug. Whereas Fathi *et.al* on their literature survey studies reported that chitosan displayed a rapid release of DOX upon the increase of the acidity[127]. The objective of this research was to synthesize the NPs that could be stable at low pH to provide the long and sustained release of the peptide for the NPs. Chitosan alone failed to achieve those goal and further investigations were made to ensure the stability of loaded CNPs at low pH.

Table 4. 6: The behaviour of the loaded NPs when exposed in different conditions

Amount	Buffer	pH	Time (hrs)	Action	Qubit reading
0.5 mg	PBS	7.4	24	Incubation 37 ºC	83.2 µg/ml
0.5 mg	PBS + acetic	3.7	24	Incubation 37 ºC	103 µg/ml
0.5 mg	BPS+ HCl	6.0	0	Sonication	0 µg/ml
0.25 mg	PBS+ 1% Ac	3.44	24	Incubation 37 ºC	61.6 µg/ml
0.25 mg	PBS+ 1% Ac	3.44	0	Vortex	-
0.25 mg	PBS+ 1% Ac	3.96	0	None	66.8 µg/ml
0.25 mg	PBS+ 1% Ac	3.96	24	Incubation	73.2 µg/ml
0.25 mg	PBS	7.4	0	none	0 µg/ml
0.25 mg	PBS	7.4	24	Incubation	68.4 µg/ml

4.8 Characterization of KCP NPs and HCP NPs

4.8.1 Introduction.

Polyacrylic acid (PAA), the carboxylic group containing polymer offer many advantageous elements for oral drug delivery, which include pH-responsiveness, inhibition of enzymes, mucoadhesion and the ability to open epithelial tight junctions [128].

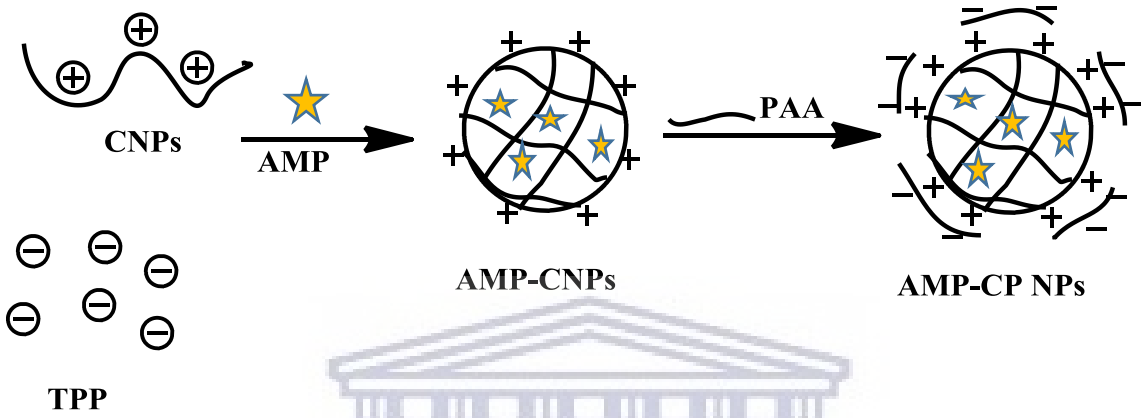

Figure 4. 8: Illustration of the impact of PAA on loaded NPs by LBL technique[129]

Unlike other coatings used before, the extra uniform structural and release behaviour is possibly observed in the case of loaded CS/PAA NPs described in Fig. 4.8 regardless of the conditions used. In this discussion we are using loaded NPs crosslinked with 0.3 TPP that are coated with PAA.

4.8.2 Dynamic light scattering

The DLS NPs showed aggregated NPs that are polydispersed, which could be due to the high molecular weight of two polymers loading peptides and plus the effect of the freeze drying process in the NPs. The excellent zeta potentials which confirmed the stability of the NPs was also shown by DLS. Another interesting findings from these coated CNPs was that, the PAA did not affect the charge of peptide loaded CNPs. This means that these NPs mucus penetrating properties remain intact. It should also be mentioned that the Zeta potential for K2-7CNPs in table 4.7 increased from 15.9 to 37.2 while Hβd-3 decreased from 54.7 to 38.3, probably because of excess and unbounded PAA polymer on the surface.

Table 4. 7: Particle size, polydispersity index and Zeta potential of peptide-loaded NPs with poly(acryilic acid). PAA, CNPs- CNPs. Kn2-7 and Hβd-3 peptide concentration 0.5 mg/ml.

Peptide-PAA/CNPs	Size (nm)	PDI	Zeta Potential (mV)
Hβd-3	847.7	0.698	+38.3
Kn2-7	997	0.840	+37.2

4.8.3 FTIR of Hβd-3 and Kn2-7 CNPs

The KCP NPs in table 4.8 shows the absorption peaks at 3033 cm^{-1} which represents the OH from the carboxylic groups of the PAA. The C-H stretching on methyl was also observed at 2984cm^{-1}. The two characteristic peaks at 1645 cm^{-1} and 1553 cm^{-1} for CS decreased, and a new absorption band at 1713cm^{-1} appeared, which could be attributed to the absorption peaks of the carboxyl groups of PAA. A broad peak appeared at 2669 cm^{-1}, which confirmed the presence of NH_3^+ in the Kn2-7 CS–PAA NPs. In addition, the absorption peaks at 1453 and 1416 cm^{-1} were assigned to asymmetric and symmetric stretching vibrations of COO^- anion groups (see Fig. 4.9). Another peak found at 1397 cm^{-1} was related to CH_2 groups, similar results were also reported by Khan and co-workers[97]. The shift of P=O peaks to 1260 and 1265 cm^{-1} was observed in both spectra, which confirmed that the crosslinking was not affected by this coating. These results indicate that the carboxylic groups of PAA were dissociated into COO^- groups, which completed with protonated amino groups of chitosan through electrostatic interactions to form the polyelectrolyte complex during the mixing procedure.

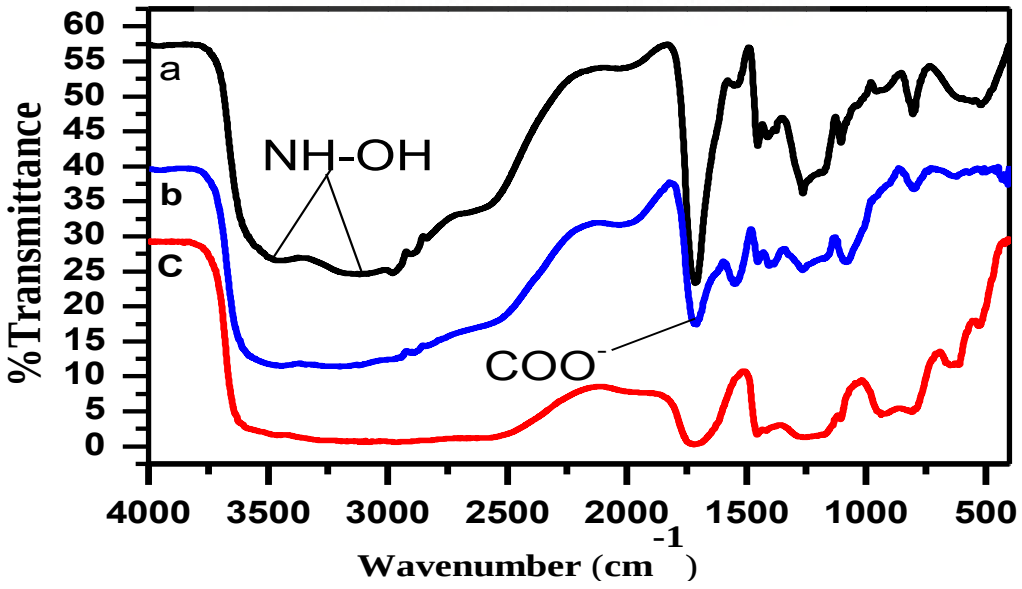

Figure 4. 9: FTIR of (a) KCP NPs (b) Hβd-3CS/PAA NPs and (c) Raw PAA

In table 4.8 Kn2-7CNPs are compared to coated CNPs (KCP NPs) according to the shifts and new bond formed during the coating process.

Table 4. 8: FTIR results for CNPS, Kn2-7 CNPs.

Wavenumber			**Functional groups**		
Kn2-7CNPs	**KCP NPs**	**Vibration**	**Kn2-7CNPs**	**KCP NPs**	**Shift**
3400	3033	Stretching vibration	O-H,N-H	O-H, carboxylic	Yes
2929	2980	Asymmetric stretch	C-H	C-H (methyl)	Yes
1643	1713	Bending vibration	COO^-	COO^-	New peak
1540	1453	Carbonyl stretch	Amide II	Amide II	Yes
1381	1376	Stretching	C-H (CH2),OH	C-H (CH2),OH	New peak
1226	1265	Stretching vibrations	P=O	P=O	Yes

The FTIR spectra of Hβd-3 and Kn2-7 CNPs with different pH values are shown in table 4.9 (appendix, Fig.2 g-i).The basic characteristics of CS at 3449 cm^{-1} (OH stretching and N-H stretching) and 2984 cm^{-1} (C-H stretching on methyl) were observed. However, in the HCP NPs, the two characteristic peaks of CS decreased dramatically, and a new absorption band at 1721-1708 cm^{-1}, which could be assigned to the absorption peaks of the carboxyl groups of PAA[130] (the absorption peak of carboxyl groups in pure PAA appeared at 1737 cm^{-1}) was observed. In addition, the absorption peak at 1556 was assigned to asymmetric and symmetric stretching vibrations of COO^- anion groups in Fig. 4.9 and a peak at 1376 cm^{-1} which was attributed to CH_2 stretch.

Table 4. 9: FTIR results for CNPS, Kn2-7 CNPs.

Wavenumber			Functional groups		
Hβd-3CNPs	**HCP NPs**	**Vibration**	**Hβd-3CNPs**	**HCP NPs**	**Shift**
3253	3203	Stretching vibration	O-H,N-H	O-H, carboxylic	Yes
2924	2984	Asymmetric stretch	C-H	C-H (methyl)	Yes
-	1721	Bending vibration	COO^-	COO^-	New peak
1548	1556	Carbonyl stretch	Amide II	Amide II	Yes
-	1397	Stretching	C-H (CH2),OH	C-H (CH2),OH	New peak
1260	1260	Stretching vibrations	P=O	P=O	Yes

4.8.4 HRSEM of Hβd-3 and Kn2-7 CNPs

In the HRSEM we obtain the oval shaped NPs with three layers in Fig. 4.10&4.11 showing that our NPs were successfully coated with PAA. In addition, this results bring confidence to conclude that we can use our NPs for stability test to see how they behave at low temperature. To the best of our knowledge this work has never been reported before because no article has reported the same work on coating the peptide loaded CNPs with poly acrylic acid**.**

HCP NPs in 1mg TPP

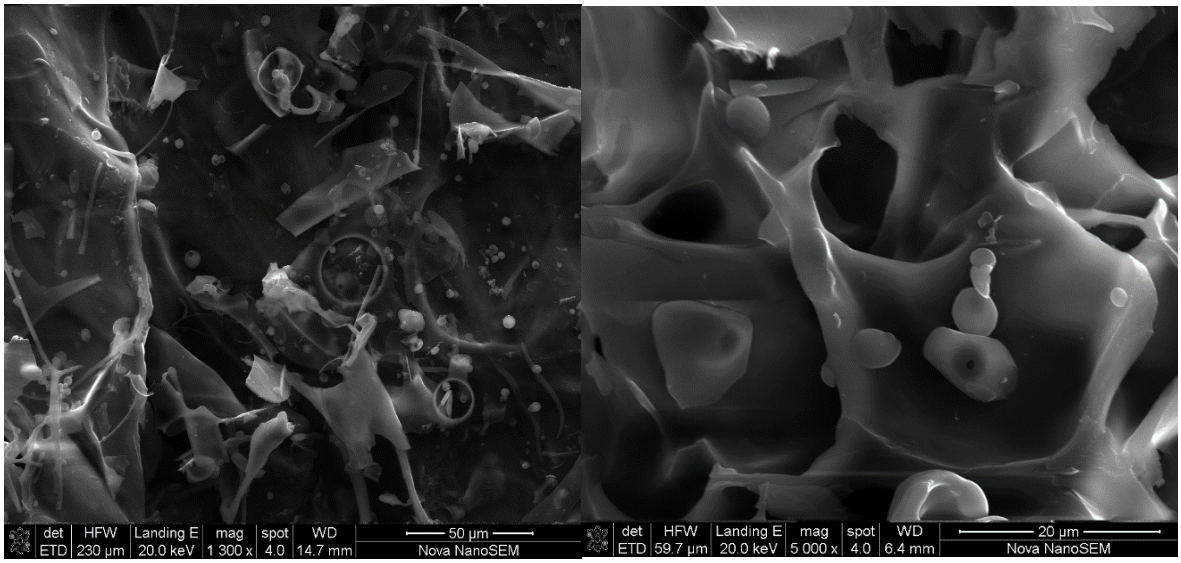

Figure 4. 10: HRSEM images of human beta defensin-3

The NPs are arranged in the sheet surfaces which represents the gel that surrounds them. The first image in Fig. 4.11 was zoomed to show how the layers look from the spectrum.

KCP NPs in1mg TPP

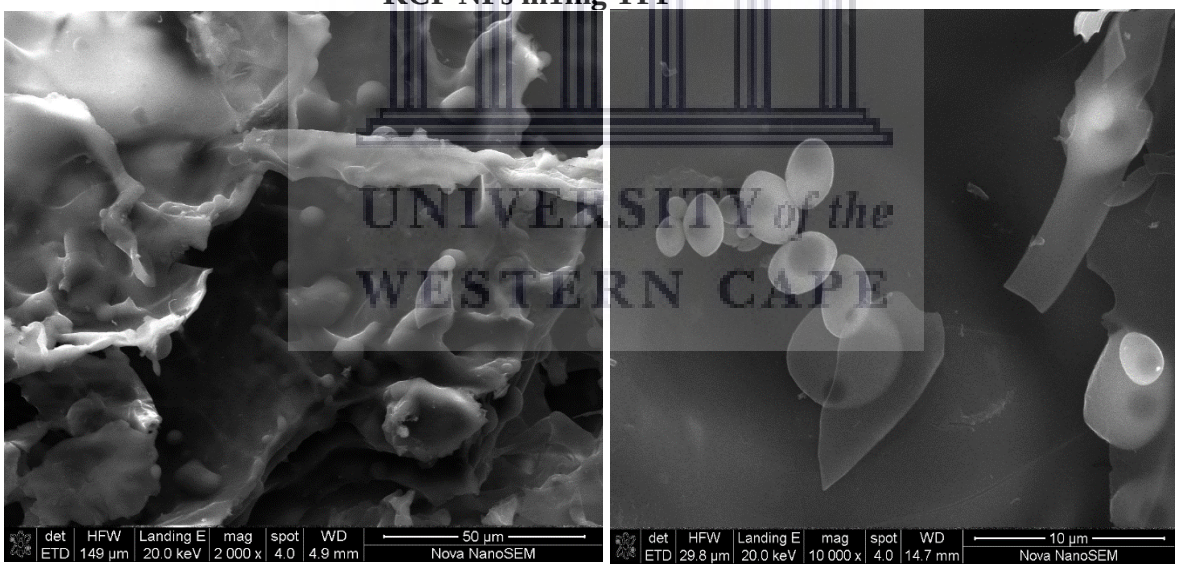

Figure 4. 11: SEM results for (a) HβD-3 chitosan NPs (b) Kn2-7 chitosan NPs

4.9 Stability test of AMP-CNPs coated with PAA

The study of stability was carried out using two samples which are 0.3 kn2-7 and 0.3 Hβd-3 CNPs. The Table 4.10 shows the detailed results of what was observed during this process. From the observations it was noticed that when NPs are dispersed in a buffer of pH 3.71 and shook with a hand the peptide was not released. Another trial was made by vortex on the NPs for 5 minutes but still there was nothing released according to the qubit. Following the same procedure the loaded NPs showed same results upon exposure at pH 4.27 which indicated that NPs are stable at that pH level. The 24 hours incubation of the NPs revealed the release of the peptide from CNPs/PAA.

Table 4. 10: The behaviour of the loaded NPs when exposed in different conditions.

Amount	Buffer	pH	Time (hrs)	Peptide	Action	Qubit reading
0.25 mg	PBS+ 1% Ac	3.71	0	Kn2-7	none	0 µg/ml
0.25 mg	PBS+ 1% Ac	3.71	24	Kn2-7	Incubation 37 degrees	48 µg/ml
0.25 mg	PBS+ 1% Ac	3.71	0	Hβd-3	Vortex	0 µg/ml
0.25 mg	PBS+ 1% Ac	3.71	24	Hβd-3	Incubation 37 degrees	44.0
0.25 mg	PBS+ 1% Ac	4.27	0	Kn2-7	None	0 µg/ml
0.25 mg	PBS+ 1% Ac	4.27	24	Kn2-7	Incubation 37 degrees	53.2 µg/ml
0.25 mg	PBS+ 1% Ac	4.27	0	Hβd-3	Vortex	0 µg/ml
0.25 mg	PBS+ 1% Ac	4.27	24	Hβd-3	Incubation 37 degrees	44.0 µg/ml

4.10 Antibacterial activity of PAA coated CNPs

The antimicrobial peptide, Kn2-7 has been reported to have anti-HIV and anti-microbial activities[13]. Peptides like Kn2-7 could be applied in the development of intravaginal microbicidal agents, which could be used to prevent the transmission of STIs. However, one of the problems is that the intravaginal environment, which has a pH of 3.5-4.5 is a very harsh environment that could degrade the peptide and leading to the loss of its antimicrobial activity. In this study the Kn2-7 peptide was loaded into CNPs (KCP NPs) to protect the peptide from rapid degradation in environment where the pH is low. In this Chapter the antimicrobial activity of Kn2-7/CNP is investigated under low pH conditions. We did not investigate the Hβd-3 peptide in antibacterial activity, it will be investigated in the next study considering the results and stability we obtained from this study.

4.10.1 Growth kinetics of *S. aureus* in normal and acidic conditions

The growth curve in Fig. 4.12 revealed that *S. aureus* grows more or less the same in both normal (pH 7.4) and acidic (pH 3.8) conditions. At 6 hours the growth of bacteria in acidic media started to decline while the bacteria in normal media continued to increase. After 24 hours the bacterial growth in both media was reduced, an indication that the bacteria might have overgrown and depleted their nutrients and started to die.

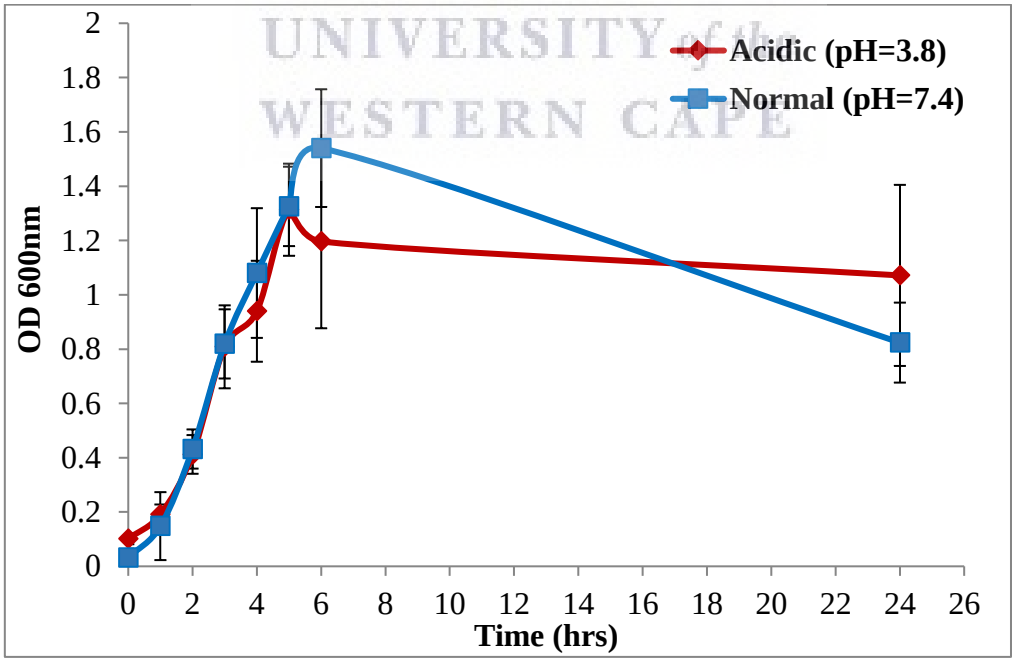

Figure 4. 12: Growth kinetics of *S aureus* in acidic and normal broth. Bacterial growth was measured as a function of optical density at 600nm for 24 hours

4.10.2 Assessing the antibacterial activity of the peptides and peptide loaded CNPs

The Minimum Inhibitory Concentration (MIC) was established for the Kn2-7 peptide and KCP NPs as described in Chapter 3, Section 3.7.2. Two cultures of *S. aureus* were prepared; one was cultured in media at pH 3.8 and the other at pH 7.4. To determine the MIC the bacteria were treated with the Kn2-7 peptide (up to 50ug/mL), the KCP NPs (up to 12.5ug/mL) and the CS/PAA NPs. For the Kn2-7, the MIC was determined at both pH 3.8 and 6.25, while for KCP NPs the MIC was only determined at pH 3.8 as shown in Table 4.11. The MIC for Kn2-7 was 6.25ug/mL at pH 7.4. The same peptide (Kn2-7) was reported in literature to have MIC value of 3.13 μg/mL in normal media (pH 7.4) against *S. aureus* [18], the current study obtained a MIC value of 6.25 μg/mL (Table 4.11). The MIC for Kn2-7 at pH 3.8 could not be established and is likely to be higher than 50ug/mL. It is also possible that the peptide is completely degraded at this low pH, resulting in the complete loss of antibacterial activity. The MIC for KCP NPs at pH 3.8 was 6.25ug/mL. This suggests that when encapsulated in CNP, the antibacterial activity of Kn2-7 is preserved even at a low pH. CNP thus protect the Kn2-7 from degradation. The MIC for NPs that were not loaded with peptide, CS/PAA NPs was also higher than the maximum concentration used (>12.5ug/mL) and could not be determined. This suggest CS/PAA NPs under these conditions do not have any antibacterial activity against *S. aureus* and that the activity observed for KCP NPs was as a result of the Kn2-7 peptide loaded onto CS/PAA NPs

Table 4. 11: MICs values for the Kn2-7 peptide and KCP NPs

Treatment	**Kn2-7 Peptide**		**CS/PAA NPs**	**KCP NPs**
pH	7.4	3.8	3.8	3.8
MIC (μg/mL)	6.25	>50	>12.5	6.25

CHAPTER 5

GENERAL CONCLUSIONS AND RECOMMENDATIONS

5.1 Conclusion

The objective of this study was to synthesize nanocarriers that will serve as vehicles, protect the AMPs and deliver them to the conditions that have low pH. The NPs used in this study were synthesized and characterized. They are non-toxic, biodegradable, biocompatible and most importantly stable in acidic conditions which make them suitable as microbicides. The microbicides made from these NPs can be used as topical vaginal gels or condom gels for an extra layer protection to prevent the transmission of STIs**.**

The CNPs were prepared successfully by ionic gelation of CS with different concentrations TPP. TEM, SEM, FTIR, UV and DLS analysis was used to confirm this. The characterization techniques revealed that the NPs were spherical in shape with a mean diameter of 2.5-15 nm and a zeta potential more than + 30 mV, which ensures their physical stability and render them suitable for transportation through mucosa and uptake by cells in the human body. The phosphate band observed by FTIR confirmed the formation of the NPs.

The successful loading of peptide into the CNPs was also confirmed by FTIR, DLS, HRSEM, HRTEM, and UV-Vis spectroscopy. The FTIR spectra of peptide-loaded CNPs showed the shifts in band and formation of new peaks, which can be attributed to the presence of peptides. CNPs cross-linked with 1 mg/ml TPP showed excellent stability as demonstrated by the DLS analysis. HRTEM revealed NPs with an average size less than 100 nm for both CNPs and peptide loaded CNPs were synthesized via ionic gelation method. Poly electrolyte formation between PAA and CS with peptides loading was confirmed by FTIR, DLS, and HRSEM spectroscopy. The FTIR spectra of peptide-loaded CS/PAA NPs amide absorption bands characteristic of peptide and also showed that carboxylic groups of PAA associated with amine and OH groups of CS through electrostatic interactions to form the polyelectrolyte. Exothermic peaks of physical mixture were different from those of the uncoated NPs, which also indicate that coating of the AMP-CNPs with PAA results in new chemical bonds formed. The Zeta potential of AMP-CP NPs remained positively charged an indication that conjugation of PAA will not affect the mucus penetration properties of CNPs.

The encapsulation efficiency EE (%) of the peptide loaded CNPs cross-linked with 1mg/ml TPP was 79.6% and it was observed that the entrapment efficiency of these NPs was higher compared to NP synthesised with higher/lower concentrations of TPP. The stability of the CS/PAA NPs allows for modulated release of the encapsulated drug. It also showed improvement in the in vitro release profiles of these coated NPs, by releasing the Kn2-7 in a more controlled and sustained manner. Thus, as the NPs are slowly degraded by the acidic conditions in the vagina, the peptide is released and kills the bacteria.

Antibacterial studies confirmed that free peptide (Kn2-7) does not survive the acidic conditions and that the peptide completely lose its activity. Kn2-7 loaded NPs protects the activity of the peptide in the conditions that simulate vaginal pH (~pH 3.8). Comparing the activity of all the peptide loaded NPs cross-linked with different concentrations of TPP, it was clear that TPP has an effect in the loading capacity of the drug. Approximately 87.5% of the peptide was released within 24 hours to inhibit the bacterial growth at pH 3.8. These results indicate that CS/PAA NPs are a promising carrier system for the controlled delivery of antimicrobial peptides in acidic environments such as the vagina.

In conclusion, this study demonstrated that incorporating Kn2-7, which was previously shown to have anti-HIV activity, into CNPs protected the peptide from degradation in acidic conditions and preserve the antimicrobial activity of the peptide. These NPs demonstrate potential for its application in the development of a microbicidal product that could prevent the transmission of STIs, such as HIV/AIDS.

5.2 Recommendations

- The antiviral activity against HIV must be tested, first *in vitro*, then *in vivo* in an animal study.
- To test the nanoparticles against hepatitis B, herpes and the human papilloma virus (HPV) for susceptibility.
- The mucus penetrating ability of the AMP-CP NPs still need to be tested.
- All of the above must be repeated with Hβd-3.
- The release studies on NPs over time still need to be investigated to know the exact time for the start of release.

REFERENCES

[1] Republic of South Africa Department of Health, "Sexually transmitted infections management guidelines," vol. 54, pp. 1–28, 2015.

[2] M. Waugh and H. J. C. de Vries, "Sexually Transmitted Infections," *Import. Ski. Dis. Second Ed.*, pp. 149–161, 2012.

[3] D. N. H. Muhammad Ali Tarar1 , Dr Saira Akhtar2 , Dr. Yasir Nawaz Manj3 , Dr. Manzoom Akhtar4 , Dr. Muhammad Iqbal Zafar5, "knowledge and attitude ;stis, hiv, aids, rtis, breast cancer & reproductive health among young females in faisalabad district, pakistan 1.," *Prof. Med. J.*, vol. 22, no. 6, pp. 690–704, 2015.

[4] D. M. P Mayaud, "Approaches to the control of sexually transmitted infections in developing countries: old problems and modern challenges," *Ser. Trop. Med.*, vol. 80, pp. 174–182, 2004.

[5] R. K. Malcolm, A. D. Woolfson, C. F. Toner, R. J. Morrow, and S. D. Mccullagh, "silicone elastomer vaginal rings," no. September, pp. 954–956, 2005.

[6] R. Pauwels and E. De Clercq, "Development of vaginal microbicides for the prevention of heterosexual transmission of HIV," *J. Acquir. Immune Defic. Syndr. Hum. Retrovirology*, vol. 11, no. 3, pp. 211–221, 1996.

[7] M. P. Sánchez-Sánchez, "Chitosan and Kappa-Carrageenan Vaginal Acyclovir Formulations for Prevention of Genital Herpes. In Vitro and Ex Vivo Evaluation," *Mar. Drugs*, vol. 13, no. 9, pp. 5976–5992, 2015.

[8] F. Notario-Pérez, R. Ruiz-Caro, and M. D. Veiga-Ochoa, "Historical development of vaginal microbicides to prevent sexual transmission of HIV in women: From past failures to future hopes," *Drug Des. Devel. Ther.*, vol. 11, pp. 1767–1787, 2017.

[9] B. Cutler and J. Justman, "Vaginal microbicides and the prevention of HIV transmission," *Lancet Infect. Dis.*, vol. 8, no. 11, pp. 685–697, 2008.

[10] I. J. Rosenstein, M. K. Stafford, V. S. Kitchen, H. Ward, J. N. Weber, and D. Taylor-Robinson, "Effect on Normal Vaginal Flora of Three Intravaginal Microbicidal Agents Potentially Active against Human Immunodeficiency Virus Type 1," *J. Infect. Dis.*, vol. 177, no. 5, pp. 1386–1390, 1998.

[11] J. Lei, "The antimicrobial peptides and their potential clinical applications," vol. 11, no. 7, pp. 3919–3931, 2019.

[12] J. W. Hui Zhang, "Review on Bioactive Peptides and Pharmacological Activities of

Buthus martensii Karsch," *Biochem. Pharmacol. Open Access*, vol. 04, no. 02, 2015.

[13] Y. Chen, "Anti-HIV-1 Activity of a New Scorpion Venom Peptide Derivative Kn2-7," vol. 7, no. 4, pp. 1–9, 2012.

[14] B. Hmed, H. T. Serria, and Z. K. Mounir, "Scorpion Peptides: Potential Use for New Drug Development," *J. Toxicol.*, vol. 2013, pp. 1–15, 2013.

[15] L. Cao, "Antibacterial Activity and Mechanism of a Scorpion Venom Peptide Derivative In Vitro and In Vivo," vol. 7, no. 7, 2012.

[16] M. Tohidnezhad, "Thrombocytes are effectors of the innate immune system releasing human beta defensin-3," *Injury*, vol. 42, no. 7, pp. 682–686, 2011.

[17] Q. Lu, L. P. Samaranayake, R. P. Darveau, and L. Jin, "Expression of human β-defensin-3 in gingival epithelia," *J. Periodontal Res.*, vol. 40, no. 6, pp. 474–481, 2005.

[18] D. Cui, "Human β-defensin 3 inhibits periodontitis development by suppressing inflammatory responses in macrophages," *Mol. Immunol.*, vol. 91, no. September, pp. 65–74, 2017.

[19] C. Zhu, H. Tan, T. Cheng, and H. Shen, "Human b -defensin 3 inhibits antibiotic-resistant Staphylococcus biofilm formation," *J. Surg. Res.*, vol. 183, no. 1, pp. 204–213, 2013.

[20] V. Dhople, A. Krukemeyer, and A. Ramamoorthy, "The human beta-defensin-3 , an antibacterial peptide with multiple biological functions," vol. 1758, pp. 1499–1512, 2006.

[21] M. Debi Prasanna, Yogesh Panditrao Palve, Debasish Sahoo, and P. L. Nayak, "Synthesis and Characterization of Chitosan/Cloisite 30B (MMT) Nanocomposite for Controlled Release of Anticancer Drug Curcumin," *Int. J. Pharm. Res. Allied Sci.*, vol. 1, no. 4, pp. 52–62, 2012.

[22] J. Robertson, "11119," *Am. Math. Mon.*, vol. 111, no. 10, p. 915, 2004.

[23] Y. Zambito, "Nanoparticles Based on Chitosan Derivatives," *Adv. Biomater. Sci. Biomed. Appl.*, pp. 243–263, 2013.

[24] T. Kean and M. Thanou, "Biodegradation , biodistribution and toxicity of chitosan ☆," *Adv. Drug Deliv. Rev.*, vol. 62, no. 1, pp. 3–11, 2010.

[25] C. E. Kast, C. Valenta, M. Leopold, and A. Bernkop-schnurch, "Design and in vitro evaluation of a novel bioadhesive vaginal drug delivery system for clotrimazole," vol. 81, pp. 347–354, 2002.

[26] I. Younes and M. Rinaudo, “Chitin and chitosan preparation from marine sources. Structure, properties and applications,” *Mar. Drugs*, vol. 13, no. 3, pp. 1133–1174, 2015.

[27] A. Anitha, V. G. Deepagan, V. V. D. Rani, D. Menon, S. V Nair, and R. Jayakumar, “Preparation , characterization , in vitro drug release and biological studies of curcumin loaded dextran sulphate – chitosan nanoparticles,” *Carbohydr. Polym.*, vol. 84, no. 3, pp. 1158–1164, 2011.

[28] T. Sahasathian, T. Kerdcholpetch, A. Chanweroch, N. Praphairaksit, N. Suwonjandee, and N. Muangsin, “Sustained release of amoxicillin from chitosan tablets,” *Arch. Pharm. Res.*, vol. 30, no. 4, pp. 526–531, 2007.

[29] L. Qi, Z. Xu, X. Jiang, C. Hu, and X. Zou, “Preparation and antibacterial activity of chitosan nanoparticles,” vol. 339, pp. 2693–2700, 2004.

[30] Y. Zambito, “World ’ s largest Science , Technology & Medicine Open Access book publisher c,” *Nanoparticles Based Chitosan Deriv.*, pp. 243–263, 2013.

[31] B. C. Tang, “Biodegradable polymer nanoparticles that rapidly penetrate the human mucus barrier,” *Proc. Natl. Acad. Sci.*, vol. 106, no. 46, pp. 19268–19273, 2009.

[32] S. K. Lai, Y. Y. Wang, and J. Hanes, “Mucus-penetrating nanoparticles for drug and gene delivery to mucosal tissues,” *Adv. Drug Deliv. Rev.*, vol. 61, no. 2, pp. 158–171, 2009.

[33] F. Laffleur and A. Bernkop-Schnurch, “Development and in vitro evaluation of mucus inert nanoparticles for mucosal diseases,” *NANOCON 2012 - Conf. Proceedings, 4th Int. Conf.*, vol. 10, pp. 23–25, 2012.

[34] B. V. N. Nagavarma, H. K. S. Yadav, A. Ayaz, L. S. Vasudha, and H. G. Shivakumar, “Different techniques for preparation of polymeric nanoparticles- A review,” *Asian J. Pharm. Clin. Res.*, vol. 5, no. SUPPL. 3, pp. 16–23, 2012.

[35] T. Yu, “Biodegradable mucus-penetrating nanoparticles composed of diblock copolymers of polyethylene glycol and poly(lactic-co-glycolic acid),” *Drug Deliv. Transl. Res.*, vol. 2, pp. 124–128, 2012.

[36] K. Berginc, S. Suljaković, N. Škalko-Basnet, and A. Kristl, “Mucoadhesive liposomes as new formulation for vaginal delivery of curcumin,” *Eur. J. Pharm. Biopharm.*, vol. 87, no. 1, pp. 40–46, 2014.

[37] C. Li, C. Han, Y. Zhu, W. Li, Q. Li, and Y. Liu, “In vivo evaluation of an in-situ hydrogel system for vaginal administration,” *Pharmazie*, vol. 69, no. 6, pp. 458–460, 2014.

[38] R. Jayakumar, M. Prabaharan, P. T. Sudheesh Kumar, S. V. Nair, and H. Tamura, "Biomaterials based on chitin and chitosan in wound dressing applications," *Biotechnol. Adv.*, vol. 29, no. 3, pp. 322–337, 2011.

[39] F. Y. Nakano, R. de B. F. Leão, and S. C. Esteves, "Insights into the role of cervical mucus and vaginal pH in unexplained infertility," *Med. Express*, vol. 2, no. 2, pp. 1–8, 2015.

[40] A. Choudhury, S. Das, and M. Kar, "A review on novelty and potentiality of vaginal drug delivery," *Int. J. PharmTech Res.*, vol. 3, no. 2, pp. 1033–1044, 2011.

[41] A. A. Date and V. B. Patravale, "Current strategies for engineering drug nanoparticles," *Curr. Opin. Colloid Interface Sci.*, vol. 9, no. 3–4, pp. 222–235, 2004.

[42] A. Bayat, B. Larijani, and S. Ahmadian, "Preparation and characterization of insulin nanoparticles using chitosan and its quaternized derivatives," vol. 4, pp. 115–120, 2008.

[43] M. Thanou, J. C. Verhoef, P. Marbach, and H. E. Junginger, "Intestinal Absorption of Octreotide : N-Trimethyl Chitosan Chloride (TMC) Ameliorates the Permeability and Absorption Properties of the Somatostatin Analogue In Vitro and In Vivo," vol. 89, no. 7, pp. 951–957, 2000.

[44] M. Thanou, J. C. Verhoef, J. H. M. Verheijden, and H. E. Junginger, "Intestinal Absorption of Octreotide Using Trimethyl Chitosan Chloride : Studies in Pigs," vol. 18, no. 6, 2001.

[45] S. K. Sahoo and V. Labhasetwar, "Nanotech approaches to drug delivery and imaging," *Drug Discov. Today*, vol. 8, no. 24, pp. 1112–1120, 2003.

[46] S. Vrignaud, J. P. Benoit, and P. Saulnier, "Strategies for the nanoencapsulation of hydrophilic molecules in polymer-based nanoparticles," *Biomaterials*, vol. 32, no. 33, pp. 8593–8604, 2011.

[47] C. Perez, A. Sanchez, D. Putnam, D. Ting, R. Langer, and M. J. Alonso, "Poly(lactic acid)-poly(ethylene glycol) nanoparticles as new carriers for the delivery of plasmid DNA," *J. Control. Release*, vol. 75, no. 1–2, pp. 211–224, 2001.

[48] M. N. V. R. Kumar, R. A. A. Muzzarelli, C. Muzzarelli, H. Sashiwa, and A. J. Domb, "Chitosan chemistry and pharmaceutical perspectives," *Chem. Rev.*, vol. 104, no. 12, pp. 6017–6084, 2004.

[49] M. Islam, "Mucoadhesive Chitosan Derivatives as Novel Drug Carriers," *Curr. Pharm. Des.*, vol. 21, no. 29, pp. 4285–4309, 2015.

[50] T. R. Hoare and D. S. Kohane, "Hydrogels in drug delivery: Progress and challenges,"

Polymer (Guildf)., vol. 49, no. 8, pp. 1993–2007, 2008.

[51] A. K. Bajpai, S. K. Shukla, S. Bhanu, and S. Kankane, "Responsive polymers in controlled drug delivery," *Prog. Polym. Sci.*, vol. 33, no. 11, pp. 1088–1118, 2008.

[52] P. Legrand, "Influence of polymer behaviour in organic solution on the production of polylactide nanoparticles by nanoprecipitation," *Int. J. Pharm.*, vol. 344, no. 1–2, pp. 33–43, 2007.

[53] M. Jahanshahi and Z. Babaei, "Protein nanoparticle: A unique system as drug delivery vehicles," *African J. Biotechnol.*, vol. 7, no. 25, pp. 4926–4934, 2008.

[54] R. N. Saha, S. Vasanthakumar, G. Bende, and M. Snehalatha, "Nanoparticulate drug delivery systems for cancer chemotherapy," *Mol. Membr. Biol.*, vol. 27, no. 7, pp. 215–231, 2010.

[55] C. Vauthier and K. Bouchemal, "Methods for the Preparation and Manufacture of Polymeric Nanoparticles," *Pharm. Res.*, vol. 26, no. 5, pp. 1025–1058, 2009.

[56] P. N. Ezhilarasi, P. Karthik, N. Chhanwal, and C. Anandharamakrishnan, "Nanoencapsulation Techniques for Food Bioactive Components: A Review," *Food Bioprocess Technol.*, vol. 6, no. 3, pp. 628–647, 2013.

[57] J. Poirier, "MASTER ' S THESIS Porous Scaffolds of Cellulose Nanofibres Bound with Crosslinked Chitosan and Gelatine for Cartilage Applications :," 2013.

[58] K. S. Krzysztof Cal, "Thermodynamic Modeling of Activity Coefficient and Prediction of Solubility: Part 2. Semipredictive or Semiempirical Models," *Online*, vol. 95, no. 4, pp. 798–809, 2006.

[59] C. Sun, J. S. H. Lee, and M. Zhang, "Magnetic nanoparticles in MR imaging and drug delivery," *Adv. Drug Deliv. Rev.*, vol. 60, no. 11, pp. 1252–1265, 2008.

[60] B. Sarmento, A. Ribeiro, F. Veiga, P. Sampaio, R. Neufeld, and D. Ferreira, "Alginate/chitosan nanoparticles are effective for oral insulin delivery," *Pharm. Res.*, vol. 24, no. 12, pp. 2198–2206, 2007.

[61] J. Meng, T. F. Sturgis, and B. C. Youan, "European Journal of Pharmaceutical Sciences Engineering tenofovir loaded chitosan nanoparticles to maximize microbicide mucoadhesion," *Eur. J. Pharm. Sci.*, vol. 44, no. 1–2, pp. 57–67, 2011.

[62] M. Ariza-Sáenz, "Penetration of polymeric nanoparticles loaded with an HIV-1 inhibitor peptide derived from GB virus C in a vaginal mucosa model," *Eur. J. Pharm. Biopharm.*, vol. 120, no. March, pp. 98–106, 2017.

[63] A. Makhlof, M. Werle, Y. Tozuka, and H. Takeuchi, "Nanoparticles of glycol chitosan and its thiolated derivative significantly improved the pulmonary delivery of

calcitonin," *Int. J. Pharm.*, vol. 397, no. 1–2, pp. 92–95, 2010.

[64] M. Garcia-fuentes, D. Torres, and M. Jos, "New surface-modified lipid nanoparticles as delivery vehicles for salmon calcitonin," vol. 296, pp. 122–132, 2005.

[65] C. Prego, M. Garcı, D. Torres, and M. J. Alonso, "Transmucosal macromolecular drug delivery," vol. 101, pp. 151–162, 2005.

[66] Q. Gan and T. Wang, "Chitosan nanoparticle as protein delivery carrier-Systematic examination of fabrication conditions for efficient loading and release," *Colloids Surfaces B Biointerfaces*, vol. 59, no. 1, pp. 24–34, 2007.

[67] W. Ajun, S. Yan, G. Li, and L. Huili, "Preparation of aspirin and probucol in combination loaded chitosan nanoparticles and in vitro release study," *Carbohydr. Polym.*, vol. 75, no. 4, pp. 566–574, 2009.

[68] J. Duan, "Synthesis and in vitro / in vivo anti-cancer evaluation of curcumin-loaded chitosan / poly (butyl cyanoacrylate) nanoparticles," vol. 400, pp. 211–220, 2010.

[69] A. V Samrot, U. Burman, S. Ann, N. Shobana, and K. Chandrasekaran, "Informatics in Medicine Unlocked Synthesis of curcumin loaded polymeric nanoparticles from crab shell derived chitosan for drug delivery," *Informatics Med. Unlocked*, vol. 10, no. November 2017, pp. 159–182, 2018.

[70] F. Akhtar, M. M. Alam, and S. Kumar, "Oral delivery of curcumin bound to chitosan nanoparticles cured Plasmodium yoelii infected mice," *Biotechnol. Adv.*, vol. 30, no. 1, pp. 310–320, 2012.

[71] H. Yamamoto, Y. Kuno, S. Sugimoto, H. Takeuchi, and Y. Kawashima, "Surface-modified PLGA nanosphere with chitosan improved pulmonary delivery of calcitonin by mucoadhesion and opening of the intercellular tight junctions," vol. 102, pp. 373–381, 2005.

[72] P. K. Chutima Sinsuebpol, Jittima Chatchawalsaisin, "Preparation and in vivo absorption evaluation of spray dried powders containing salmon calcitonin loaded chitosan nanoparticles for pulmonary delivery," *dovepress*, no. 7, pp. 861–873, 2013.

[73] S. Alam, "Development and evaluation of thymoquinone- encapsulated chitosan nanoparticles for nose-to- brain targeting : a pharmacoscintigraphic study," *Int. J. Nanomedicine*, vol. 7, pp. 5705–5718, 2012.

[74] F. Ballout, Z. Habli, O. N. Rahal, M. Fatfat, and H. Gali-muhtasib, "Thymoquinone-based nanotechnology for cancer therapy : promises and challenges," *Drug Discov. Today*, vol. 23, no. 5, pp. 1089–1098, 2018.

[75] A. S. Hanafy, "Pharmacological , toxicological and neuronal localization assessment

of galantamine / chitosan complex nanoparticles in rats : future potential contribution in Alzheimer ' s disease management Pharmacological , toxicological and neuronal localization assessment of galantamine / chitosan complex nanoparticles in rats : future potential contribution in Alzheimer ' s disease management," vol. 7544, 2016.

[76] Z. Liu, "Alginic Acid-Coated Chitosan Nanoparticles Loaded with Legumain DNA Vaccine : Effect against Breast Cancer in Mice," *PLoS One*, vol. 8, no. 4, pp. 1–11, 2013.

[77] O. Borges, M. Silva, A. De Sousa, G. Borchard, H. E. Junginger, and A. Cordeiro-da-silva, "International Immunopharmacology Alginate coated chitosan nanoparticles are an effective subcutaneous adjuvant for hepatitis B surface antigen," *Int. Immunopharmacol.*, vol. 8, no. 13–14, pp. 1773–1780, 2008.

[78] O. Borges, G. Borchard, "Immune response by nasal delivery of hepatitis B surface antigen and codelivery of a CpG ODN in alginate coated chitosan nanoparticles," *Eur. J. Pharm. Biopharm.*, vol. 69, no. 2, pp. 405–416, 2008.

[79] K. Zhao, "Preparation and Efficacy of a Live Newcastle Disease Virus Vaccine Encapsulated in Chitosan Nanoparticles," *PLoS One*, vol. 7, no. 12, pp. 1–11, 2012.

[80] A. Khan, S. H. Mehdi, I. Ahmad, and M. M. A. Rizvi, "International Journal of Biological Macromolecules Characterization and anti-proliferative activity of curcumin loaded chitosan nanoparticles in cervical cancer," *Int. J. Biol. Macromol.*, vol. 93, pp. 242–253, 2016.

[81] L. Mazzarino, "Elaboration of chitosan-coated nanoparticles loaded with curcumin for mucoadhesive applications," *J. Colloid Interface Sci.*, vol. 370, no. 1, pp. 58–66, 2012.

[82] M. de la Fuente, B. Seijo, and M. J. Alonso, "Bioadhesive hyaluronan-chitosan nanoparticles can transport genes across the ocular mucosa and transfect ocular tissue," *Gene Ther.*, vol. 15, no. 9, pp. 668–676, 2008.

[83] M. Fazil, "Development and evaluation of rivastigmine loaded chitosan nanoparticles for brain targeting," *Eur. J. Pharm. Sci.*, vol. 47, no. 1, pp. 6–15, 2012.

[84] B. Bu, Q. Wang, P. Kiptoo, J. M. Stewart, C. Berkland, and T. J. Siahaan, "Vaccine-like Controlled-Release Delivery of an Immunomodulating Peptide To Treat Experimental Autoimmune Encephalomyelitis," *Mol. Pharm.*, no. 9, pp. 979–985, 2012.

[85] M. Marciello, S. Rossi, C. Caramella, and C. Remu, "Freeze-dried cylinders carrying chitosan nanoparticles for vaginal peptide delivery," vol. 170, pp. 43–51, 2017.

[86] J. Y. Kim, W. Il Choi, Y. H. Kim, and G. Tae, "Brain-targeted delivery of protein

using chitosan- and RVG peptide-conjugated, pluronic-based nano-carrier," *Biomaterials*, vol. 34, no. 4, pp. 1170–1178, 2013.

[87] F. Chen, Z. Zhang, F. Yuan, X. Qin, M. Wang, and Y. Huang, "In vitro and in vivo study of N -trimethyl chitosan nanoparticles for oral protein delivery," *Int. J. Pharm.*, vol. 349, pp. 226–233, 2008.

[88] M. D. N, R. Eskandari, H. Zolfagharian, and M. Mohammad, "Preparation and in vitro characterization of chitosan nanoparticles containing Mesobuthus eupeus scorpion venom as an antigen delivery system," *J. Venom. Anim. Toxins Incl. Trop. Dis.*, vol. 18, no. 1, pp. 44–52, 2012.

[89] M. K. Yeh, K. M. Cheng, C. S. Hu, Y. C. Huang, and J. J. Young, "Novel protein-loaded chondroitin sulfate-chitosan nanoparticles: Preparation and characterization," *Acta Biomater.*, vol. 7, no. 10, pp. 3804–3812, 2011.

[90] N. Mohammadpourdounighi, A. Behfar, A. Ezabadi, H. Zolfagharian, and M. Heydari, "Preparation of chitosan nanoparticles containing Naja naja oxiana snake venom," *Nanomedicine Nanotechnology, Biol. Med.*, vol. 6, no. 1, pp. 137–143, 2010.

[91] B. Wilson, M. K. Samanta, K. Santhi, K. P. S. Kumar, M. Ramasamy, and B. Suresh, "Chitosan nanoparticles as a new delivery system for the anti-Alzheimer drug tacrine," *Nanomedicine Nanotechnology, Biol. Med.*, vol. 6, no. 1, pp. 144–152, 2010.

[92] A. Grenha, C. Remuñán-López, E. L. S. Carvalho, and B. Seijo, "Microspheres containing lipid/chitosan nanoparticles complexes for pulmonary delivery of therapeutic proteins," *Eur. J. Pharm. Biopharm.*, vol. 69, no. 1, pp. 83–93, 2008.

[93] A. Makhlof, Y. Tozuka, and H. Takeuchi, "Design and evaluation of novel pH-sensitive chitosan nanoparticles for oral insulin delivery," *Eur. J. Pharm. Sci.*, vol. 42, no. 5, pp. 445–451, 2011.

[94] Q. Y. Deng, C. R. Zhou, and B. H. Luo, "Preparation and characterization of chitosan nanoparticles containing lysozyme," *Pharm. Biol.*, vol. 44, no. 5, pp. 336–342, 2006.

[95] E. Gavini, V. Sanna, C. Juliano, M. C. Bonferoni, and P. Giunchedi, "Mucoadhesive vaginal tablets as veterinary delivery system for the controlled release of an antimicrobial drug, acriflavine," *AAPS PharmSciTech*, vol. 3, no. 3, 2002.

[96] A. S. Tzeyung, "Fabrication, optimization, and evaluation of rotigotine-loaded chitosan nanoparticles for nose-to-brain delivery," *Pharmaceutics*, vol. 11, no. 1, pp. 1–17, 2019.

[97] S. Khan and N. Anwar, " Highly Porous pH-Responsive Carboxymethyl Chitosan-Grafted -Poly (Acrylic Acid) Based Smart Hydrogels for 5-Fluorouracil Controlled

Delivery and Colon Targeting ," *Int. J. Polym. Sci.*, vol. 2019, pp. 1–15, 2019.

[98] M. W. Jøraholmen, Ž. Vanić, I. Tho, and N. Škalko-Basnet, "Chitosan-coated liposomes for topical vaginal therapy: Assuring localized drug effect," *Int. J. Pharm.*, vol. 472, no. 1–2, pp. 94–101, 2014.

[99] L. Perioli, V. Ambrogi, C. Pagano, S. Scuota, and C. Rossi, "FG90 chitosan as a new polymer for metronidazole mucoadhesive tablets for vaginal administration," *Int. J. Pharm.*, vol. 377, no. 1–2, pp. 120–127, 2009.

[100] Y. Wu, "Facile fabrication of poly(acrylic acid) coated chitosan nanoparticles with improved stability in biological environments," *Eur. J. Pharm. Biopharm.*, vol. 112, pp. 148–154, 2017.

[101] M. He, C. Zhong, H. Hu, Y. Jin, and Y. Chen, "Cyclodextrin / chitosan nanoparticles for oral ovalbumin delivery : Preparation , characterization and intestinal mucosal immunity in mice," *Asian J. Pharm. Sci.*, vol. 14, no. 2, pp. 193–203, 2019.

[102] S. H. Hussein-al-ali, A. Kura, M. Z. Hussein, and S. Fakurazi, "Preparation of Chitosan Nanoparticles as a Drug Delivery System for Perindopril Erbumine," *Polym. Compos.*, pp. 2–10, 2016.

[103] Z. L. Wang, "New developments in transmission electron microscopy for nanotechnology," *Adv. Mater.*, vol. 15, no. 18, pp. 1497–1514, 2003.

[104] Z. . Wang, "Transmission Electron Microscopy of Shape-Controlled Nanocrystals and Their Assemblies," *j.phys.Chem.B*, vol. 104, pp. 1153–1175, 2000.

[105] Jeol Ltd, "SEM Scanning Electron Microscope A To Z Basic Knowledge For Using The SEM Construction of Instrument Electron Gun Construction of Lens Condenser Lens and Objective Lens Specimen Stage Secondary Electron Detector Image Display and Recording Vacuum System," *Jeol Ltd*, pp. 1–32, 2009.

[106] K. S. P. PL.RM. Palaniappan, "Fourier Transfrom Infrared Spectroscopy," *Fourier Transform Infrared Spectrosc.*, vol. 48, no. 8–9, pp. 2337–2343, 2016.

[107] M. Bodnar, J. F. Hartmann, and J. Borbely, "Preparation and characterization of chitosan-based nanoparticles," *Biomacromolecules*, vol. 6, no. 5, pp. 2521–2527, 2005.

[108] W. Fan, W. Yan, Z. Xu, and H. Ni, "Formation mechanism of monodisperse, low molecular weight chitosan nanoparticles by ionic gelation technique," *Colloids Surfaces B Biointerfaces*, vol. 90, no. 1, pp. 21–27, 2012.

[109] J. Kumirska, "Application of spectroscopic methods for structural analysis of chitin and chitosan," *Mar. Drugs*, vol. 8, no. 5, pp. 1567–1636, 2010.

[110] M. Agarwal, M. K. Agarwal, N. Shrivastav, S. Pandey, R. Das, and P. Gaur,

"Preparation of Chitosan Nanoparticles and their In-vitro Characterization," *Int. J. Life-Sciences Sci. Res.*, vol. 4, no. 2, pp. 1713–1720, 2018.

[111] B. Krishnaveni and P. Priya, "International Journal of Chemical Studies Green synthesis and antimicrobial activity of silver," *Int. J. Chem. Stud.*, vol. 1, no. 6, pp. 10–20, 2014.

[112] G. B. Martínez-Hernández, M. L. Amodio, and G. Colelli, "Carvacrol-loaded chitosan nanoparticles maintain quality of fresh-cut carrots," *Innov. Food Sci. Emerg. Technol.*, vol. 41, pp. 56–63, 2017.

[113] S. Woranuch and R. Yoksan, "Eugenol-loaded chitosan nanoparticles: I. Thermal stability improvement of eugenol through encapsulation," *Carbohydr. Polym.*, vol. 96, no. 2, pp. 578–585, 2013.

[114] S. Honary, K. Ghajar, P. Khazaeli, and P. Shalchian, "Preparation , Characterization and Antibacterial Properties of Silver-Chitosan Nanocomposites Using Different Molecular Weight Grades of Chitosan," vol. 10, no. July 2010, pp. 69–74, 2011.

[115] S. W. Ali, S. Rajendran, and M. Joshi, "Synthesis and characterization of chitosan and silver loaded chitosan nanoparticles for bioactive polyester," *Carbohydr. Polym.*, vol. 83, no. 2, pp. 438–446, 2011.

[116] Y. Zhang, Y. Yang, K. Tang, X. Hu, and G. Zou, "Physicochemical Characterization and Antioxidant Activity of Quercetin-Loaded Chitosan Nanoparticles," 2007.

[117] G. Chen, W. Wang, G. Chen, and W. Wang, "Role of Freeze Drying in Nanotechnology Role of Freeze Drying in Nanotechnology," vol. 3937, 2007.

[118] T. Banerjee, S. Mitra, A. Kumar Singh, R. Kumar Sharma, and A. Maitra, "Preparation, characterization and biodistribution of ultrafine chitosan nanoparticles," *Int. J. Pharm.*, vol. 243, no. 1–2, pp. 93–105, 2002.

[119] D. Chen, "Comparative study of Pluronic® F127-modified liposomes and chitosan-modified liposomes for mucus penetration and oral absorption of cyclosporine A in rats," *Int. J. Pharm.*, vol. 449, no. 1–2, pp. 1–9, 2013.

[120] K. C. Hembram, S. Prabha, R. Chandra, B. Ahmed, and S. Nimesh, "Advances in preparation and characterization of chitosan nanoparticles for therapeutics," *Artif. Cells, Nanomedicine Biotechnol.*, vol. 44, no. 1, pp. 305–314, 2016.

[121] C. P. Kiilll, "Synthesis and factorial design applied to a novel chitosan/sodium polyphosphate nanoparticles via ionotropic gelation as an RGD delivery system," *Carbohydr. Polym.*, vol. 157, pp. 1695–1702, 2017.

[122] N. Hasheminejad, F. Khodaiyan, and M. Safari, "Improving the antifungal activity of

clove essential oil encapsulated by chitosan nanoparticles," *Food Chem.*, vol. 275, no. April 2018, pp. 113–122, 2019.

[123] M. Amidi, S. G. Romeijn, G. Borchard, H. E. Junginger, W. E. Hennink, and W. Jiskoot, "Preparation and characterization of protein-loaded N-trimethyl chitosan nanoparticles as nasal delivery system," *J. Control. Release*, vol. 111, no. 1–2, pp. 107–116, 2006.

[124] A. Grenha, B. Seijo, and C. Remuñán-López, "Microencapsulated chitosan nanoparticles for lung protein delivery," *Eur. J. Pharm. Sci.*, vol. 25, no. 4–5, pp. 427–437, 2005.

[125] D. Kavaz, F. Kirac, M. Kirac, and A. Vaseashta, "Low Releasing Mitomycin C Molecule Encapsulated with Chitosan Nanoparticles for Intravesical Installation," *J. Biomater. Nanobiotechnol.*, vol. 08, no. 04, pp. 203–219, 2017.

[126] P. Bhardwaj and S. Singh, "formulation and in vitro evaluation of ph-sensitive chitosan beads of flurbiprofen 1* 1," vol. 1, no. 2, pp. 48–54, 2013.

[127] M. Fathi, P. S. Zangabad, S. Majidi, J. Barar, H. Erfan-niya, and Y. Omidi, "Stimuli-responsive chitosan-based nanocarriers for cancer therapy," vol. 7, no. 4, pp. 269–277, 2017.

[128] X. Gao, "Biodegradable , pH-Responsive Carboxymethyl Cellulose / Poly (Acrylic Acid) Hydrogels for Oral Insulin Delivery a," pp. 565–575, 2014.

[129] C. W. N. S. S. J. R. B. Usselman, "乳鼠心肌提取 HHS Public Access," *Physiol. Behav.*, vol. 176, no. 3, pp. 139–148, 2017.

[130] J. Wang and Y. Kuo, "Preparation and Adsorption Properties of Chitosan – Poly (acrylic acid) Nanoparticles for the Removal of Nickel Ions," 2007.

678

Appendix 1

ZETA POTENTIAL AND SIZE DISTRIBUTION CURVES

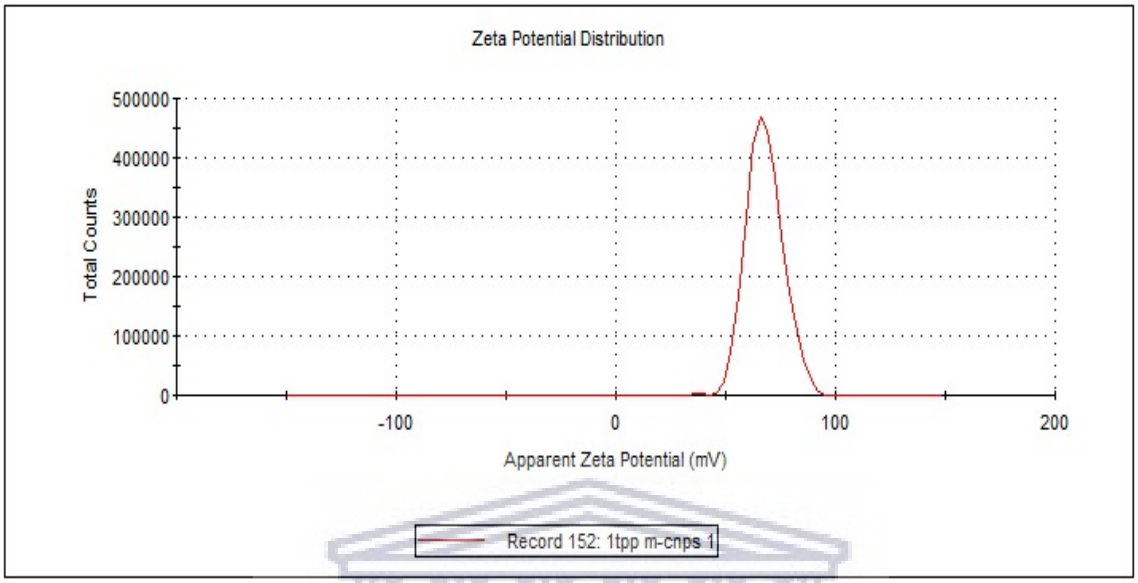

Figure 1(a): Zeta potential of Kn2-7 CNPs

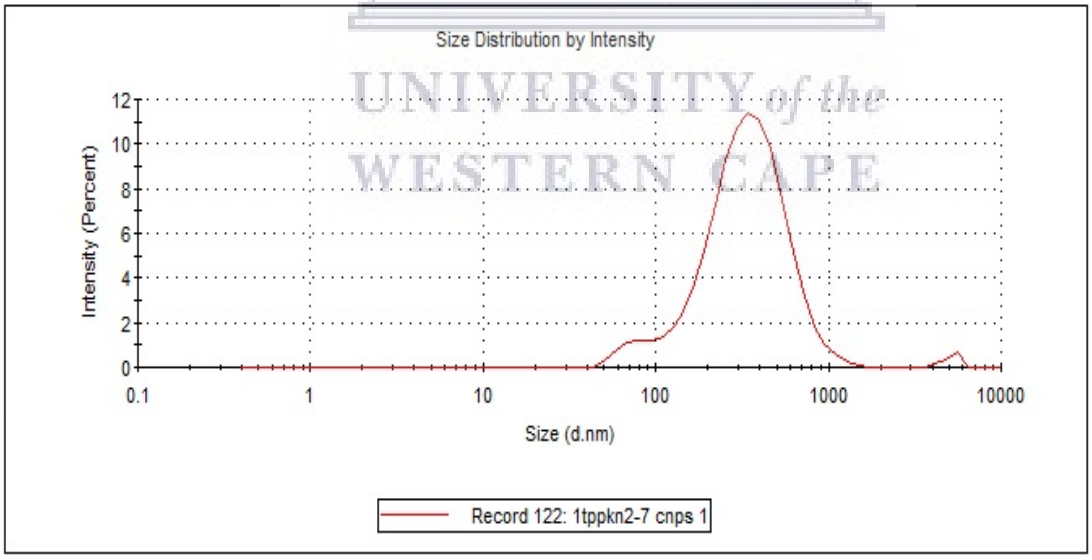

Figure 1(b): Size distribution of Kn2-7 CNPs

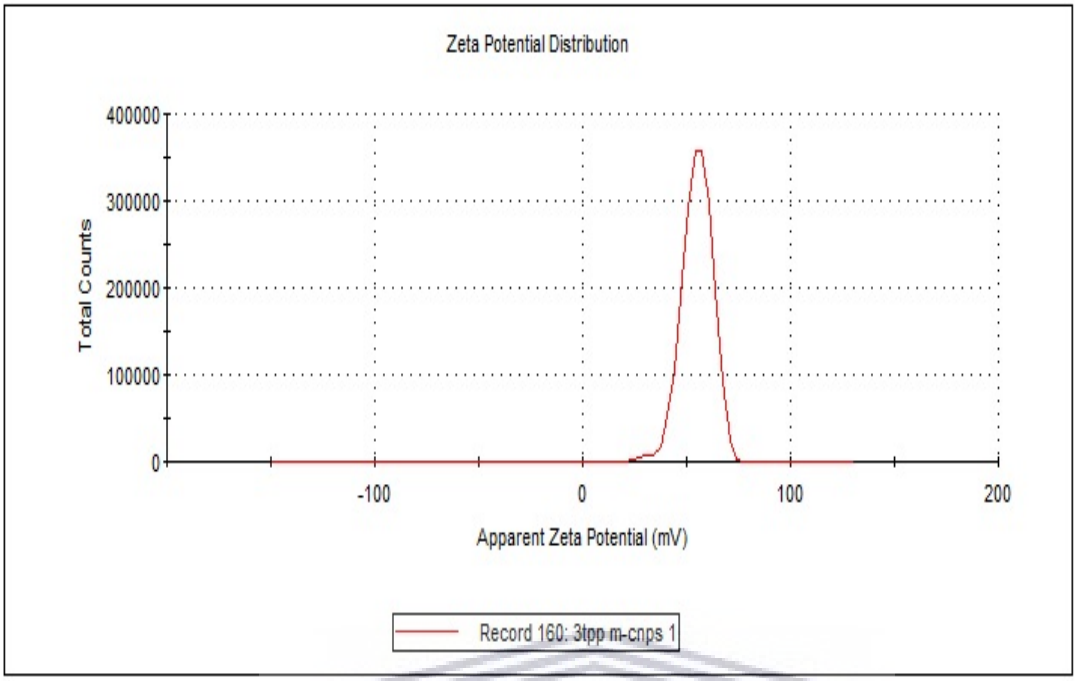

Figure 1(c): Zeta potential of Hβd-3 CNPs

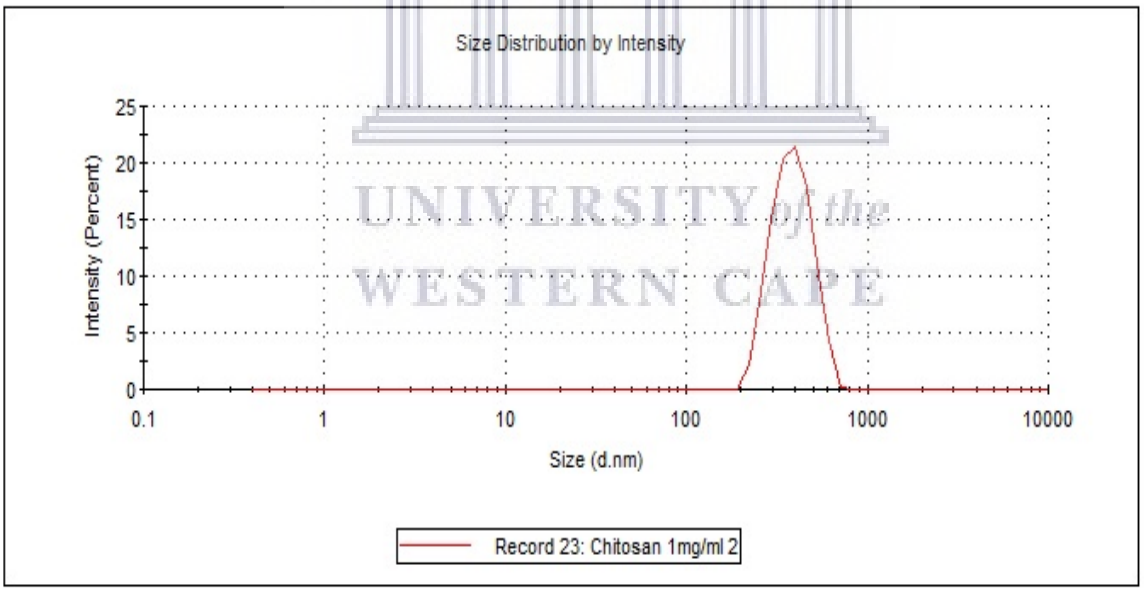

Figure 1(d): Size distribution of Hβd-3 CNPs.

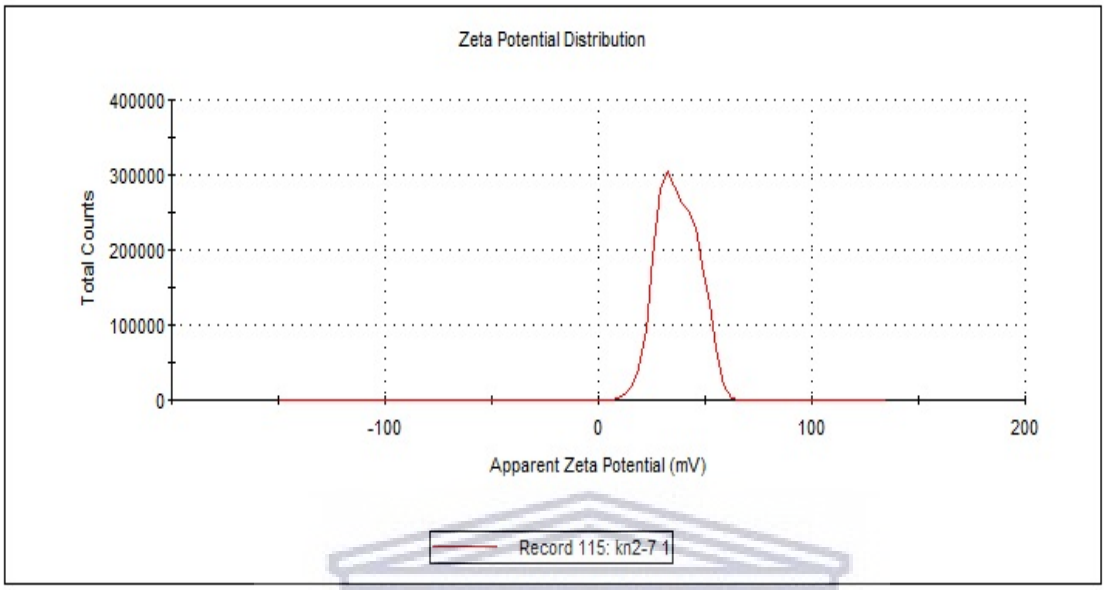

Figure 1(e): Zeta potential of Kn2-7 CS/PAA NPs

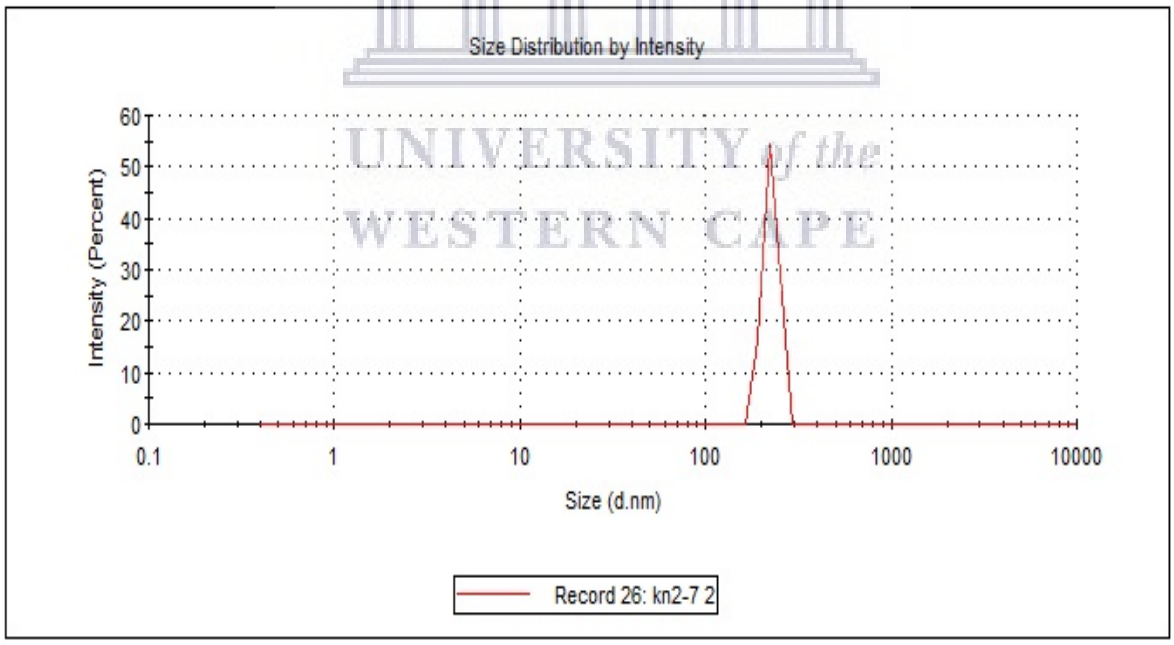

Figure 1(f): Size distribution of Hβd-3 CNPs.

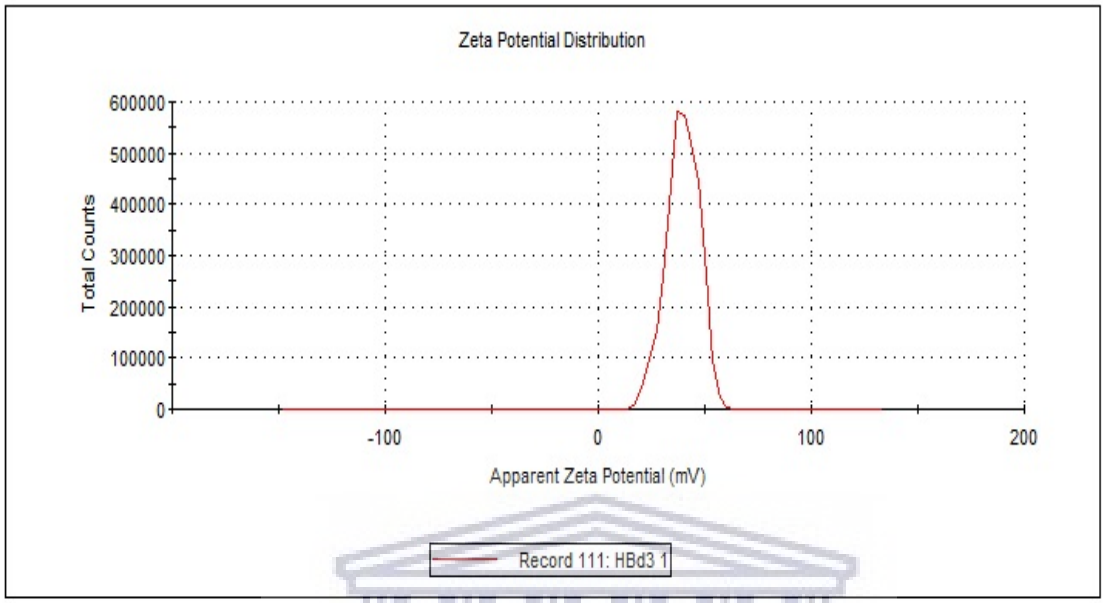

Figure 1(g): Zeta potential of Kn2-7 CS/PAA NPs

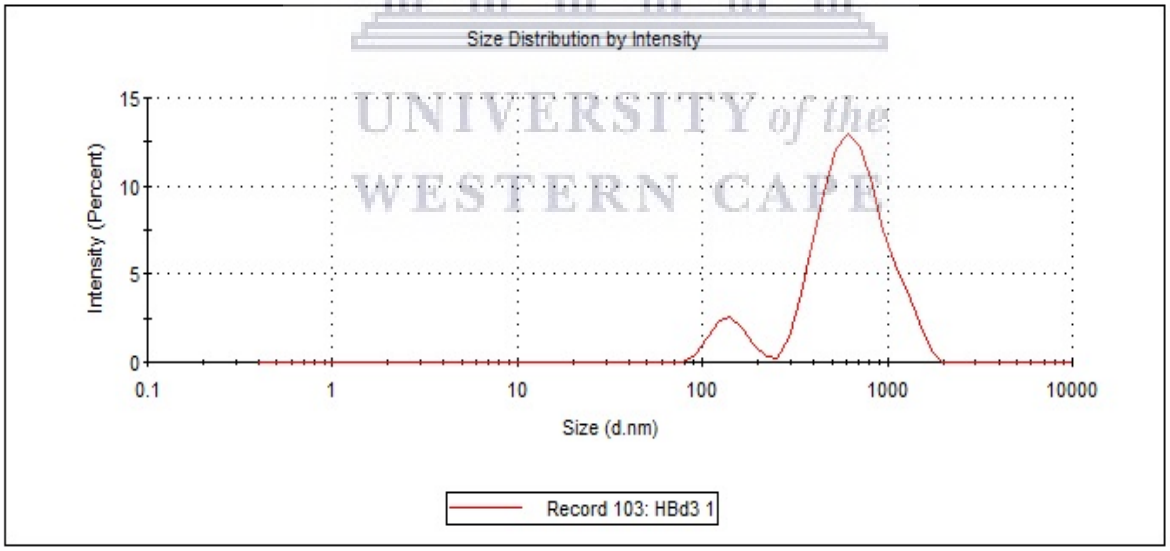

Figure 1(h): Size distribution of HCPNPs.

Appendix 2

FTIR SPECTRUM.

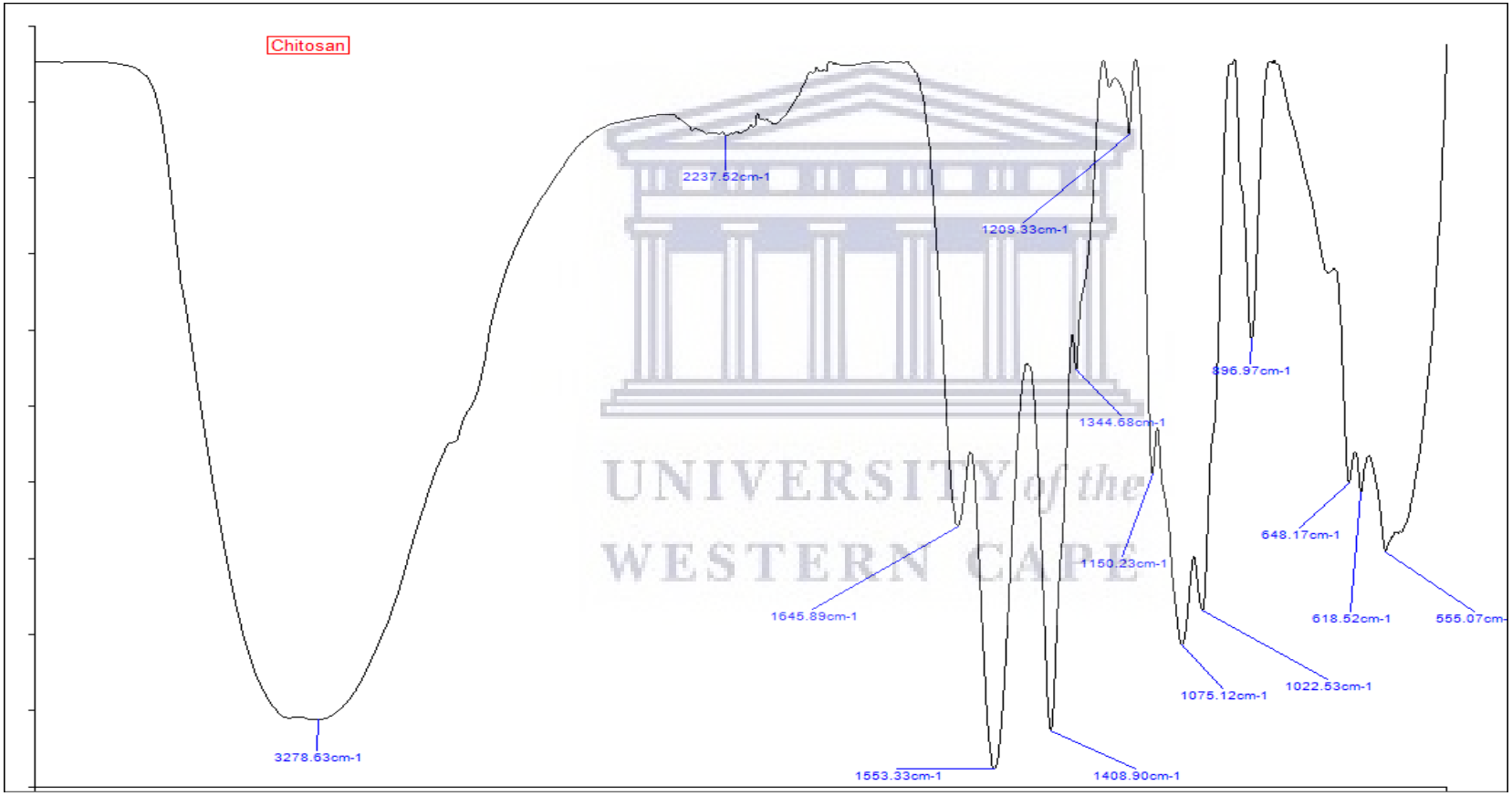

Figure 2(a): FTIR of Kn2-7 CS.

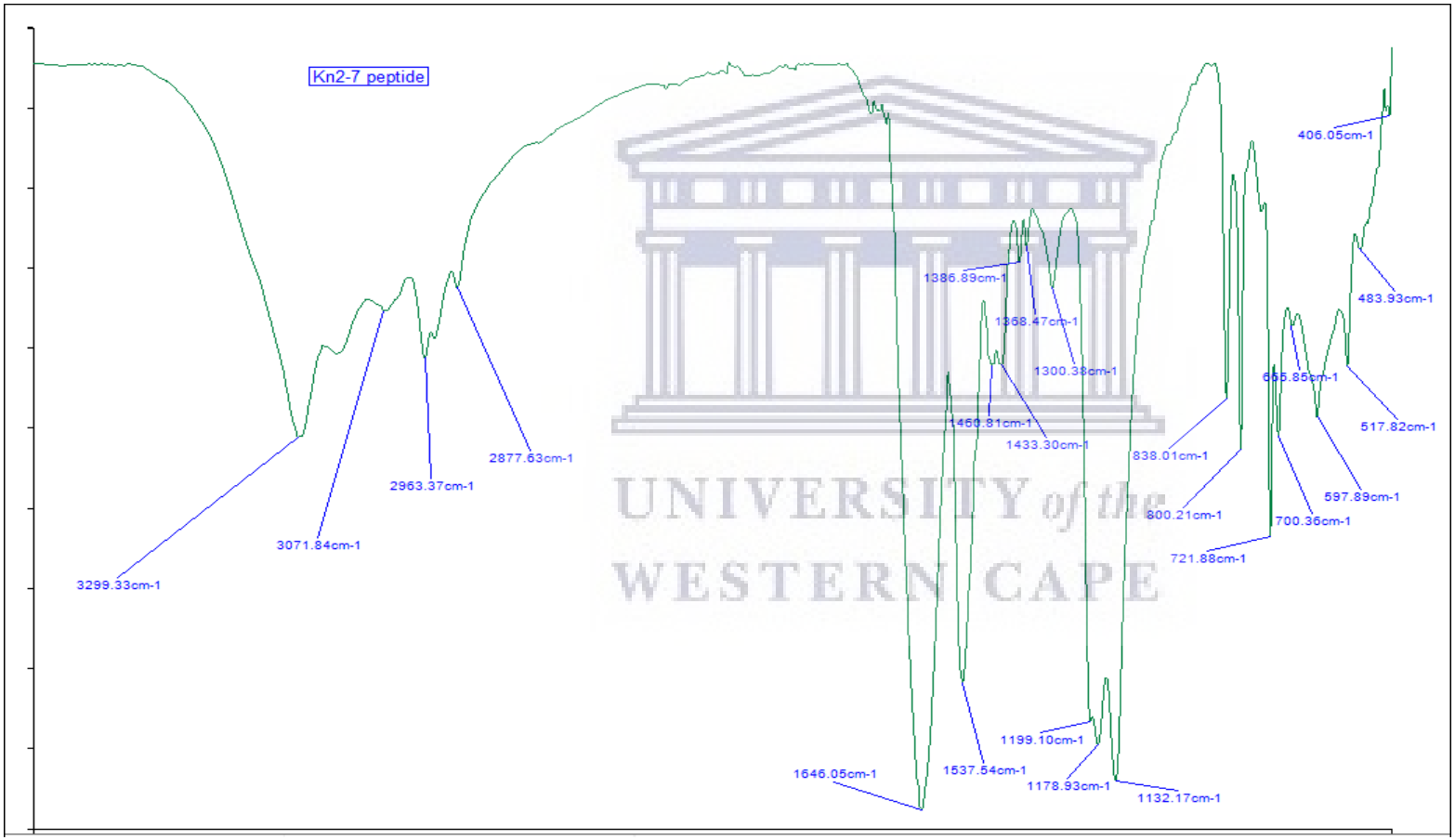

Figure 2(b): FTIR of Kn2-7 peptide.

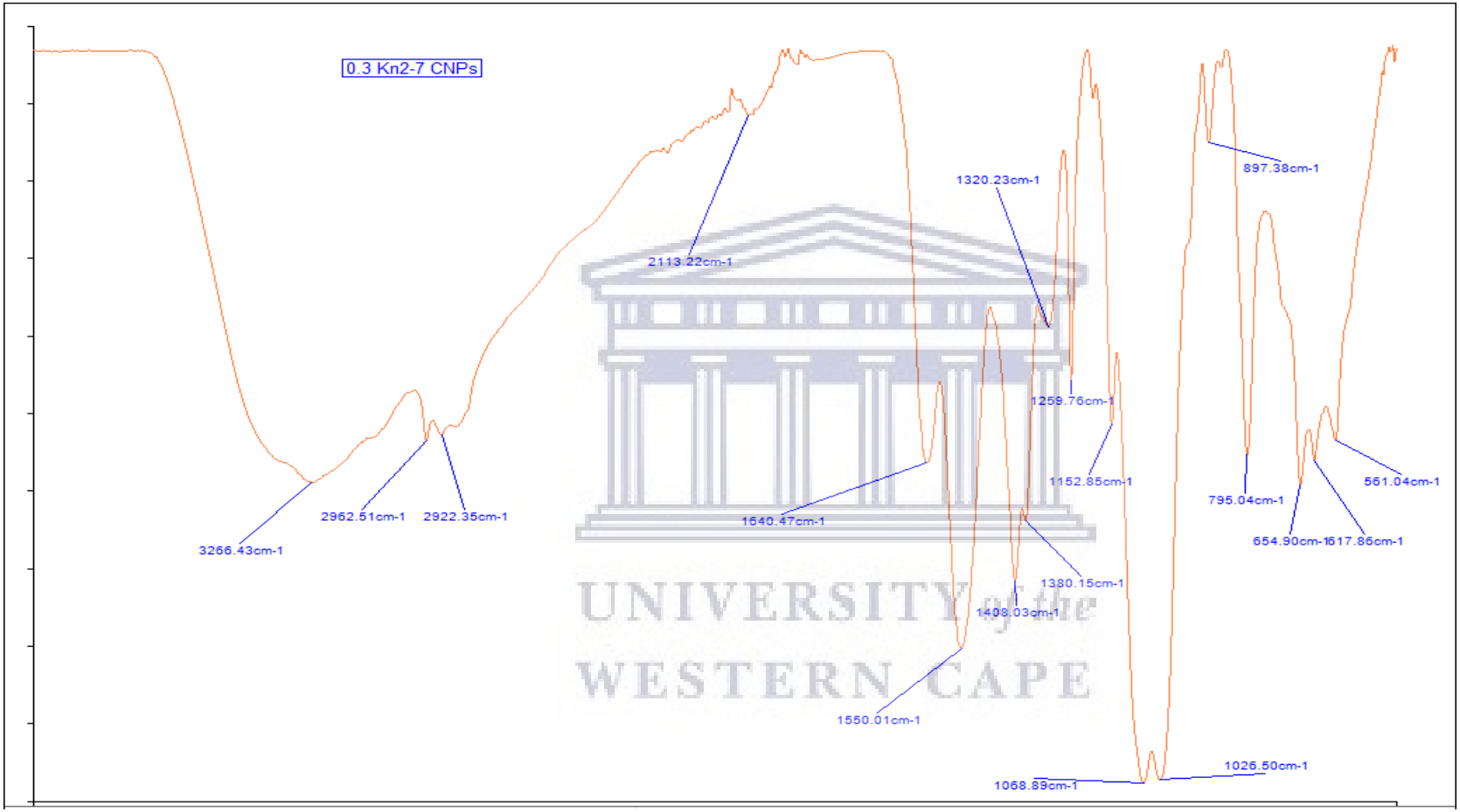

Figure 2(c): FTIR of Kn2-7 CNPs in 0.3 mg/mL TPP

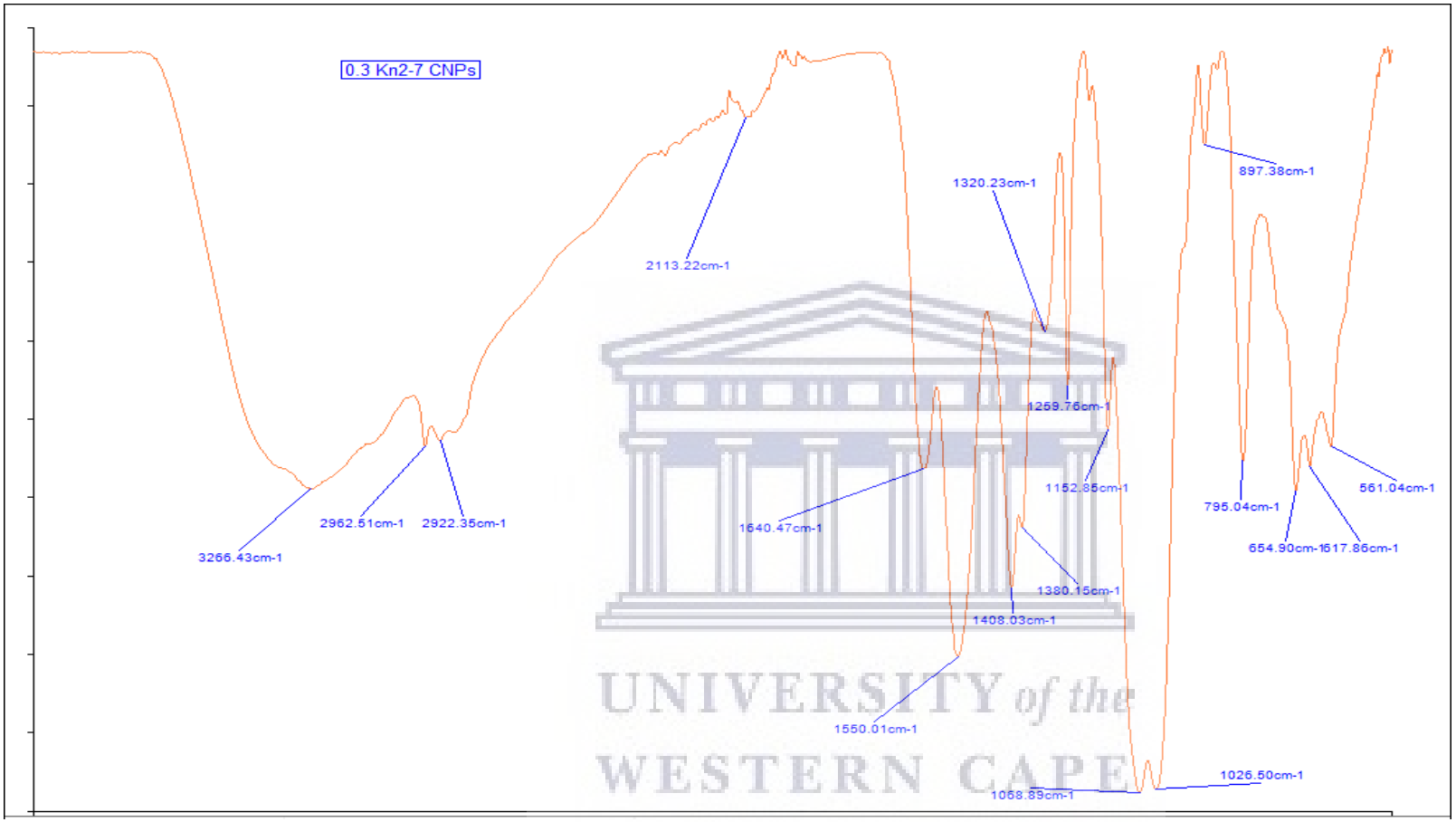

Figure 2(d): FTIR of Kn2-7 CNPs in 0.3mg/mL TPP

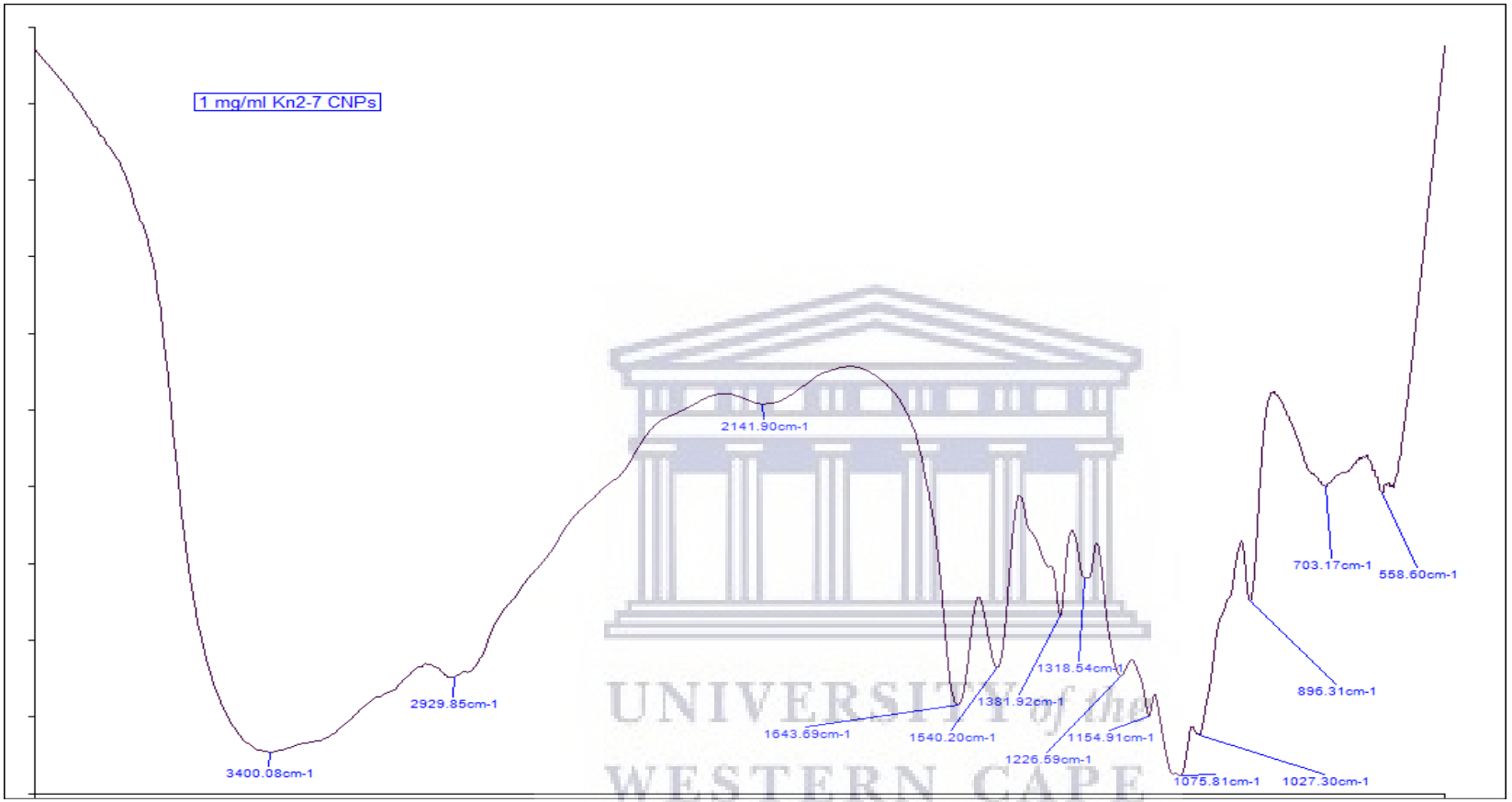

Figure 2(e): FTIR of Kn2-7 CNPs in 1mg/mL TPP

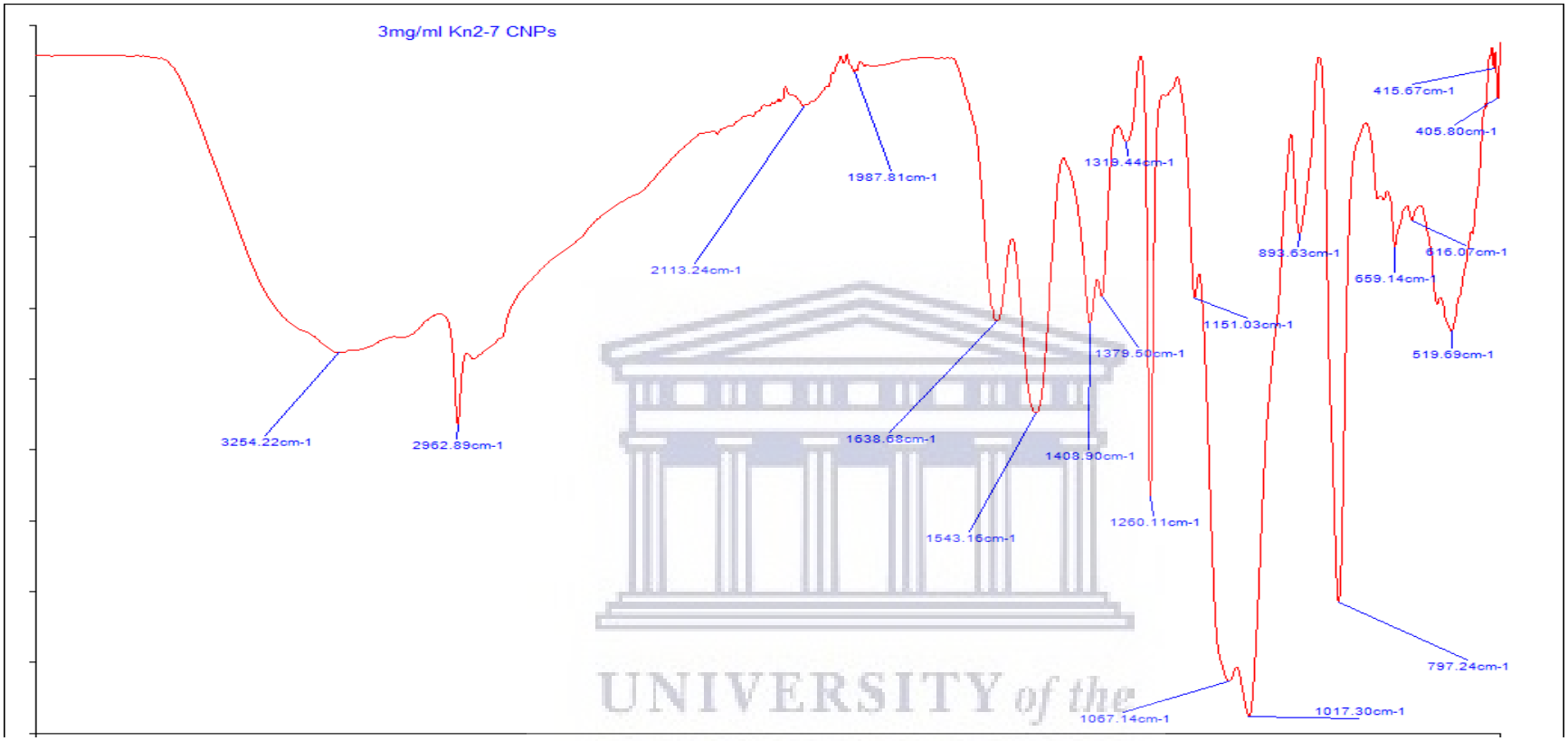

Figure 2(f): FTIR of Kn2-7 CNPs in 3mg/mL TPP

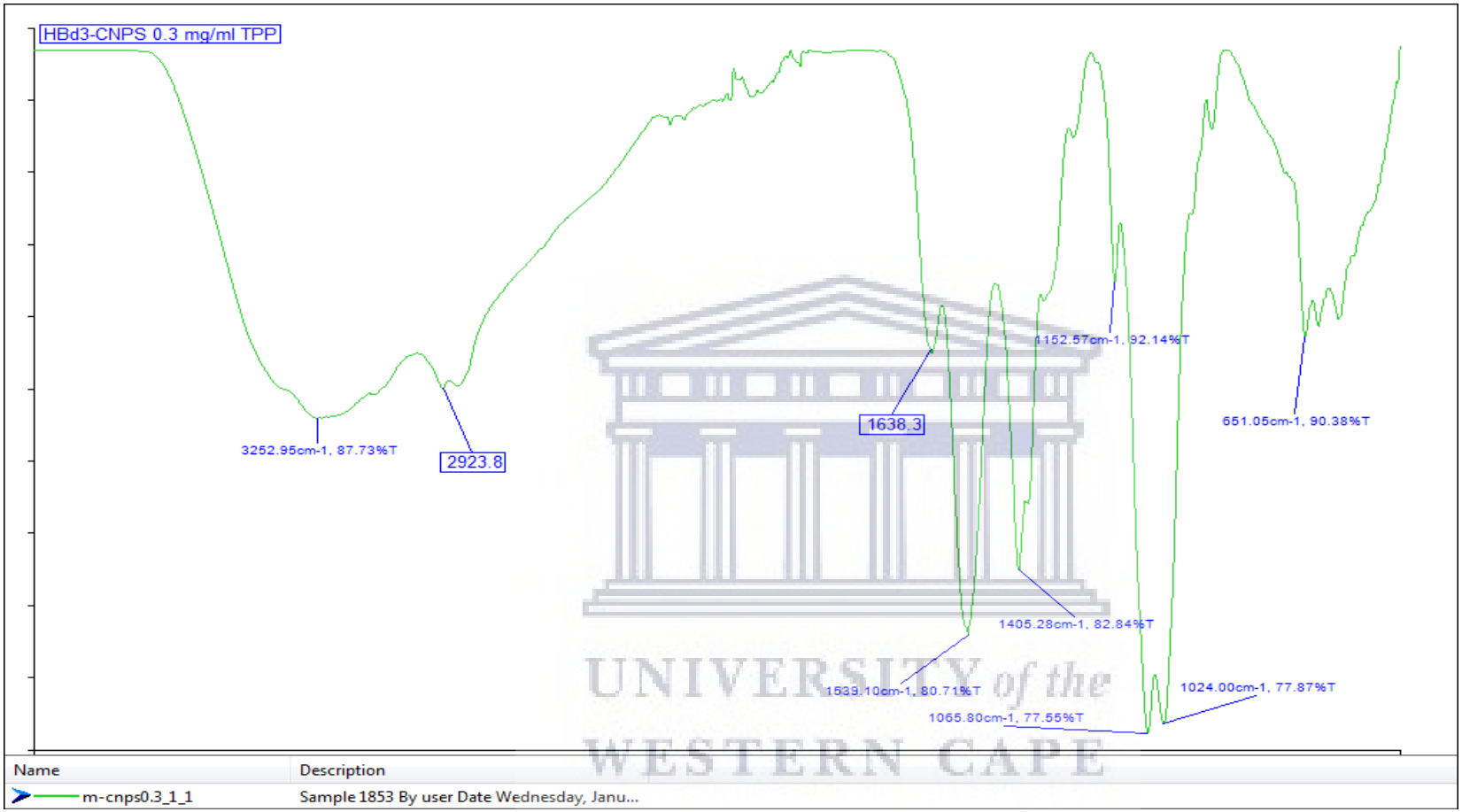

Figure 2(g): FTIR of Hβd-3 CNPs in 0.3mg/mL TPP.

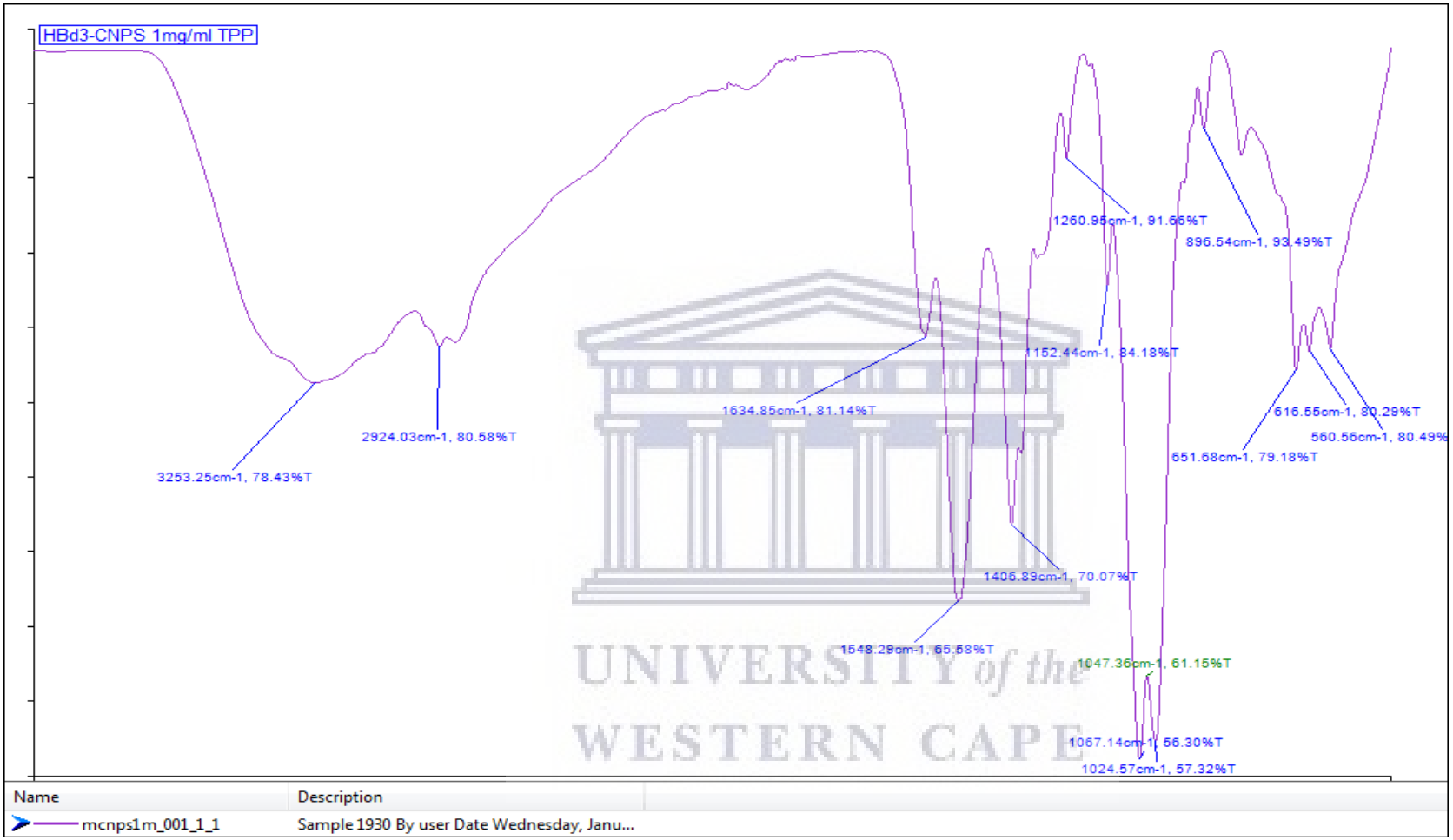

Figure 2(h): FTIR of Hβd-3 CNPs in 1mg/mL TPP.

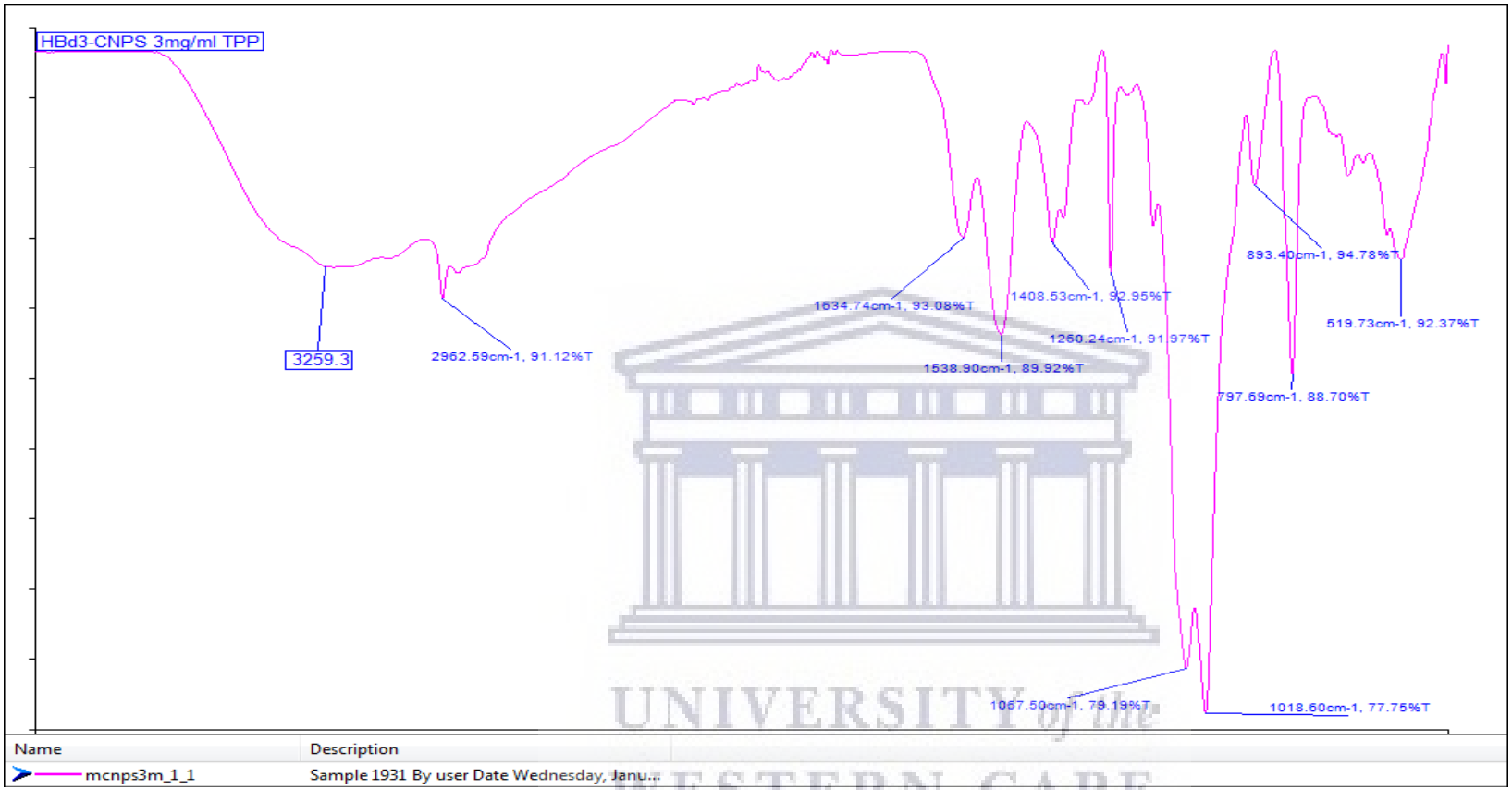

Figure 2(i): FTIR of Hβd-3 CNPs in 3mg/mL TPP